PERFORMANCE EVALUATION OF KDOT W-BEAM SYSTEMS

Volume II:
Component Testing and Computer Simulation

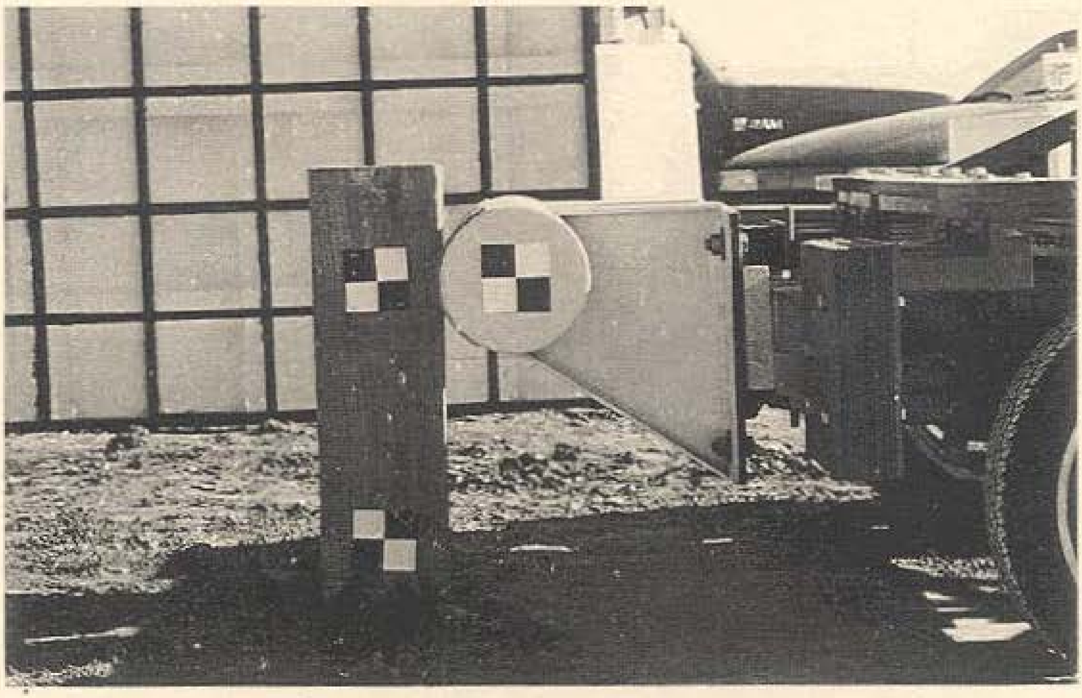

Prepared by:
Midwest Roadside Safety Facility (MwRSF)
Center for Infrastructure Research
Civil Engineering Department
University of Nebraska-Lincoln
1901 Y Street, Building C
Lincoln, Nebraska 68588-0601
(401) 472-9198

May 1996

1. Performing Organization Report No.	2. Report Date	3. Type of Report
TRP-03-39-96	May 1996	Final Report

4. Title and Subtitle

Performance Evaluation of KDOT W-Beam Systems
Volume II: Component Testing and Computer Simulation

5. Author(s)

Holloway, J.C., M.G. Bierman, B.G. Pfeifer, B.T. Rosson, and D.L. Sicking

6. Performing Organization Name and Address

Midwest Roadside Safety Facility (MwRSF)
Civil Engineering Department
University of Nebraska - Lincoln
1901 Y St., Bldg C
Lincoln, Nebraska 68588-0601
(402) 472-9198

7. Sponsoring Agency Name and Address

Midwest States Regional Pooled Fund
Nebraska Department of Roads
1500 Nebraska Highway 2
Lincoln, Nebraska 68509-4567

8. Contract or Grand No.

SPR-3(017), FY-94 Midwest States Regional Pooled Fund Program

9. Abstract

Typical Kansas Department of Transportation (KDOT) guardrail installations use single W-beams with steel posts spaced at 6 ft. - 3 in. The first phase of this study evaluated the strengthening effects of half-post spacing and nested W-beams on the performance of guardrail systems using four full-scale crash tests.

As part of this research, simulations using the computer program BARRIER VII were performed on the same configurations and with timber posts. The necessary post inputs for the program were obtained by using the results of a post testing program. A total of twenty-one dynamic post tests were conducted, consisting of timber and steel posts with lengths of 6 ft and 6 ft - 6 in., in clay and sandy soils and with varying soil moisture contents.

BARRIER VII post parameters were calculated by interpolating stiffness and strength values from the force-deflection plots obtained in the post tests. Using the resulting steel post parameters in a BARRIER VII simulation of the full-scale crash tests, the results of both the full-scale crash tests and the simulations were compared. The results of the simulation were satisfactorily validated by the full-scale tests, and therefore, the results of the other post tests could be used to calculate reliable BARRIER VII inputs for each guardrail strengthening scheme. The various post parameters were also then used in simulations of the KSWB installations to predict the deflections of guardrails using various post types in different soils with varying moisture contents. The predicted deflections of each guardrail simulation were compared with the others to evaluate the effect the post and soil conditions have on the guardrail's ability to control deflections.

If the moisture content of the clay was high, the stiffness and yield moment post parameters calculated from post testing were lower than the parameters for posts in a drier clay. Consequently, guardrail simulations using the clay post parameters with high moisture contents resulted in higher maximum dynamic and permanent set deflections than the simulations using post parameters in clay soil with a lower moisture content. The post type did no affect the deflections greatly, as both steel and timber posts behaved similarly for all soil conditions and guardrail configurations.

When simulations of the guardrail using the strengthening techniques were compared, the deflection reductions resulting from half-post spacings were considerably greater than those of W-beam nesting. Guardrails strengthened by half-post spacing reduced deflections by 17 to 29% whereas nesting W-beams reduced the deflections by a relatively small amount in comparison. Guardrail simulations with both modifications decreased the deflections only slightly more than simulations conducted with half-post spacings alone. Therefore, the strengthening technique of a single W-beam with a half-post spacing is recommended, unless the additional purchase necessary to nest the W-beam is justified for a particular installation adjacent to a roadside hazard.

10. Keywords	11. Distribution Statement
Highway Safety, Crash Tests, Guardrail, Posts, Dynamic Post Testing, W-Beam	No restrictions. This document is available to the public from the sponsoring agency.

12. Security Classification (of this report)	13. Security Classification (of this page)	14. No. of Pages
Unclassified	Unclassified	

Disclaimer Statement

The contents of this report reflect the views of the authors who are responsible for the facts and the accuracy of the data presented herein. The contents do not necessarily reflect the official views or policies of the Kansas Department of Transportation. This report does not constitute a standard, specification, or regulation.

Acknowledgements

The authors wish to express their appreciation and thanks to the Midwest Regional States Pooled Fund and the Center for Infrastructure Research for funding the research described herein. A special thanks is also given the following individuals who made a contribution to this research study.

Kansas Department of Transportation
Ron Seitz, P.E., Squad Leader

Nebraska Department of Roads
Larry Brown, Midwest States Regional Pooled Fund Chairman
Leona Kolbet, Research Coordinator

Missouri Highway Transportation Department
Pat McDaniel, P.E., Special Assignments Design Engineer

Minnesota Department of Transportation
Khani Sahebjam, P.E., State Aid Bridge Engineer

Center for Infrastructure Research
Maher Tadros, Ph.D., P.E., Director

Midwest Roadside Safety Facility
Ronald K. Faller, P.E., Research Associate Engineer
John R. Rohde, Ph.D., P.E., Associate Professor
John D. Reid, Ph.D., Assistant Professor
Graduate and Undergraduate Assistants

Table of Contents

List of Figures

List of Tables

1. Introduction

Guardrails are placed adjacent to highways and roadways to redirect errant vehicles away from roadside hazards. These hazards may include light poles, abutments, bridge piers, and other obstacles. Guardrail designs that have proven very effective are being continuously redesigned to improve their efficiency, and these redesigned systems must then be analyzed in detail and tested to prove their crash worthiness. Full-scale crash testing on such systems provides a valuable tool for evaluating their performance.

The Kansas Department of Transportation (KDOT) has designed several guardrail systems to control deflections and safely redirect vehicles from roadside obstacles. If an obstacle is close to the road, a stiffer modified barrier is needed to decrease deflections and minimize the possibility of snagging or striking the hazard. There are many different modifications that can be employed to stiffen a guardrail. The two modifications investigated as part of this research are nested W-beams and half-post spacing. W-beam nesting increases the stiffness of the rail by sandwiching two W-beams together and mounting them at the same point on the post. Half-post spacing is reducing the spacing from the standard 6 ft - 3 in. to 3 ft - $1^1/_2$ in. One aspect of this research is to evaluate the effects these two strengthening techniques have on the performance of a guardrail.

In 1993, a series of full-scale crash tests (26) were performed on Kansas W-Beam (KSWB) guardrails employing the strengthening techniques described above. The tests consisted of single and nested W-beams with full and half-post spaced steel posts. The purpose of the tests was to determine the effects that nesting and reduced post-spacing have on the dynamic lateral deflections of the guardrail. KSWB-1, the baseline system configuration, consisted of a typical W-beam installation with a single rail and full post spacings (6 ft - 3 in.). KSWB-2 was identical to the first with the only modification being nested W-beams on the inner five of the seven sections. KSWB-3 was also identical to the baseline configuration except the inner five sections had half-post spacings (3 ft - $1^1/_2$ in.). KSWB-4, the final test in the series, employed nested W-beams and half-post spacings on the inner five sections. The plan view and section details of the KSWB installations are illustrated in Figure 1.

The interaction of a vehicle and a roadside barrier is complex, requiring extensive analysis. The interaction can only be properly and reliably analyzed through full-scale testing and computer simulations. Full-scale crash tests on guardrail systems have proven to be an accurate and reliable means of evaluating the performance of a system, but the cost associated with them is high. Because of this fact, full-scale testing is not a cost effective way to develop new guardrail systems. Hand calculations of dynamic vehicular impacts can be too simplistic and cannot analyze the process thoroughly. Computer simulations, however, can provide a reliable and relatively inexpensive means of analyzing the impact into a guardrail. Thus they have the potential to reduce the cost or even enlarge the extent of an existing test program, without substantially increasing the cost. For these reasons,

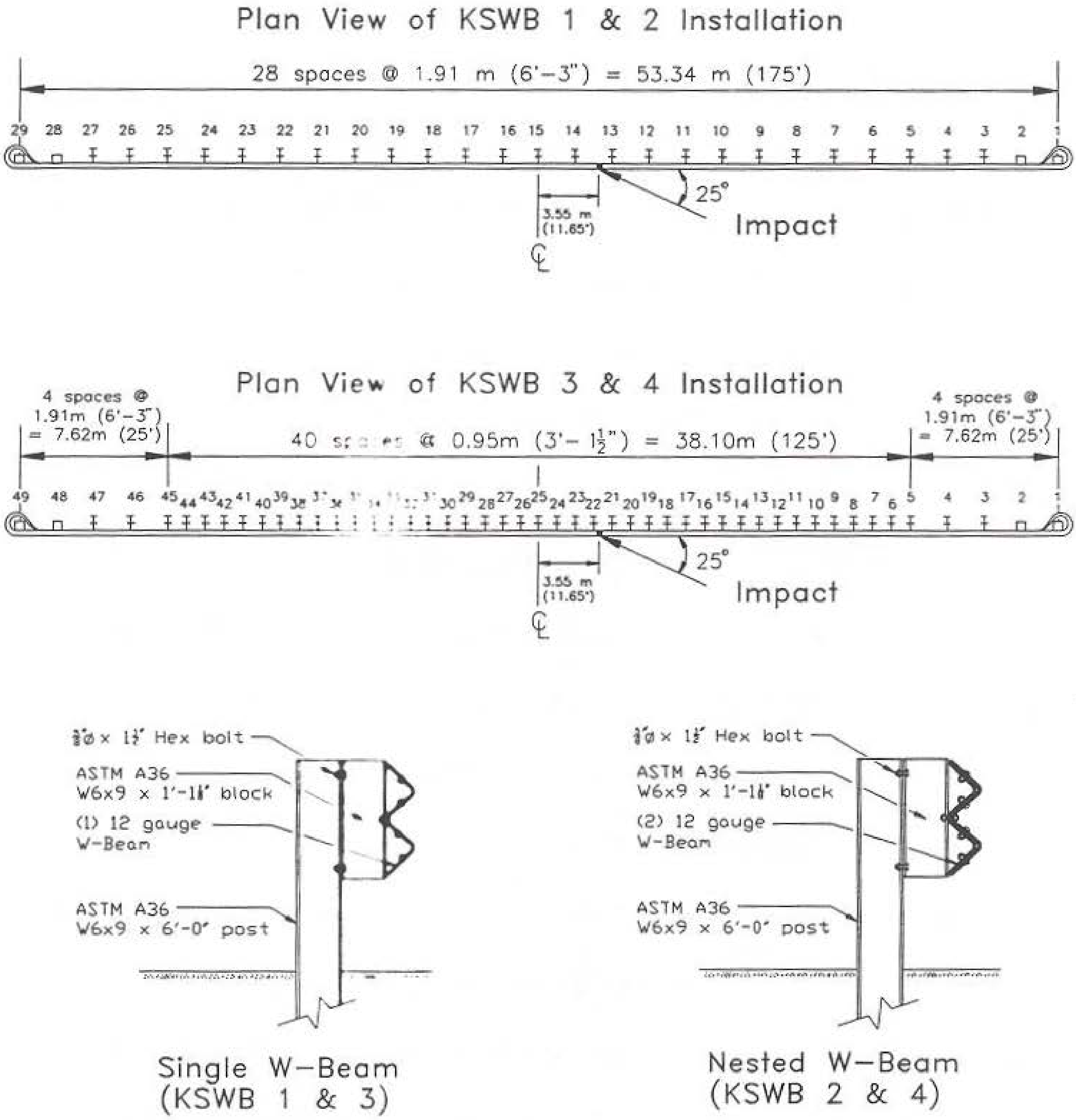

Figure 1. Plan view and section details of KSWB installations.

computer simulation programs have become an extremely valuable tool for use in the development of guardrail designs.

One such computer program, known as BARRIER VII, was first developed in 1970 by G.H. Powell (1,2) and has since been used extensively by state agencies to simulate full-scale vehicle impacts. The computer program performs a two-dimensional analysis of a vehicle impacting deformable barriers. While more advanced computer simulation programs have evolved since BARRIER VII, this program continues to be widely used due to its proven reliability and familiarity by the roadside safety community.

Over the years since the inception of the program, research has focused on validating and refining the parameters input to the program. In particular, much of this research effort has been directed toward developing the post stiffness input parameters that describe the behavior of the post for the various post and soil conditions. Post testing in various soil conditions provides for a better understanding of the relationship between these conditions and the behavior of the post under dynamic loading. Conditions investigated in this research effort include: the post type, and the soil material and moisture content, and the embedment depth.

The original proposal for this research was to validate a BARRIER VII model for steel posts typically used in Kansas, and to determine the deflections of the KSWB guardrail systems with timber posts by computer simulations. The posts to be investigated were W6 x 9 steel and 6 x 8 inch timber posts, each 6 ft in length. KDOT and many other highway agencies are considering the potential use of one length of post for both its W-beam and Thrie beam systems. A Thrie-Beam guardrail system requires a $6^1/_2$ ft post, whereas a W-beam system typically utilizes a 6 ft post. In order to reduce post inventories, it would be desirable to use $6^1/_2$ ft posts for both guardrails. The longer posts must be embedded an additional six inches for W-beam systems, so the testing matrix was expanded to examine the effect this increase in embedment has on the post behavior under dynamic impact load.

The soils used in the study include a lean clay and a fine poorly graded sand. The clay soil was chosen because the four guardrails which were tested were installed in this soil, and the sand was chosen because it provided for a well drained soil condition.

Varying the moisture content of the soil during post tests has been given little attention in past research even though the moisture content directly affects the compaction of the soil around the post, and hence the lateral resistance of the soil. As part of this research, three different moisture contents were studied - varying from low (8%), optimum (17%), to high (28%).

Twenty-one dynamic tests were conducted on various posts embedded in the aforementioned soil conditions. The posts were impacted with a bogie - a steel frame cart designed for testing components of roadside safety appurtenances - at approximately 20 mph. The bogie is very rigid, therefore most of the impact energy is absorbed by the soil and post.

After the bogie post testing phase, the resulting force and deflection plots were used to develop the BARRIER VII post models for each of the various post types and soil conditions. Four of the models were validated by comparing the computer simulation results with the full-scale crash test results (KSWB 1-4).

After validation of the post model, simulations were conducted using the other post parameters in the matrix to predict the dynamic deflections for similar guardrail systems with different post types and soil conditions. The various strengthening techniques were assessed for each structural change by comparing the maximum dynamic deflections of the strengthened rails with those of the corresponding standard installation. Comparisons were also made between identical configurations with different post and soil conditions to evaluate the effect of each condition on the maximum dynamic deflections.

2. Literature Review

2.1 Computer and BARRIER VII Simulations

The interaction of a vehicle with a flexible barrier system is a particularly complex process. When analyzing this process, dynamic effects, extremely large displacements, and inelastic behavior must all be considered. Dynamic loads used in the interaction are not explicitly specified, but must be determined by satisfying force equilibrium and displacement compatibility equations between the automobile and barrier. Computer simulation using the finite element method for the dynamic interaction problem is ideal for studying this interaction.

In the late sixties, the Highway Vehicle Object Simulation Model (HVOSM) was developed (3). The computer simulation program simulated the three-dimensional behavior of a vehicle as it interacts with roadside objects. Although this program is still widely used by many research agencies, usually in a modified form of the original version for specific needs, its success on longitudinal barriers is limited.

In 1970, Graham Powell developed two guardrail computer simulation programs, BARRIER IV and BARRIER V for the Federal Highway Administration (FHWA) (1). The BARRIER programs simulate two-dimensional impacts of various vehicles with deformable barriers. The two programs were intended to provide information at two stages in the evaluation of barrier systems: (1) at the initial design stage, the programs could be used to compare design concepts and assist in prototype design; and (2) at the testing stage, if the programs provided reasonable results for the range of parameters considered in the tests, the behavior could be predicted for other values of the parameters, and the number of tests reduced. In other words, if one set of parameters could be validated by full-scale test results, then this reliability could be projected toward other values of the parameters.

In 1973, Powell published the next version of the simulation program, BARRIER VII (2). This update contained the features of both BARRIER IV and BARRIER V with additional capabilities. BARRIER VII included an energy balance computation and the ability to simulate barriers with members at different heights above the ground, such as rubrails.

BARRIER VII idealizes the barrier as a structural framework of arbitrary configuration and the automobile as a body surrounded by a cushion of springs in the horizontal plane. Large displacements and inelastic behavior, including hysteresis effect on unloading, are considered in the barrier structure. As the automobile slides along the barrier, the effects of normal forces, friction forces, and wheel drag forces are considered in determining its motion. Input data to the program consists of the configuration of the barrier, the properties of the barrier members and the automobile, and the trajectory of the automobile before impact. Output data consists of the time histories of automobile positions, velocities and accelerations, and barrier deflections and member forces.

The vehicle model used in BARRIER VII is composed of 3 major segments: the vehicle as a rigid body, the steering mechanism, and the deformable body. The barrier is modeled as a structured beam on many flexible supports. The rail, is divided into discrete elements connected to each other at the support nodes.

The reliability of BARRIER VII has been proven numerous times, and the range over which the simulation program can be successfully used has been demonstrated in many validation studies. Simulations in 1987 by Post (4) proved the accuracy of the program when the snagging potential of wheel hubs and rims predicted by BARRIER VII was verified by full-scale crash tests. Snagging of wheels occurs when the path of the wheel overlaps a post or other potential snag points and direct contact is possible, resulting in excessive vehicle decelerations and unacceptable occupant impact velocities. Wheel contact cannot be simulated, but its occurrence can be predicted. The predicted snagging of $3^1/_2$ inches compared well with the field measured value of 3 inches.

Research in 1988 by Bligh, et al. (5) verified, with full-scale vehicle crash tests, that BARRIER VII could be employed to predict vehicle snagging for W-beam transitions without a rubrail by plotting the path of the undeformed wheel hub. These findings indicated that the wheel hub and rim were able to slide under the W-beam guardrail member easily. These results from BARRIER VII demonstrated the benefits of rubrails in preventing snagging problems on guardrail installations.

Work by Tuan in 1989, et al. (6) on Kansas Guardrail to Bridge-rail Transition Designs proved the model effective at predicting the vehicle exit speed and angle, and maximum dynamic deflections of transitions. A methodology was developed for wheel-snagging prediction and was validated against test data. It was shown that reliable simulation results could be obtained if the input parameters for simulation were assessed accurately.

2.2 Previous Post Testing Studies

Post testing can be accomplished by a number of different methods. For posts loaded statically, a continuously increasing load is applied until failure of the post or soil occurs. The basic static test configuration consists of the post, embedded in soil or fixed to an immovable block, and a loading mechanism, typically a hydraulic cylinder. As the load is increased, the resulting deflections are recorded. Post model constants used as input in simulations are calculated using the force-deflection plots created from the test results. These static values, although easily obtained, do not replicate the actual load a post in a guardrail system is subject to during a vehicular impact because the strain rates are typically much lower. The dynamic response of a post to an impact load is very complex and much more difficult to determine.

Dynamic impact tests with moving carts or pendulums more closely replicate the actual force transmission to the posts when a guardrail is impacted, thus producing more viable results. Typically these tests are performed by impacting a post, embedded in soil or fixed in a rigid base, by a pendulum or a bogie. However, for dynamic testing of posts in soil, adequate post rotation is needed in order to develop a force-deflection relationship that accurately models the common behavior of strong posts in guardrails. If the post is not allowed to rotate sufficiently and fractures or yields soon after impact, the force levels will be of shorter duration than what is commonly observed in full-scale guardrail impact tests with strong posts embedded in soil.

Due to the complexity of post / soil interaction, much effort has been devoted to the behavior of posts under lateral load. Many different aspects of the post and soil interaction have been studied in prior research projects. In 1961, General Motors, (7) studied the performance characteristics of various materials and found that reinforced concrete is undesirable for guardrail posts. However, timber and steel posts were found to be acceptable for strong and weak post designs.

In 1967, the New York State Department of Public Works (8) found that the behavior of guardrail posts directly affects the performance of guardrails. This was determined using the results of dynamic post testing. They also found that an 8 by 24 in. steel plate attached to the posts was adequate to replace a more expensive concrete footing.

In 1970, the Southwest Research Institute (9) conducted a study of the post-soil interaction behavior of guardrail posts. A total of 72 tests were conducted, both dynamic and static, using two types of soils, four embedment depths and three different posts. They found that the dynamic response of the post and the energy absorbed by the soil is directly related to the shear strength of non-cohesive soils, embedment depth, and post width. Also, the study found that the dynamic response of guardrail posts was greater than what was indicated by static tests. Results also showed that the performance of a highway guardrail system is clearly affected by the post/soil characteristics of the system.

Michie et al. (10) conducted pendulum tests to experimentally determine the performance properties of timber posts under impact loads. Steel posts were also tested for comparison with the timber posts. The posts were secured to a rigid fixture to test the post strength and not the more complex post/soil composite properties. The post dynamic peak force, average force and fracture energy were found to vary directly with the moment of inertia. Presented in Table 1 is a summary of the results obtained from the study.

Post Material	Dimensions or Specifications	Average Force (kips)	Deflection (in.)
Douglas Fir	8 x 8	9.08	11.7
Douglas Fir	6 x 8	6.84	9.8
Douglas Fir	4 x 6	3.00	9.1
Douglas Fir	4 x 4	1.78	8.9
Steel	6B8.5	7.4	9.7
Steel	3I5.7	3.58	12

Table 1. Michie post test results.

In 1974, a series of pendulum tests was performed by Gatchell (11) to evaluate the dynamic performance of wooden guardrail posts. The major finding was that specifications for timber guardrail posts based on grades or stress ratings can be eliminated. Wooden-guardrail-post specifications should be based on the amount of knot-associated grain distortion in the middle third of the tension face. Such knot-associated grain distortion should not exceed one-third the width of the tension face.

A series of 102 pendulum tests on two typical guardrail posts installed in five different soil types was performed by Calcote, et al. (12,13) of the Southwest Research Institute (SwRI) in 1978. The purpose of the tests was to determine post property variations as a function of soil conditions. The results were then used as post input properties in the BARRIER VII computer program to estimate the ultimate effect soil conditions have on guardrail performance. It was concluded that guardrail failure could be expected for severe impacts on short installations (less than 150 ft) with poor soil conditions and that guardrails of this length or shorter should not be used unless precautions are taken to ensure the integrity of each post, particularly if the available space behind the barrier is limited. It was felt that embedding the post in a concrete footing or lengthening the embedment depth in the soil could provide the necessary integrity of the posts. Shown in Table 2 are the parameters developed as a result of this study. It should be noted the force-deflection curves provided showed that the forces absorbed by the post returned to zero once the maximum force was reached. That is, no sustained force was apparent in the models developed from this post testing study.

Input Parameter		Soil and Post Type									
		Fixed Support		Base Material		Stiff Clay		Sat Clay		Sandy Loam	
		Steel	Wood	Steel	Wood	Steel	Wood	Steel	Wood	Steel	Wood
Stiffness Strong Axis	K_A k/in.	1.02	3.56	1.15	1.95	0.61	1.18	0.74	1.40	0.78	1.57
Stiffness Weak Axis	K_B k/in.	3.95	4.55	2.46	1.56	1.16	1.42	1.13	1.22	1.94	1.28
Base Yield Moment Strong Axis	M_B k-in.	353.14	339.87	231.00	172.59	125.68	108.86	71.69	73.46	138.96	107.09
Base Yield Moment Weak Axis	M_A k-in.	107.09	247.82	96.47	192.95	71.69	102.67	56.64	77.89	73.46	119.49
Shear Force Strong Axis	F_A kips	5.10	11.80	4.61	9.19	3.39	4.90	2.70	3.71	3.51	5.71
Shear Force Weak Axis	F_B kips	16.79	16.21	10.99	8.21	6.00	5.19	3.39	3.51	6.61	5.10
Max. Deflection Strong Axis	D_A in.	4.96	3.31	3.98	4.72	5.55	4.17	3.66	2.64	4.49	3.62
Max. Deflection Weak Axis	D_B in.	4.25	3.54	4.49	5.28	5.16	3.66	2.99	2.87	3.39	3.98

Table 2. Calcote post test results.

In 1983, Jeyapalan et al. (14) of the Texas Transportation Institute (TTI) conducted a study of the post/soil interaction to determine the relationship between laterally applied loads and the rotational displacements of 6 inch wide guardrail posts in dry soils. The load-displacement relationship was idealized as elastic-plastic with complete failure occurring at a post deflection of 20 in. Series of both static and dynamic tests were conducted to verify the performance capabilities of the posts. The results of the tests indicate that the steel guardrail post, embedded without a concrete footing which was required by specifications at the time, performs similarly to the timber post. The results of the dynamic testing program are presented in Table 3.

Test No.	Post Material	Soil Conditions	Impact Velocity (fps)	Maximum Force (kips)	Force at 18 in. Movement (kips)	Total Energy (ft-kips)
C1	Timber	Cohesionless	26.6	13.3	-	1.3
C2	Steel	Cohesionless	26.1	22.4	22.4	29.2
C3	Timber	Cohesive	22.7	16.3	19.2	27.2
C4	Steel	Cohesive	24.1	17.1	17.1	29.9

Table 3. Jeyapalan post test results.

In 1984, Eggers et al. (15) studied the effects of different backfill materials and concrete footings on guardrail posts. Static load tests were performed on posts in clay, sand, weathered limestone and concrete. They found that posts behaved acceptably in all conditions; however, sand or weathered limestone was recommended as a backfill material due to the ease of placing and compaction.

In 1985, Bedewi (16) conducted a series of pendulum tests to verify a simplified elastic-viscoplastic lumped parameter model for the analysis of guardrail posts in soil subjected to three-dimensional applied loads. Results from the post tests compared favorably with the results of the computer program developed.

TTI conducted static load post tests (17) in 1986 to study the effect of embedment depth, soil properties, and post type on the load-deformation characteristics of guardrail posts. They found that a successful guardrail can be designed using more posts when full embedment is not possible. Posts with only 18 or 24 inch embedment could be used at 3 ft. - $1^1/_2$ in. spacing and still produce the required strength.

In 1988 Bronstad, et al. (18) conducted 12 pendulum tests on timber and steel posts. His findings were different from the results of previous research conducted by Calcote (13). He concluded that the posts maintained significant reserve strength after the maximum load was reached when strong posts yield the soil. Bronstad used BARRIER VII computer simulations for guidance in selecting test conditions for the various transition configurations. For systems using larger posts, pendulum tests were conducted to determine post properties for BARRIER VII input. Results from testing indicated that the 18 x 24 inch soil paddle used on W6 x 15.5 posts apparently has little effect on the stiffness or maximum force, and a W6 x 15.5 post is only slightly less stiff than a 10 x 10 inch wood post but yields at greater maximum force. The results of the post testing study are summarized in Table 4.

Post Material	Size	Axis	Maximum Force	Distance d_1	Stiffness	Distance d_2	Remarks
			(kips)	(in.)	(k/in.)	(in.)	
Wood	12 x 12	NA	22.3	6.54	3.41	17.15	Soil Yield
Wood	10 x 10	NA	16.4	6.42	2.55	18.12	Soil Yield
Wood	8 x 8	NA	12.4	7.44	1.67	20.07	Soil Yield
Wood	6 x 8	Weak	9.2	4.71	1.95	NA	Post Fracture
Wood	6 x 8	Strong	8.2	5.26	1.56	15.47	Soil Yield
Steel	W6x15.5	Strong*	19.4	8.10	2.40	20.26	Soil Yield
Steel	W6x15.5	Strong	18.3	8.04	2.28	21.60	Soil Yield
Steel	W6x15.5	Weak	10.7	8.22	1.30	29.82	Post Yield
Steel	W6x8.5	Weak	4.6	3.99	1.15	13.65	Post Yield
Steel	W6x8.5	Strong	11.0	4.48	2.46	13.21	Soil Yield

* with Soil Paddles

Table 4. Bronstad post test results.

In 1988, Ataullah (19) utilized BARRIER VII for Nebraska Bridge-rail-Guardrail Transition designs. From the simulations, Ataullah calculated the post properties of the transition and found that guardrail post behavior in wet soil is not as stiff as it is in dry soil. The respective deflections were found to be considerably higher in the wet soil. The wet and dry soil parameters were calculated by multiplying the experimentally collected data by a factor of 0.75 and 0.50, respectively. Although the parameters were not obtained directly and were altered in order to be used in the simulation, the effect of moisture content on the performance of a guardrail system was evident and found to be significant. It was also found that for smooth redirection of vehicles, the impact point needed to be farther downstream from the transition for the weaker wet soil.

In 1988, Stout et al. (20) conducted static and dynamic post tests, as well as full-scale tests for guardrail designs near foreslopes to determine the effects that embedment depth, slope, and distance to slope have on the guardrail behavior. It was found that 7 ft posts could develop full strength while 6 ft posts pushed away causing the soil to displace without the post bending. They concluded that on steeper slopes, 6 ft posts should be set farther in from the break point of the slope.

3. BARRIER VII

3.1 Program Input & Output

BARRIER VII uses a formatted field input file that contains the simulation models for the guardrail and automobile. The post model is defined in the barrier section of the input file. A portion of this research is to create guardrail post models for the various conditions a post may encounter as part of a guardrail system.

The flexibility of the simulation is easily seen by the range of different inputs that are available. Seven different types of members can be specified. These include: beams, cables, columns, springs, friction damping members, viscous damping members, and posts. Each individual member's stiffness characteristics are assigned by the user. Multiple members provide for a variety of strengths and stiffnesses. Members that are more complex than the basic seven can be modeled by placing two or more of the same, or different member types in parallel. It is this flexibility that provides for the large variety of guardrail simulations that can be performed.

The vehicle is modeled as a rigid frame surrounded by a layer of springs. These springs are the possible contact points where the automobile may interact with the barrier. The stiffness values for the springs are calibrated by simulating automobile impacts with rigid walls and comparing the predicted values with measured vehicle deformations from instrumented wall research results. The automobile wheels are individually specified by points so they may be free to interact with the barrier if the vehicle body experiences large deformations. The program also allows for the brakes on the automobile wheels to be on or off, and the maximum wheel drag force or friction force may be explicitly specified for each wheel. The steer angle of the wheels may also be specified in the input data for the wheels. The last card in the input file contains the automobile position and trajectory, for which a large variety of locations, velocities or rotations may be specified.

The program provides three output files from the simulation. These ASCII text files provide the simulation results in a tabular form that can be imported into BARRIER VII post-processors, spreadsheets, or other programs.

Deflections of the barrier and the forces in the members at any time step in the simulation are provided in one of the output files. This data can be used to produce plots of deflected shapes of the barrier at any time step during the impact event. The dynamic deflections can be used to determine if the guardrail can adequately control deflections. The second output file consists of the vehicle positions, velocities, accelerations, points of contact with the barrier, and magnitudes of the normal and tangential interaction forces. Velocities and accelerations are provided in both the lateral and longitudinal coordinate directions with respect to the barrier, and the forward and sideways directions with respect to the vehicle. The velocities and accelerations can provide valuable information about occupant risk during an actual crash. The vehicle position data depicts the ability of the barrier to safely redirect the automobile back onto the roadway away from roadside obstacles. Vehicle position data, in conjunction with barrier deflections effectively predict snagging potential of the vehicle and barrier critical sections, such as transitions. The third output file presents the contents of both of the other two as well as an input echo, energy balance, and contact information in a format that is more easily read by the computer operator.

3.2 Post / Soil Interaction Model

The post/soil model for BARRIER VII, as shown in Figure 2, is similar to the model presented by Bronstad et al. (18) in 1988. This model can be broken into three parts. Initially, the force increases linearly with deflection until an elastic deflection (D_1) is reached. The force level then remains constant until a yield deflection (D_B) is reached. At this specified deflection, the post is considered to have failed and the resistance of the post thereafter is taken to be zero in ten time steps.

The stiffness (K_B) is the slope of the force-deflection model up to the yield point. The post is assumed to yield at constant load by forming a plastic hinge at its base. The yield moment (M_A) at the base of the post, is found by multiplying the sustained force level (P_B) by the interaction height of the barrier (H) or as in this research, the mounting height of the rail. The shear force (F_B) is the force necessary to fail the post in shear at the base. To ensure that the yield moment controls the behavior of a strong post, the shear force can be considered to be the sustained force increased by a shear factor. In Figure 2, this shear factor is denoted by C. For this research C was taken as 1.25. At the maximum deflection (D_B) the post is considered to fail and the load it is carrying prior to failure is transferred to the barrier in ten equal time steps following the initiation of failure. The gradual reduction to zero is performed to avoid the numerical instabilities that arise from the application or removal of 'shock load'. Even though a failed post does not contribute stiffness to the system, it does however contribute mass to the system (1,2).

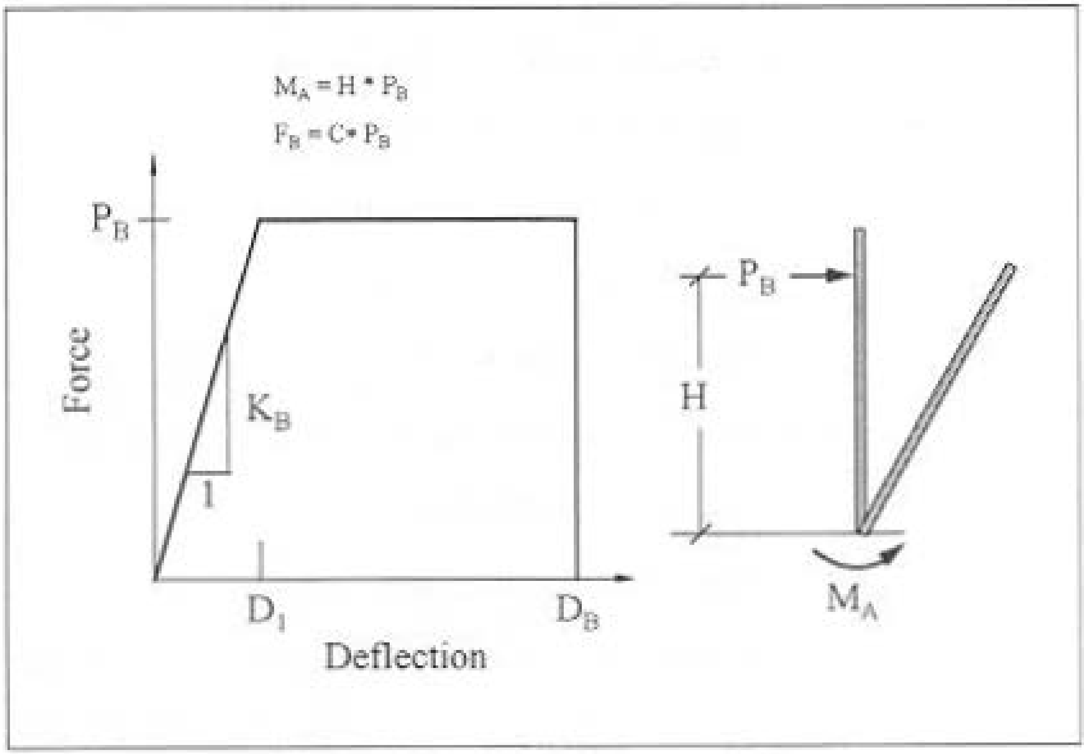

Figure 2. BARRIER VII post model.

4. Study Parameters

4.1 Scope

The original objective of the research was to determine the BARRIER VII parameters for both timber and steel 6 ft guardrail posts. The simulated steel post guardrails were to be compared with the four KSWB full-scale crash test results and validated. The steel post model, and similar timber post model could then be used in simulations to predict the strengthening effects of nesting and half-post spacing on controlling guardrail deflections under impact.

Upon review of previous tests performed on posts, and studying the results of the full-scale KSWB tests, it was necessary to expand the matrix. The original testing program was to be performed solely in the clay soil used in the KSWB tests. However, two sets of each post type were also tested in sand to determine the effect the presence of sand had on the performance of a post. Moisture content of the clay soil was included as a study variable for two reasons; (1) the KSWB full-scale crash tests were performed in clay soil with moisture contents that varied from medium to high, and (2) the moisture content of the soil is known to affect the performance of guardrail posts based on the conclusions of previous research (12,19). In addition to the above variables, $6\frac{1}{2}$ ft posts were also included in the test matrix because of the desire to use a single length post for multiple systems.

4.2 *Variables*

4.2.1 Steel and Timber Posts

The type and size of post used in a guardrail system has a direct effect on the ability of the guardrail to control deflections and to safely redirect a vehicle. This may be attributed to several reasons. Mainly, a larger area of contact that a post maintains with the soil increases its lateral load capacity in soil. Previous research indicates that the embedment depth and width of posts is directly related to the lateral resistance it offers (9,17,20). Furthermore, the cross-sectional shape and material of the post may affect the transmission of impact forces to the soil. This research investigates how these differences may exhibit themselves on the two particular post types included in this study - a 6 x 8 inch timber post and a W6x9 steel post.

The rough sawed Southern Yellow Pine 6 x 8 inch post and W6x9 steel post are used in this study because they are commonly used by various state agencies, including KDOT, for guardrail installations. Both posts are shown and described in Figures 3 and 4, respectively. The photographs were taken just prior to testing with the bogie in place to stage the impact event. Notice that the stiffness of the steel post is approximately 476 kip-in^2. This value is almost 1.5 times larger than the stiffness of the timber post, which is 309 kip-in^2.

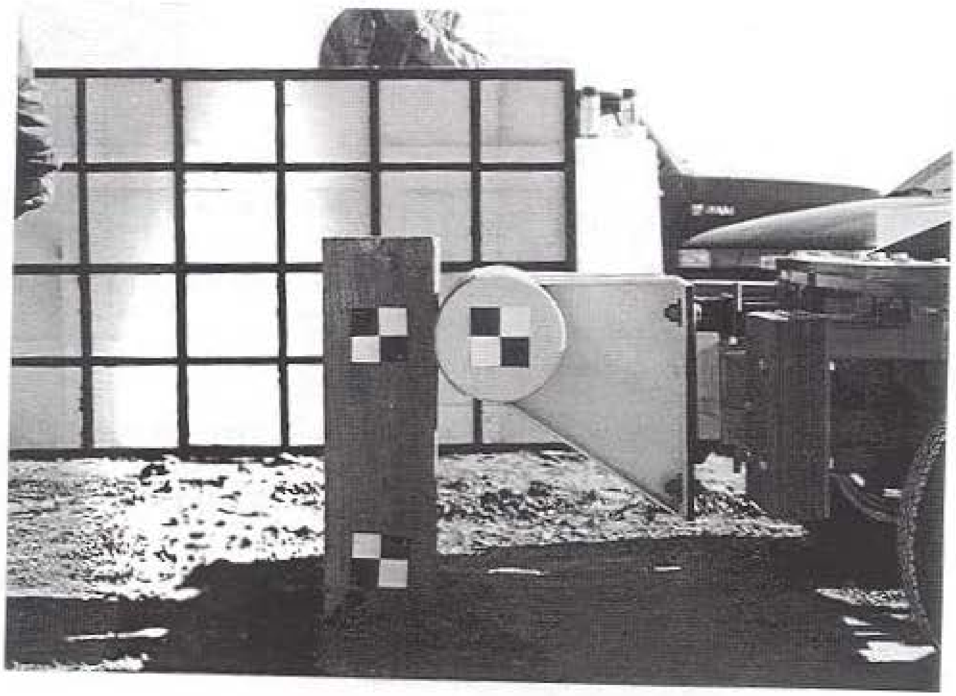

Dimensions	6 by 8 inch (Nominal)	
Material	Treated Southern Yellow Pine, Grade 2	
Density	54 plf	
Area	$A = 41.25\ in^2$	
Moment of Inertia:	Strong Axis	$I_A = 193.36\ in^4$
	Weak Axis	$I_B = 103.98\ in^4$
Modulus of Elasticity:		$E = 1600$ ksi
Stiffness	Strong Axis	$EI = 309.4$ kip-in^2
	Weak Axis	$EI = 166.4$ kip-in^2

Figure 3. Timber post photograph and description.

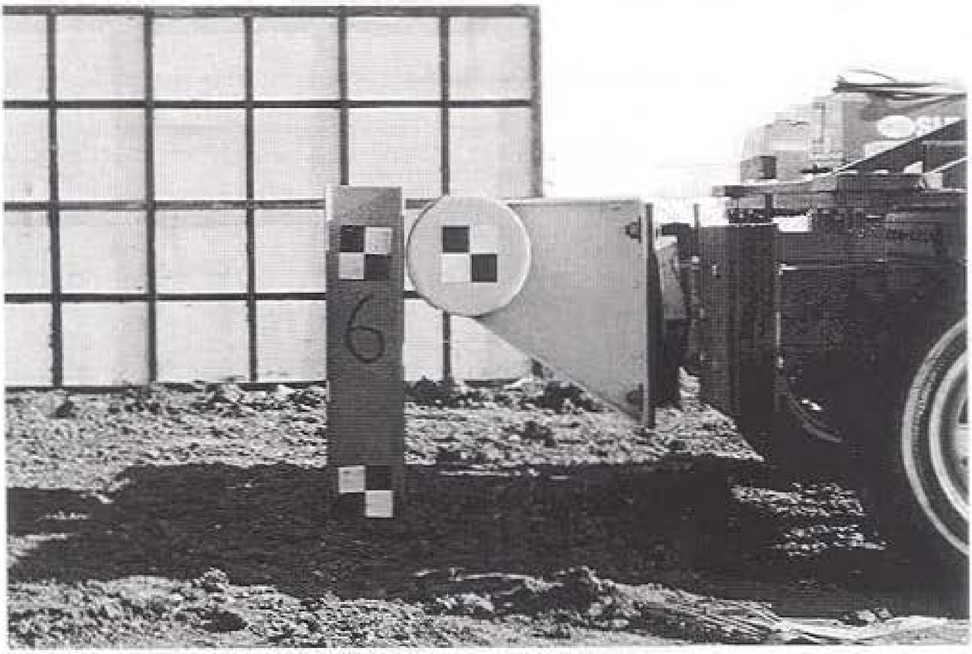

Section:	W 6 x 9	
Material:	Galvanized, A36 Mild Steel	
Dimensions:	Flange width: 3.940 in.	
	Depth: 5.90 in.	
Density:	9 plf	
Area:	$A = 2.68\ in^2$	
Moment	Strong Axis	$I_A = 16.4\ in^4$
of Inertia:	Weak Axis	$I_B = 2.19\ in^4$
Modulus of Elasticity:		$E = 29{,}000$ ksi
Stiffness:	Strong Axis	$EI = 475.6$ kip-in^2
	Weak Axis	$EI = 63.5$ kip-in^2

Figure 4. Steel post photograph and description.

4.2.2 Clay and Sand Soils

Two different soils were used for post testing in this research. A lean clay soil, classified as an A-7-6 in the AASHTO system, will be used to in order to replicate the soil conditions for the KSWB full-scale crash test series. Sand was also included in the test matrix to provide a measure of how a cohesionless soil affected the performance of a post under lateral impact load. The sand was a fine poorly graded sand, classified as an A-3 under the AASHTO soil classification system.

4.2.3 Standard and Extended Embedment Depth

Typically 6 ft posts are used for W-beam applications and $6^1/_2$ ft posts are used in Thrie-beam installations. KDOT was interested in investigating the use of $6^1/_2$ ft posts for both applications, by simply embedding the longer post 6 in. more into the ground for the W-beam guardrail installation. This changes the embedment depth from a standard 44 in. to 50 in. Studies indicate that the embedment depth of a post in soil has a direct effect on its capacity to resist lateral loads (9,19,20). As part of this research, effect of the 6 inch increase in embedment depth for a post in a low moisture content clay will be investigated.

4.2.4 Soil Moisture Content

Upon reviewing the results of the KSWB testing program, moisture content was considered to be a major factor affecting the deflections. In addition, previous research indicates that soil properties, such as soil moisture content, directly affect the performance of guardrails (9,12,19). For this reason the scope of this research was expanded to include the moisture content of the soil as a study parameter. For the clay soil, posts were tested at three different soil moisture contents; low, optimum, and high.

Standard proctor tests, presented in Appendix D, indicate an optimum moisture content for the clay of 17% with a maximum dry density of 99.9 lb/ft^3. Unconfined tests, performed at the extreme moisture contents, yielded a Young's modulus of 3000 psi and shear strength of 14.9 psi for the low moisture content (12%) clay and a Young's modulus of 500 psi and shear strength of 9.0 psi at a high moisture content (25%). The differences in these values suggest the relative performance of posts embedded in these two soils will also be different.

4.3 Test Matrix

After selection of the study parameters was completed, a test matrix was constructed. The testing matrix, shown in Table 5, consists of two different post types - timber and steel; two soils - clay and sand; two post lengths - standard 6 ft posts and extended $6^1/_2$ ft posts; and three moisture contents - low, optimum and high. Each matrix classification consisted of two tests to establish repeatability, except for PT 7.

Classification Number (PT)	Post Type	Soil Type	Moisture Content	Embedment Depth	Number of Tests
1	Timber	Clay	Low	Standard	2
2	Timber	Clay	Low	Extended	2
3	Timber	Clay	Optimum	Standard	2
4	Timber	Clay	High	Standard	2
5	Timber	Sand	Unsaturated	Standard	2
6	Steel	Clay	Low	Standard	2
7	Steel	Clay	Low	Extended	1
8	Steel	Clay	Optimum	Standard	2
9	Steel	Clay	High	Standard	2
10	Steel	Sand	Unsaturated	Standard	2

Table 5. Post testing matrix.

5. Post Testing Methodology

5.1 Test Setup

The post tests were conducted at the Midwest Roadside Safety Facility's outdoor test site located at the Lincoln Air-Park on the northwest side of the Lincoln Municipal Airport approximately 5 miles northwest of the University of Nebraska - Lincoln. The testing site is located on the south end of the facility on the 2 ft thick concrete tarmac at Pit #2. A native Nebraska soil occupies Pit #2, which is approximately 16 ft wide by 100 ft long.

A plan view of the test setup and post test soil pit is shown in Figure 5. Placement of the pit allowed for a level acceleration path for the bogie and sufficient run-out length and clearance for both the bogie and the tow vehicle. The test pit was located a sufficient distance from the edge of the concrete apron so as not to interfere with the soil response during impact.

The post testing pit shown in Figure 6 is oval in shape and approximately 36 in. wide by 75 in. long. The soil being tested occupied the entire post testing pit to a depth of approximately 60 in. Moisture content samples and sand cone compaction tests were conducted at three depths during compaction. The soil was compacted in 6 to 8 inch lifts, using a pneumatic tamper. Typical densities achieved by the tamper were 85% of the maximum dry density of clay soils at 12% moisture content and 95% of maximum dry density at 25% moisture content.

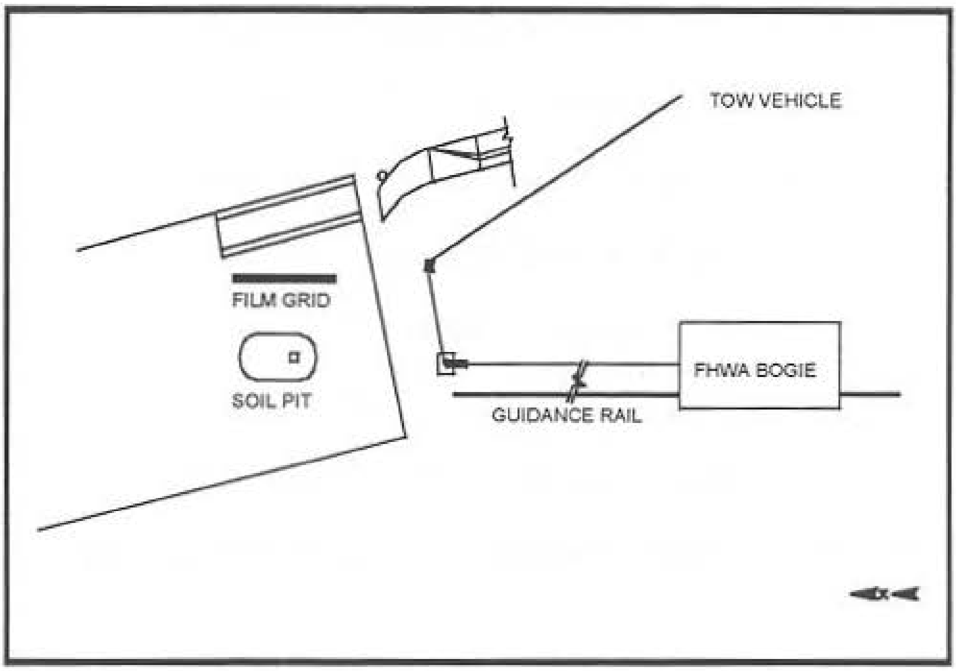

Figure 5. Plan view of the post testing site.

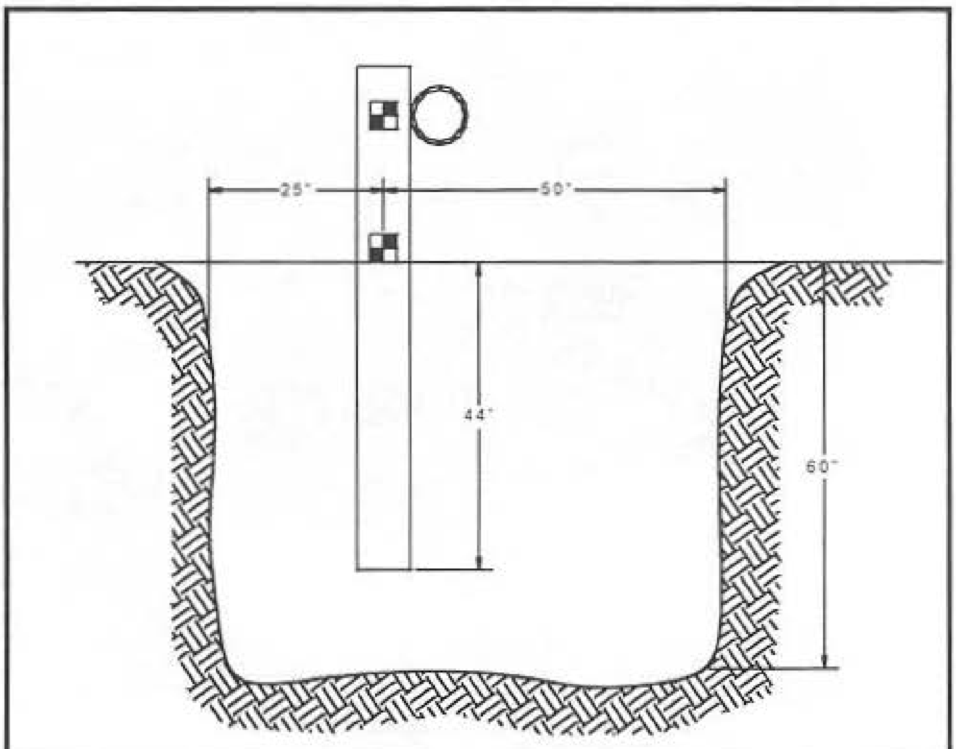

Figure 6. Cross-section view of the post testing pit.

5.2 Bogie and Test Setup

The bogie shown in Figure 7 is a rigid steel frame cart that isolates the post and soil as the primary means of absorbing the impact energy. The bogie was built according to the specifications of the bogie used at the Federal Outdoor Impact Laboratory (21). The bogie weight was set at 3060 lbs. Calculations prior to testing showed that this weight, in combination with a velocity of approximately 30 ft/sec (20 mph), would closely replicate the actual impact conditions that a post as part of a guardrail system would be subjected to in a 60 mph, 25 degree impact with a 4500 lb. sedan.

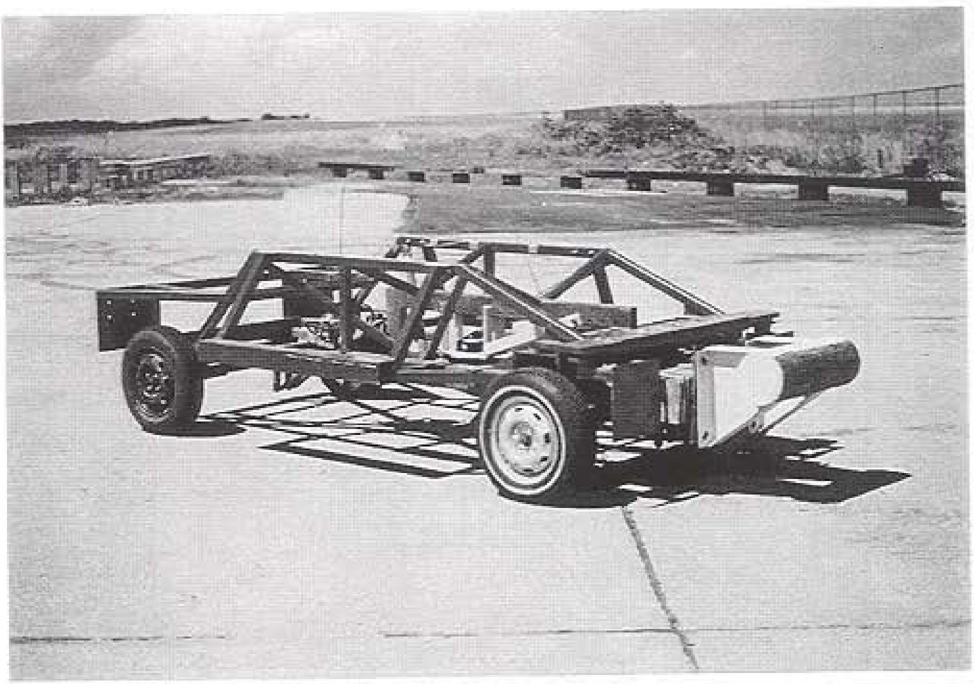

Figure 7. The MwRSF bogie.

A new bogie head was designed for the post testing program to replicate a point load on the post at the mounting height of the guardrail. The bogie head consisted of an 8 inch concrete filled standard steel pipe mounted 21 in. above the ground. A $^{1}/_{4}$ inch thick mat of belting was attached to the metal head to minimize local damage to the post from the impact. As shown in Figure 8, the head extends approximately 15 in. in front of the bogie to allow sufficient rotation of the post to take place before any other part of the bogie interacts with the post.

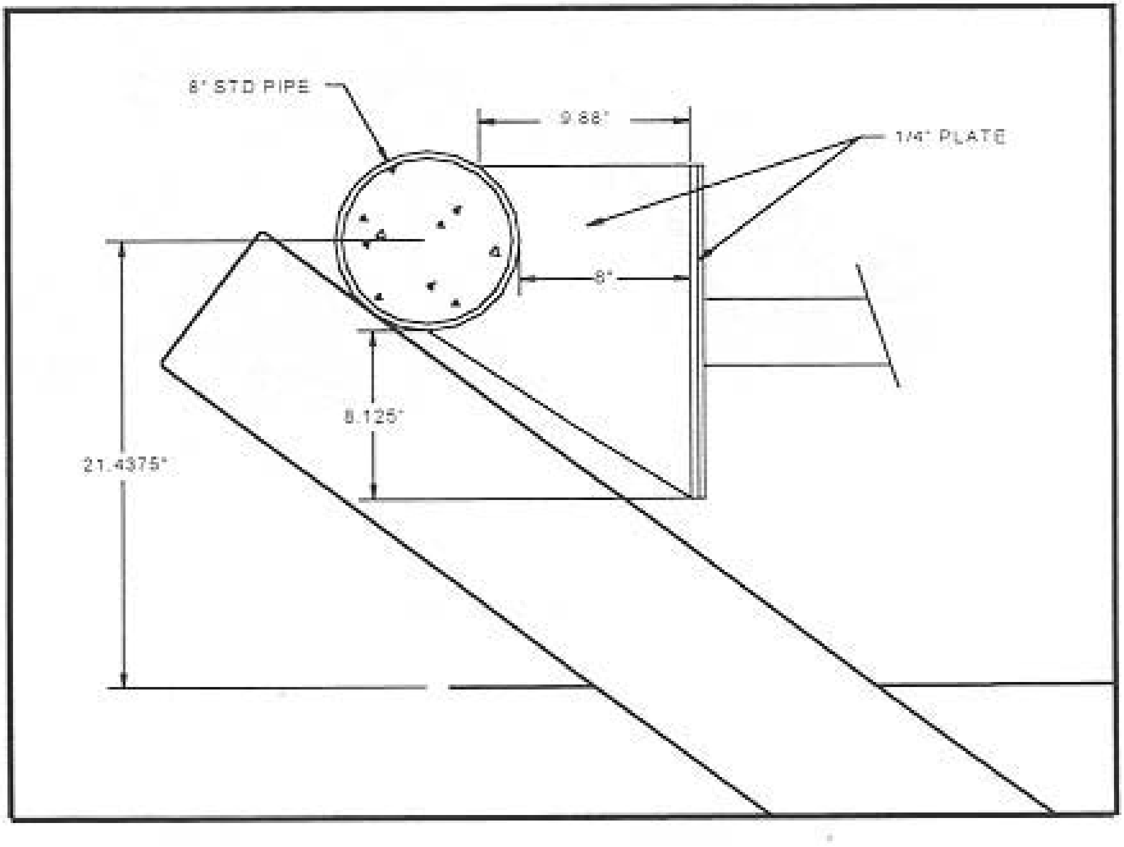

Figure 8. The post testing bogie head.

A reverse cable tow system was used to propel the test vehicle. The bogie was accelerated toward the post along a 100 ft long tracking system, which consisted of a $1^{7}/_{8}$ inch aluminum pipe that was anchored 4 in. above the tarmac. The guidance system is shown in Figure 9. Rollers attached to the underside of the bogie straddled the pipe, ensuring the proper direction and position of the bogie prior to impact.

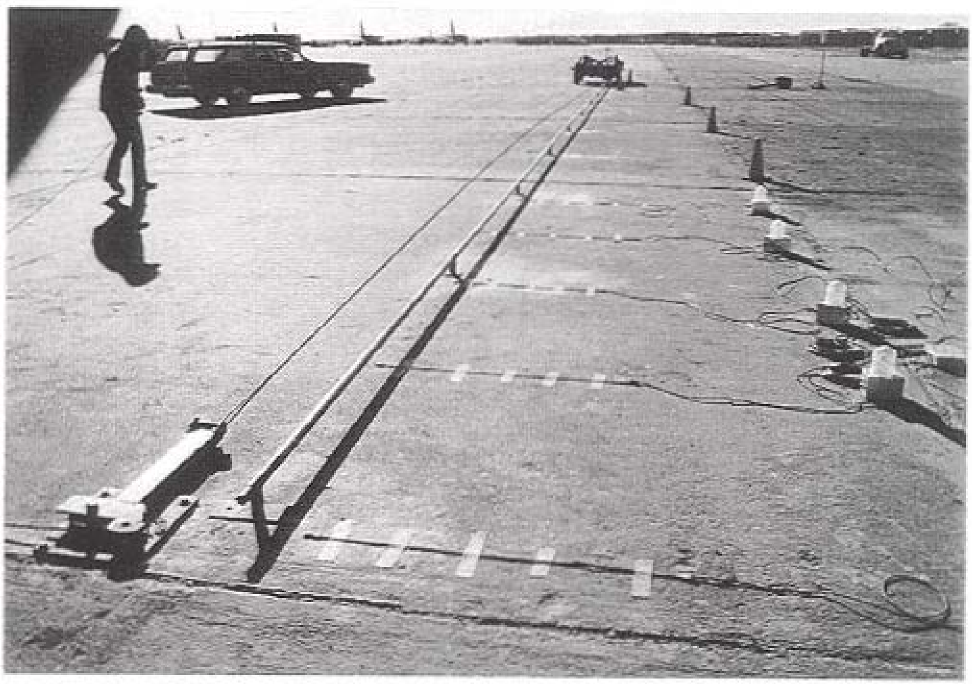

Figure 9. The post testing setup and timing strobes.

Each post test was documented by physical measurements and photographs prior to testing. The exact embedment depth, post dimensions, and post integrity (i.e. knots) were measured and recorded. The test was also documented by three cameras. A 35 mm camera provided still photographs of the site, test procedure, and the post.

A LoCam high speed camera, with a 12.5 mm - 75 mm zoom lens, recorded the impact at 250 frames per second. A grid with a 1 ft square pattern was placed in the background to provide references for the film analysis. A Super VHS Camera was also employed to provide footage for documentation and presentation purposes.

5.3 Bogie Instrumentation

In order to determine the forces transmitted to the posts during impact, the initial velocity of the bogie must be known. The impact speed of the bogie was determined using a series of pressure switches spaced at known distances adjacent to the guidance system as shown in Figure 9. As the left front tire of the bogie passes over each strip, a strobe was triggered, and an electronic timing mark was sent to a data acquisition system located in the test van. The signals were recorded for each switch on a computer using The Enhanced Graphics Acquisition and Analysis software package (22), which provides the time intervals between the signals. Using the trigger spacings and time intervals between the signals, the speed of the bogie just prior to impact could be determined accurately.

A triaxial piezoresistive accelerometer system with a range of ±200 g's was mounted on the frame of the bogie at the center of gravity. It measured the accelerations in the longitudinal direction at a sample rate of 3200 Hz. The accelerometer system known as the Model EDR-3 developed by Instrumented Sensor Technology (IST) (23) of Okemos, Michigan was configured with 256 Kb of RAM memory and a 1120 Hz filter. A laptop computer downloaded the accelerations immediately following each post test. This is the data from which the forces and deflections used in the analysis are obtained.

6. Post Testing Results

6.1 Film Analysis Data

A high speed Lo-Cam camera recorded the impact event at approximately 250 frames per second. Unfortunately, a malfunction in the high speed camera resulted in overexposed film for number of the tests. The usable film was analyzed using a VanGuard Film Analyzer to determine post deflections and rotation points, and to observe the overall behavior of the post such as pull out, fracture, and response of the soil on the surface. With the usable film, deflections were estimated using the targets placed on the side of the post. However, for most of the tests the targets were obscured by airborne soil. Therefore, an accurate determination of the position of the post was only attainable for the first 12 to 15 frames. This usually proved to be adequate in estimating the deflections and the rotation point with a high level of confidence.

The results of this analysis for a 6 ft timber post embedded in a low moisture content clay are shown in Figure 10. When the centerline of the post is drawn for each frame, an approximate rotation point can be estimated, shown as 29 in. below the surface in Figure 10. Post tests where usable film was available were analyzed in a similar manner to determine the point of rotation. The available rotation points and the ratios to the overall embedment depth for the post tests are presented in Table 6. The average point of rotation was approximately 30 in. below the ground line. This corresponds well with the commonly assumed value of 66% of the embedment depth.

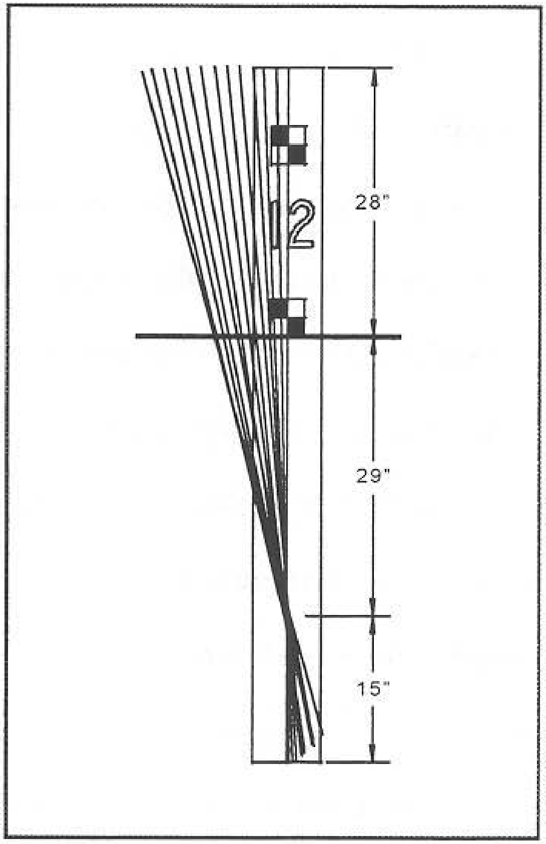

Figure 10. PT 1.1 post rotation.

Post Test (PT)	Post Number	Point of Rotation	Post Embedment	Ratio to the Embedment Depth
1.1	12	29	44	66%
1.2	13	31	44.25	70%
5.1	20	30	44	68%
5.2	21	30	44	68%
6.2	10	28	44.5	62%
7.1	11	30	50.5	60%
10.1	18	27	44.5	61%
10.2	19	32	44.5	72%

Table 6. Post rotation points.

6.2 Bogie Acceleration Data

During the impact event, the longitudinal accelerations were recorded on the EDR-3 unit at 3200 samples per second. This information was downloaded to a laptop computer and viewed to ensure the results were recorded successfully. Software known as DynaMax (DM-1) (24) extracts and processes the raw data so it can be viewed and saved as an ASCII file to be manipulated by the data analysis software, Data Analysis and Display (DaDisp) (25). Using DaDisp, the accelerometer data was filtered and force plots were created through the use of energy equations. By knowing the final speed of the bogie before impact and integrating the accelerations twice, the deflections of the post could be calculated. These deflections were verified by comparing the results with those obtained from motion analysis of the high speed film. These force and deflection data sets were then assembled into force-deflection plots for each post test and BARRIER VII post parameters were obtained. Proper idealization of the force-deflection plots was checked by comparing the energy dissipation of the force-deflection plots with that of the idealized BARRIER VII post model.

The data from test PT 1.1 is used to demonstrate in detail the procedure used to obtain the BARRIER VII post input parameters. This particular test was performed with a 6 ft long, 6 x 8 inch timber post embedded in a low moisture content (12.1%) clay. The bogie weight was 3060 lbs and impact speed was 31.3 fps.

The raw unfiltered data obtained from the EDR-3 unit for test PT 1.1 is shown in Figure 11. The data is shown with the accelerations in G's on the y-axis and time in seconds on the x-axis.

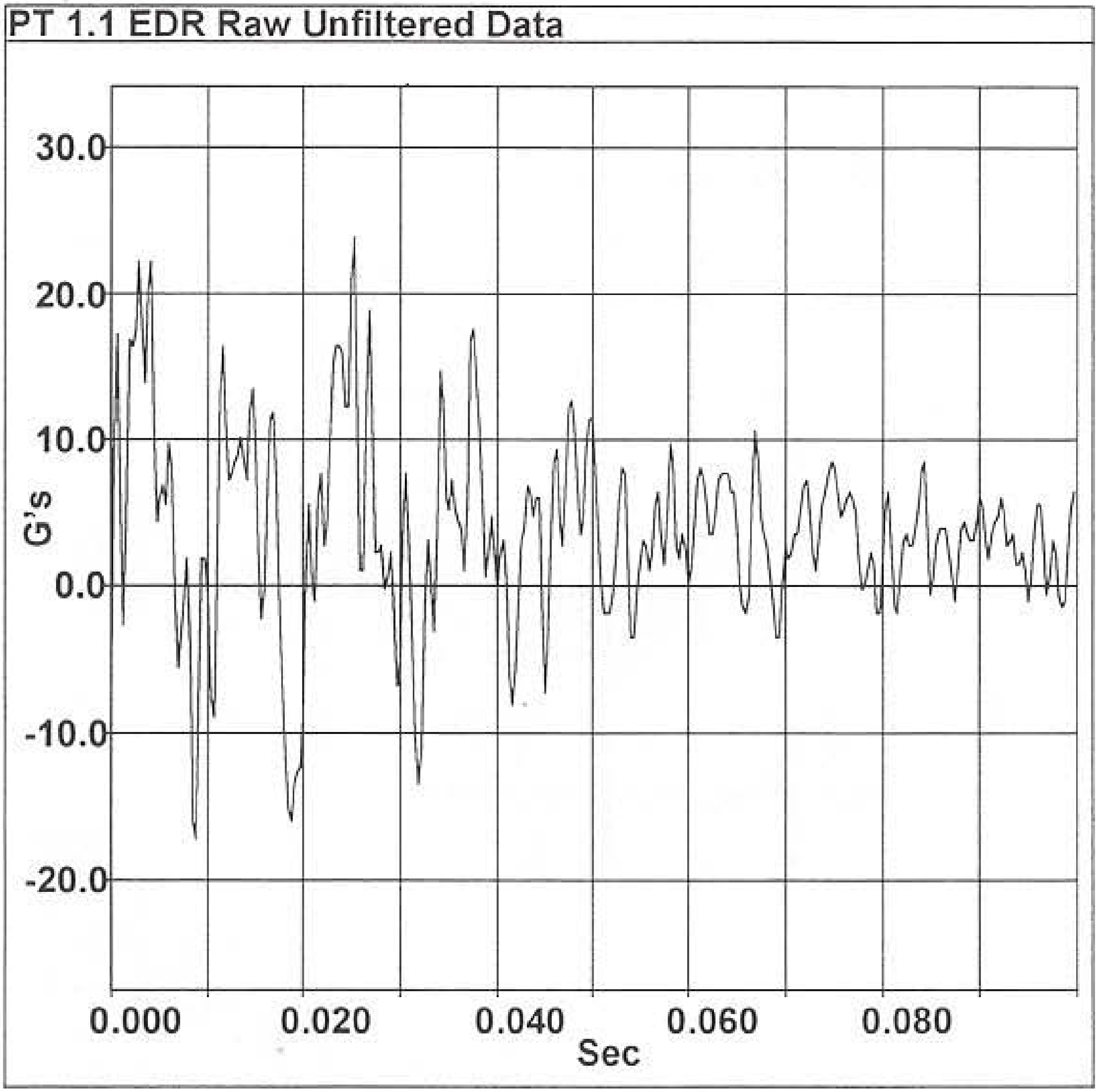

Figure 11. PT 1.1 raw data plot.

The raw data is filtered using a 90 Hz Chebychev Type II low pass filter to remove the high frequency noise. Figure 12 presents the data for test PT 1.1 after being passed through the filter. In order to obtain the forces, as shown on the *y*-axis, the accelerations are multiplied by the mass of the bogie.

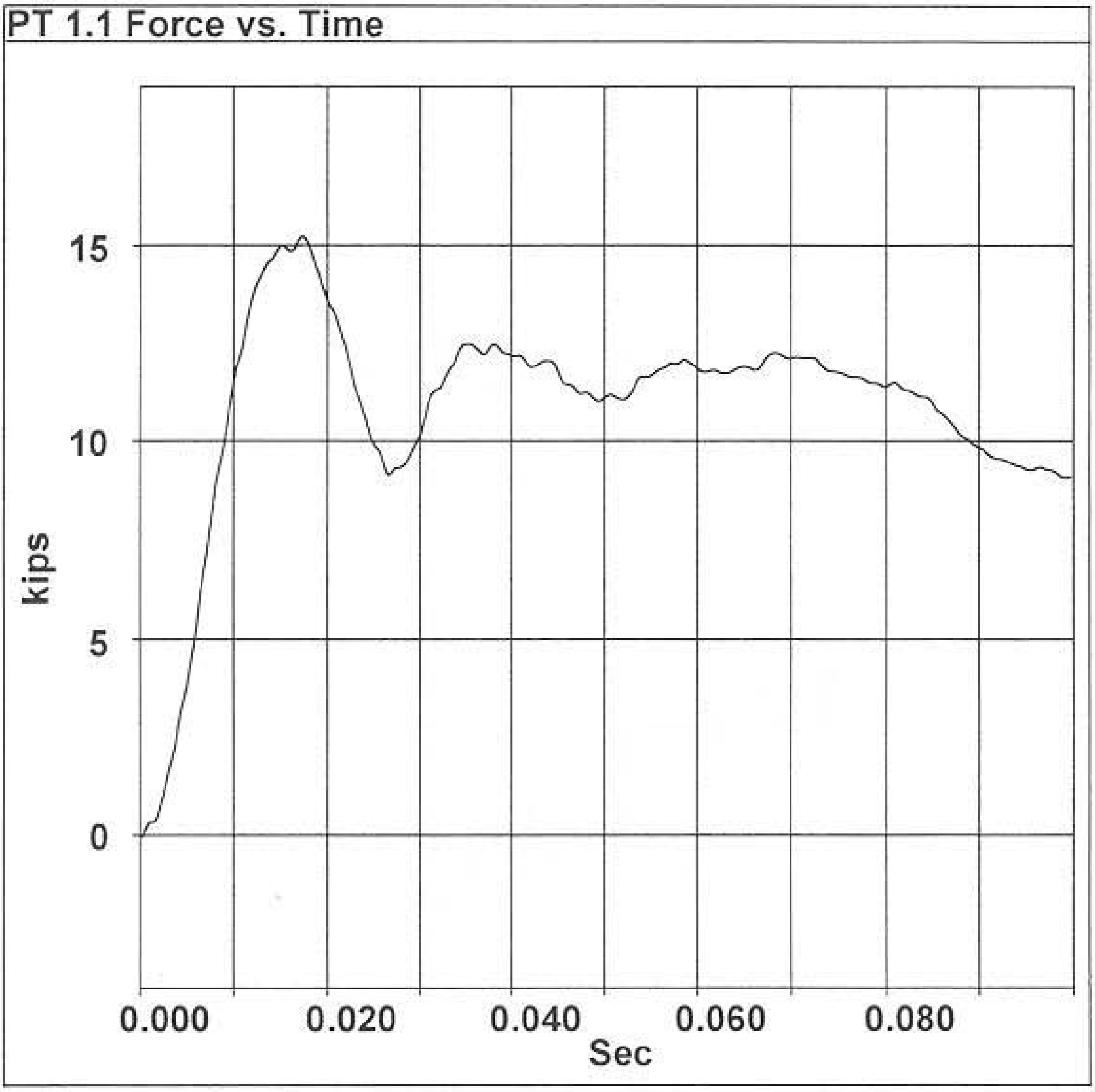

Figure 12. PT 1.1 filtered force plot.

To obtain deflections from the accelerometer plots, the data is integrated twice. A velocity plot of the bogie is created by integrating the accelerations and adding the final velocity of the bogie before impact as the integration constant. This velocity data is then integrated once more to determine the deflections, which correlated very well with the results obtained from the film analysis. The deflections calculated for test PT 1.1 are presented in Figure 13.

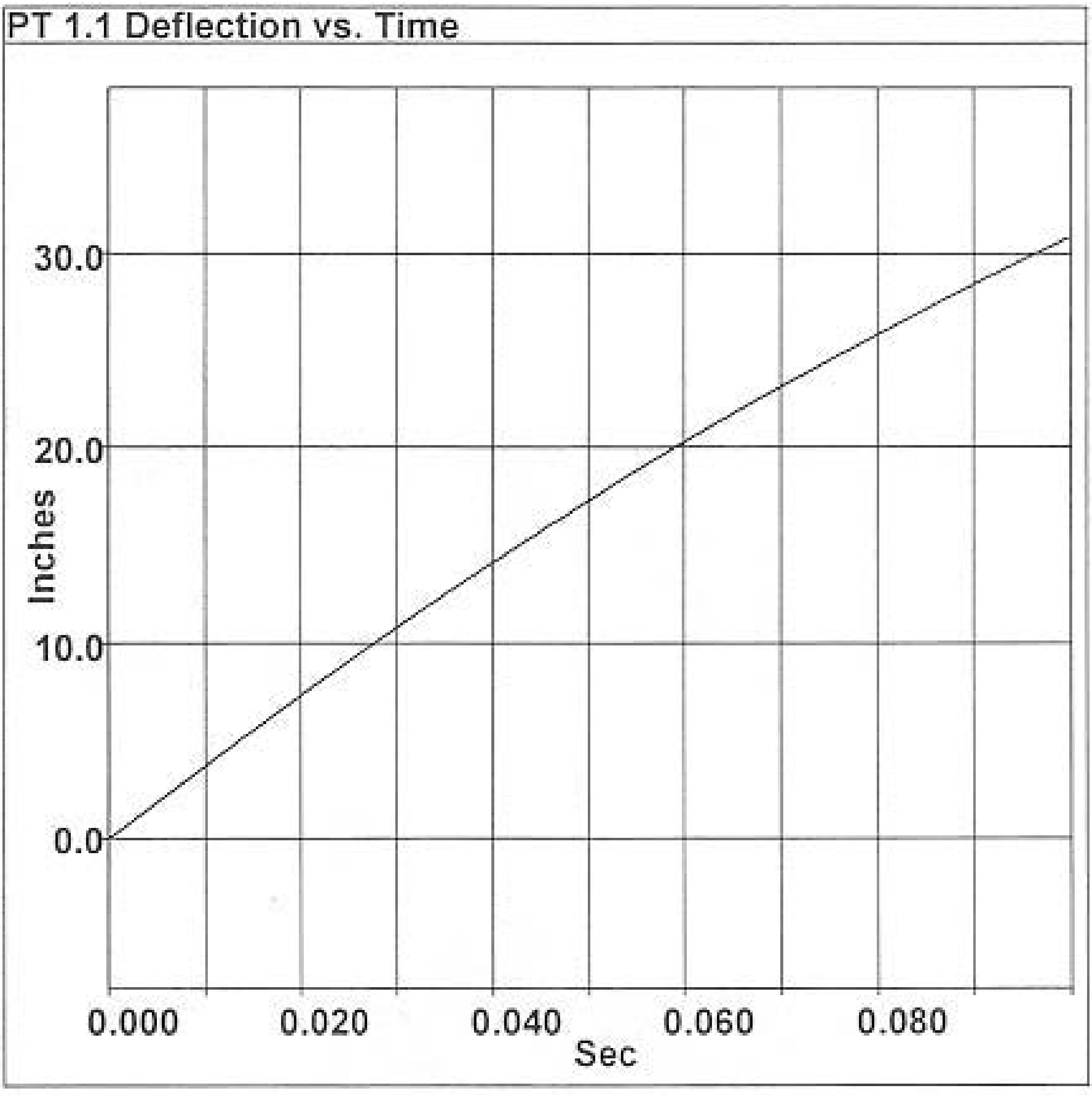

Figure 13. PT 1.1 deflection plot.

To obtain the force-deflection plot, the y-coordinates from the two previous plots are plotted against each other for each time step. Figure 14 presents the assembled force-deflection plot for test PT 1.1. Notice, the shape of the plot is similar to the BARRIER VII model illustrated in Figure 1. The force-deflection plot can now be used to determine the BARRIER VII post input properties.

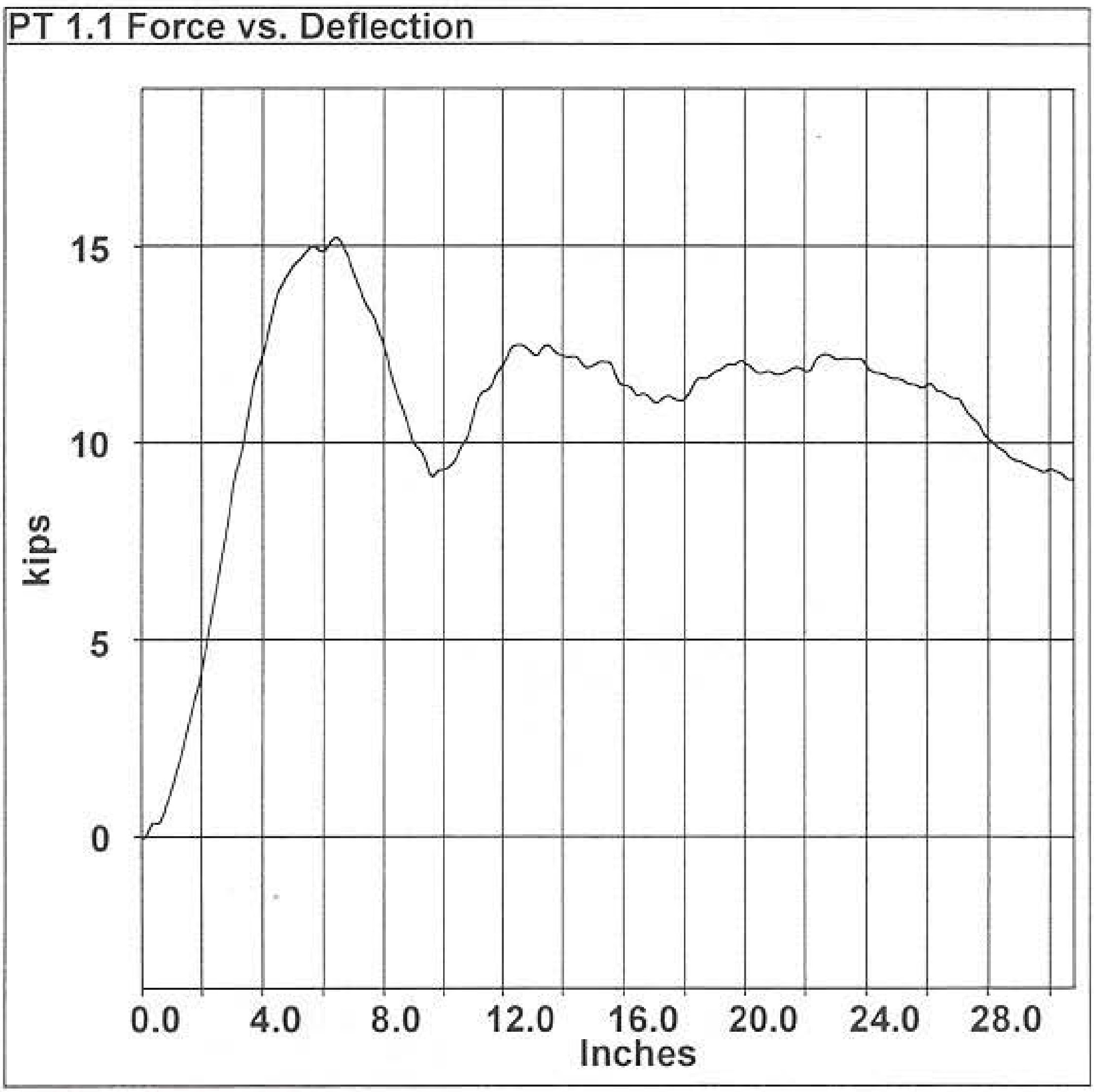

Figure 14. PT 1.1 force-deflection plot.

Using the force-deflection plots, a BARRIER VII post model was developed for each post test. The dark line in Figure 15 illustrates the approximation of the force-deflection curve for PT 1.1 that is used in the BARRIER VII post model. Similar models of the force-deflection curves for all other post tests can be found in Appendix A.

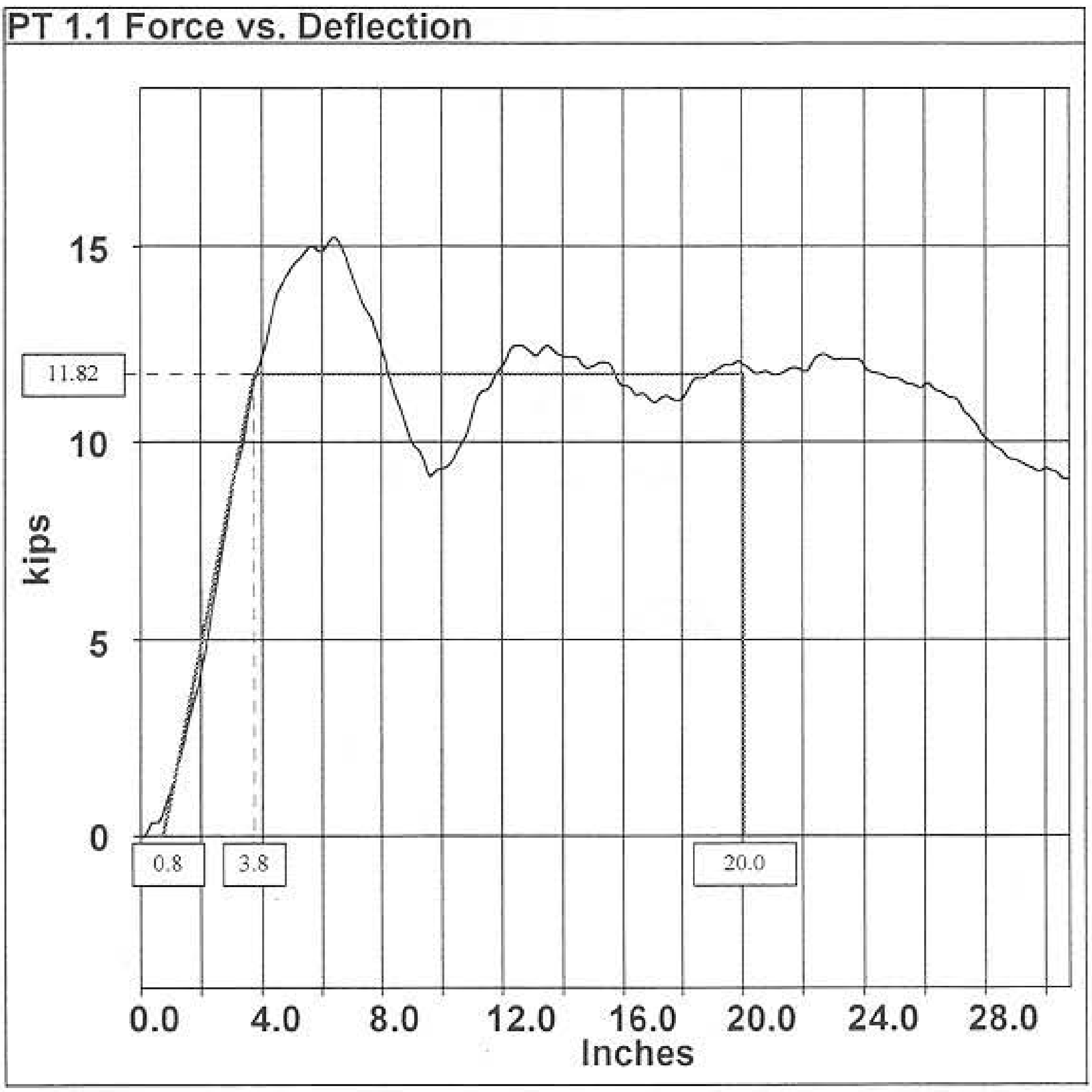

Figure 15. PT 1.1 BARRIER VII force-deflection analysis.

The BARRIER VII model was developed by matching the impact energy of the model with that of the force-deflection curve. If the areas of both the model and the force-deflection curve are similar, the impact energy is maintained. Hence, the post model shown in Figure 15 was constructed by ensuring that the area underneath the trapezoidal model was equivalent to the area underneath the actual curve.

The values that describe the post model in Figure 15 are listed in Table 7. The initial deflection, D_1, is the deflection at which point the force level is considered to level off. In Figure 15, D_1 can be estimated as 3 in. The sustained force level, F_B, is also determined as approximately 11.82 kips. Finally, a maximum deflection must be selected for the post model. Once the post has rotated a certain amount, the bolt becomes detached from the guardrail, and it no longer provides resistance to the impacting vehicle. At this point, judged to correspond with a deflection of 20 in. in this case, the post is no longer an acting part of the system, so its force is dropped to zero.

Elastic Deflection	Average Force	Final Deflection
(in.)	(kips)	(in.)
3.0	11.82	20.0

Table 7. PT 1.1 post model analysis results.

The stiffness parameter, K_B, is the slope of the line up to the initial deflection, D_1, calculated as F_B / D_1. For this example, K_B is 3.94 kip/in. (11.82 kip / 3.0 in.). The yield moment, M_A, is calculated as the force multiplied by a moment arm, whereby the moment arm is simply the height above the grade at which the rail is connected to the post, and in this guardrail, is taken to be 21 in. Hence, the yield moment is 248.22 k-in. (11.82 kips x 21 in.).

All force-deflection plots were analyzed in a manner similar to the one described above, from which a collection of parameters was developed.

7. Post / Soil Modeling and Validation

7.1 Force-deflection Data Analysis

The parameters obtained from an analysis of the force-deflection plots for each particular post test are listed in Table 8. The BARRIER VII models from which these were obtained are presented in Appendix A.

Post Test (PT)	D_1 (in.)	D_F (in.)	P_B (kips)	K_B (k/in.)	M_A (k-in.)	F_B (kips)	D_B (in.)
1.1	3.0	20.0	11.82	3.94	248.22	14.78	20.0
1.2	3.7	20.0	10.82	2.92	227.22	13.53	20.0
2.1	3.7	10.0	10.72	2.90	225.12	13.40	10.0
2.2	6.4	20.0	13.56	2.12	284.76	16.95	20.0
3.1	4.9	20.0	13.63	2.78	286.23	17.04	20.0
3.2	3.0	20.0	5.56	1.85	116.76	6.95	20.0
4.1	2.4	20.0	4.77	1.99	100.17	5.96	20.0
4.2	5.1	15.0	4.84	0.95	101.64	6.05	15.0
5.1	2.4	20.0	6.44	2.68	135.24	8.05	20.0
5.2	2.5	20.0	2.49	1.00	52.29	3.11	20.0
6.1	3.5	20.0	9.85	2.81	206.85	12.31	20.0
6.2	3.3	20.0	8.55	2.59	179.55	10.69	20.0
7.1	4.1	20.0	10.76	2.62	225.96	13.45	20.0
8.1	2.2	20.0	11.29	5.13	237.09	14.11	20.0
8.2	2.1	20.0	8.31	3.96	174.51	10.39	20.0
9.1	5.8	20.0	4.44	0.77	93.24	5.55	20.0
9.2	3.5	20.0	4.88	1.39	102.48	6.10	20.0
10.1	2.4	20.0	5.97	2.49	125.37	7.16	20.0
10.2	2.2	20.0	4.43	2.01	93.03	5.54	20.0

Table 8. Post test analysis results.

Upon comparison of the post test results, several tests were assumed to be outliers and were omitted from the final collection of parameters. The remaining tests were synthesized into a table with a set of constants for each test classification. Table 9 lists the BARRIER VII post parameters from this synthesis and are the actual values used in the KSWB simulation efforts presented in the applied results. The applicable Bronstad (18) test results listed in Table 4 compare favorably with those list here.

Class (PT)	Post Type	Moisture Content (%)	Embedment	Soil Type	Stiffness (k/in.)	Yield Moment (k-in.)	Maximum Deflection (in.)	Shear Force (kips)
1	Timber	Low	Standard	Clay	3.43	237.72	20.00	14.15
2	Timber	Low	Extended	Clay	2.51	254.94	15.00	15.18
3	Timber	Optimum	Standard	Clay	2.78	286.23	20.00	17.04
4	Timber	High	Standard	Clay	1.47	100.91	17.50	6.01
5	Timber	Unsaturated	Standard	Sand	2.68	135.24	20.00	8.05
6	Steel	Low	Standard	Clay	2.70	193.20	20.00	11.50
7	Steel	Low	Extended	Clay	2.62	225.96	20.00	13.45
8	Steel	Optimum	Standard	Clay	4.54	205.80	20.00	12.25
9	Steel	High	Standard	Clay	1.08	97.86	20.00	5.83
10	Steel	Unsaturated	Standard	Sand	2.25	109.20	20.00	6.50

Table 9 BARRIER VII post input parameters.

7.2 *Moisture Content Relationships*

Plots of the post parameters vs. the moisture content of the clay were also developed to establish a relationship between the two. For example, in Figure 16, the yield moments, M_A, for the steel posts in clay soil were plotted against the corresponding moisture contents and a curve was fitted to the data. The shape of the curve is similar to that of the proctor curve shown in Appendix D. This suggests a direct relationship between the post parameter and the density of the soil. Notice the maximum yield moment for the post occurs around 16% moisture content. This roughly agrees with a measured optimum moisture content of 17%. Also, notice that the high moisture content clay yields the lowest M_A values. Results were similar for the timber post and are presented in Appendix E.

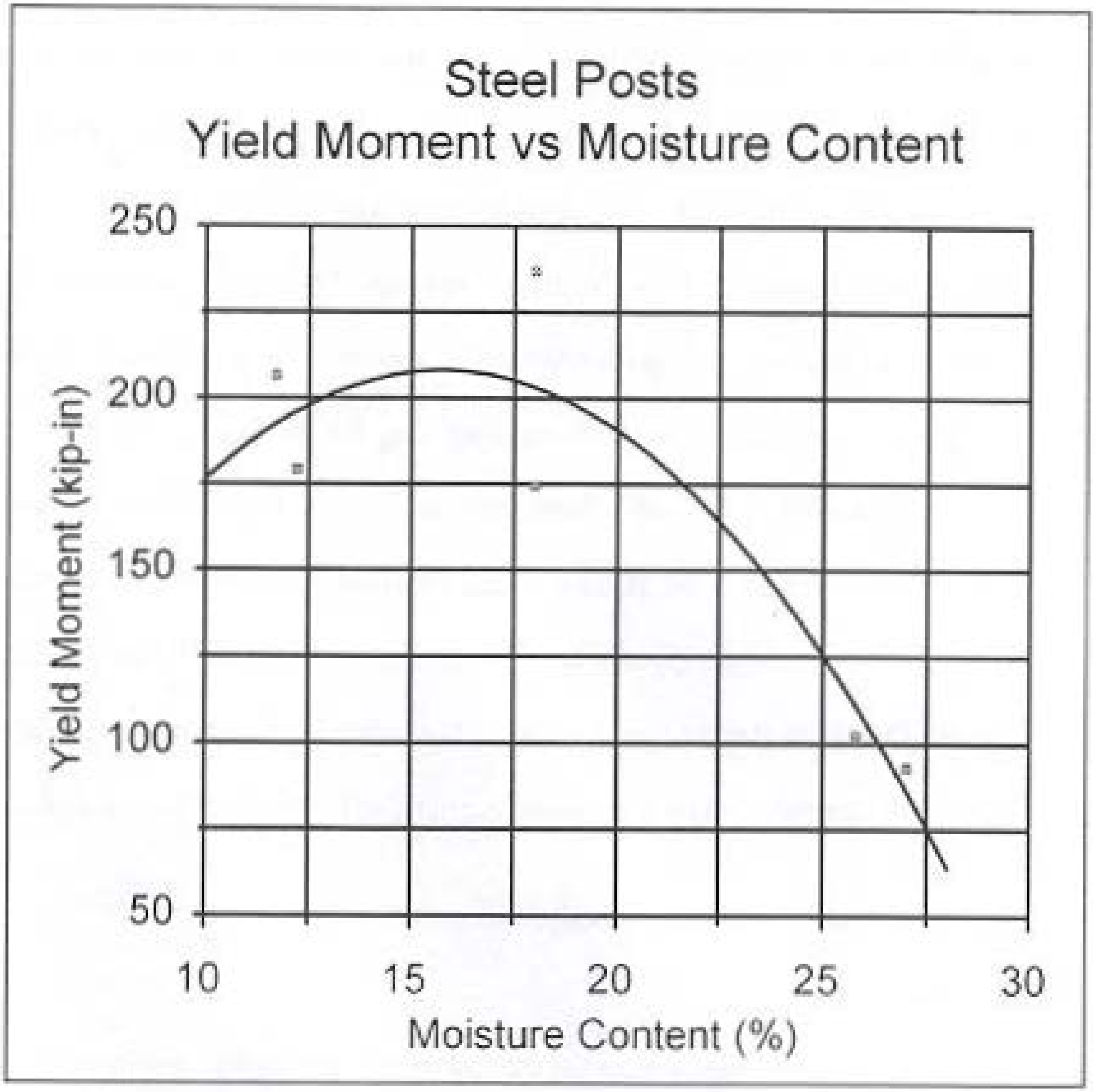

Figure 16. Moisture content relationship vs. yield moment for a steel post.

7.3 Kansas W-beam (KSWB) Full-scale-Tests

In 1993, Holloway et al. (26) conducted full-scale crash tests to evaluate the effect of nested W-beams and half-post spacing on the performance of Kansas W-beam guardrail systems (KSWB). The four test installations that were evaluated consisted of: (1) a single W-beam with 6 ft - 3 in. post spacing; (2) a nested W-beam with 6 ft - 3 in. post spacing; (3) a single W-beam with 3 ft - $1^1/_2$ in. post spacing; and (4) a nested W-beam with 3 ft - $1^1/_2$ in. post spacing. The target impact conditions for all four tests consisted of using a 4500 lb sedan impacting the guardrails at 60 mph and 25 degrees. All installations were constructed using 6 ft steel posts in a clay soil.

The KSWB tests were conducted and reported in accordance with the requirements specified in the *Recommended Procedures for the Safety Performance Evaluation of Highway Appurtenances*, National Cooperative Highway Research Program (NCHRP) Report No. 230 (27). The safety performance of each guardrail system was determined to be acceptable according to the NCHRP Report 230 criteria.

7.3.1 Full-Scale Crash Test Descriptions and Results

KSWB-1

KSWB-1 was the baseline for the four tests. The overall layout of the system installation is shown in Figure 17. The first test was conducted with full post spacings (6 ft - 3 in.) and 175 ft (seven - 25 ft sections) of single 12 gauge W-beam mounted at a height of 21 in (height to post bolt).

A total of 29 posts were in the guardrail system. Posts 3 through 27 consisted of 6 ft long W6x9 steel posts with W6x9 steel spacer blocks. While posts 1, 2, 28, and 29 were 3 ft - $6^1/_2$ in. long, $5^1/_2$ x $7^1/_2$ inch timber breakaway posts. The W-beam guardrail was anchored on both ends with a standard breakaway cable terminal (BCT). Steel backup plates were placed between the guardrail and the posts at all non-splice locations. All posts were installed by auguring holes and backfilling with the native clay soil.

This test was conducted with a 4,399 lb sedan at an impact speed of 61.9 mph and impact angle of 25.1 degrees. The impact location was approximately 12 ft upstream of post 15. These impact conditions correspond to an impact severity of 101.4 kip-ft. The film analysis results for the test indicated the vehicle had an exit speed of 40.1 mph and an exit angle of 14.5 degrees. The maximum dynamic deflections were also estimated from the film analysis and are presented in Figure 18 with the permanent set deflections measured directly in the field. The overall maximum dynamic post deflection was estimated to be 28.0 in. at post 15 and the maximum permanent set post deflection was measured as 23.0 in. at the same post. Posts 15 and 16 were disengaged from the system and post 15 was permanently twisted. There was also a small tear in the W-beam at post 15.

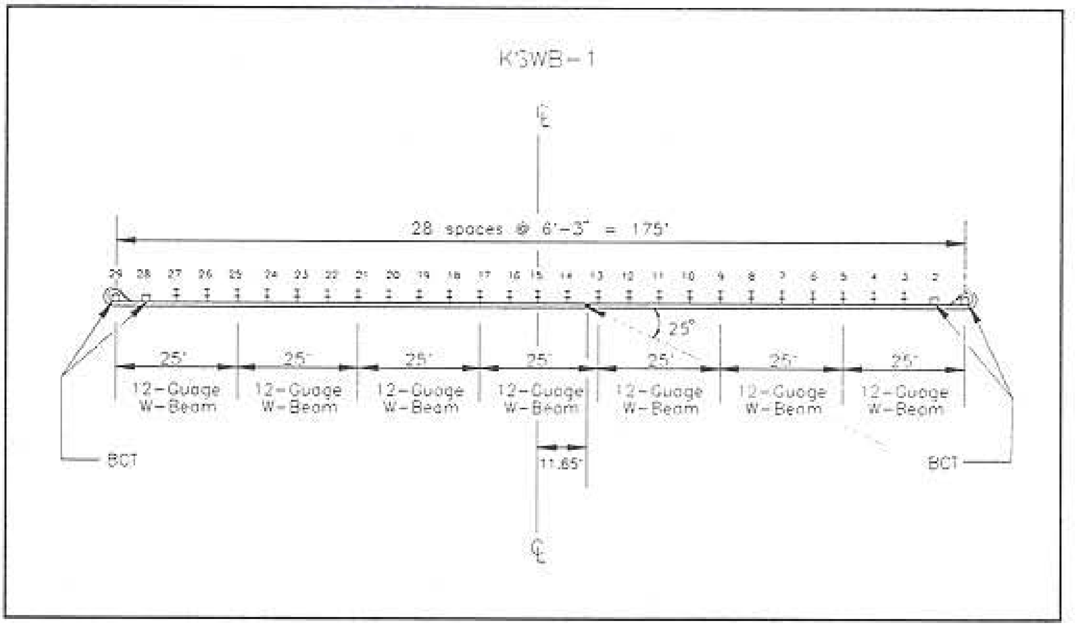

Figure 17. Plan view of KSWB-1 guardrail installation.

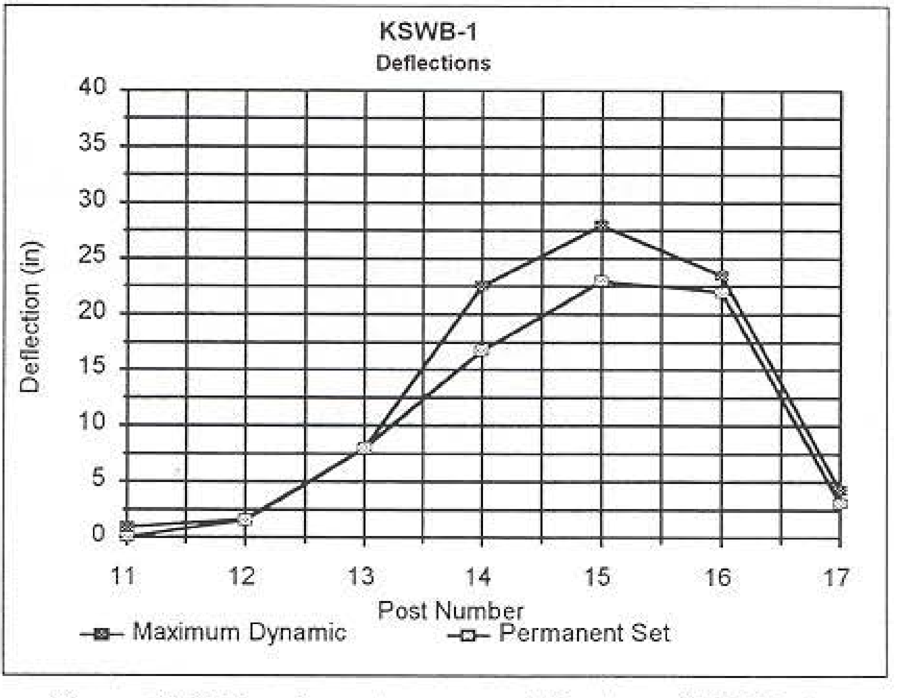

Figure 18. Full-scale crash test post deflections of KSWB-1.

KSWB-2

The second test in the series as shown in Figure 19 was constructed using the normal 6 ft - 3 in. post spacing with nested W-beam. The two end 25 ft sections of the installation consisted of a single layer of W-beam and only the five inner sections were nested. Only the inner sections were strengthened because that was the area of concern. Also, the length of modified guardrail met NCHRP 230 specifications (27) for minimum test lengths. Twenty-nine posts were used in constructing this system. Post and rail installation details are the same as previously discussed for KSWB-1.

A vehicle weighing 4,486 lbs impacted the system at 60.5 mph and 25.4 degrees, approximately 12 ft upstream of post 15. The impact severity for this test was 101.0 kip-ft. The vehicle exited the installation with a speed of approximately 52.6 mph and an angle of 12.9 degrees. The maximum dynamic and permanent set deflections are shown in Figure 20. The maximum dynamic deflection was estimated to be 35.5 in. between posts 14 and 15. The maximum dynamic post deflection occurred at post 14 and was 32.5 in. The maximum permanent set deflection of 24.8 in. occurred at the same post. None of the posts disengaged from the system although post 15 was permanently twisted and contained visible markings resulting from contact with the vehicle.

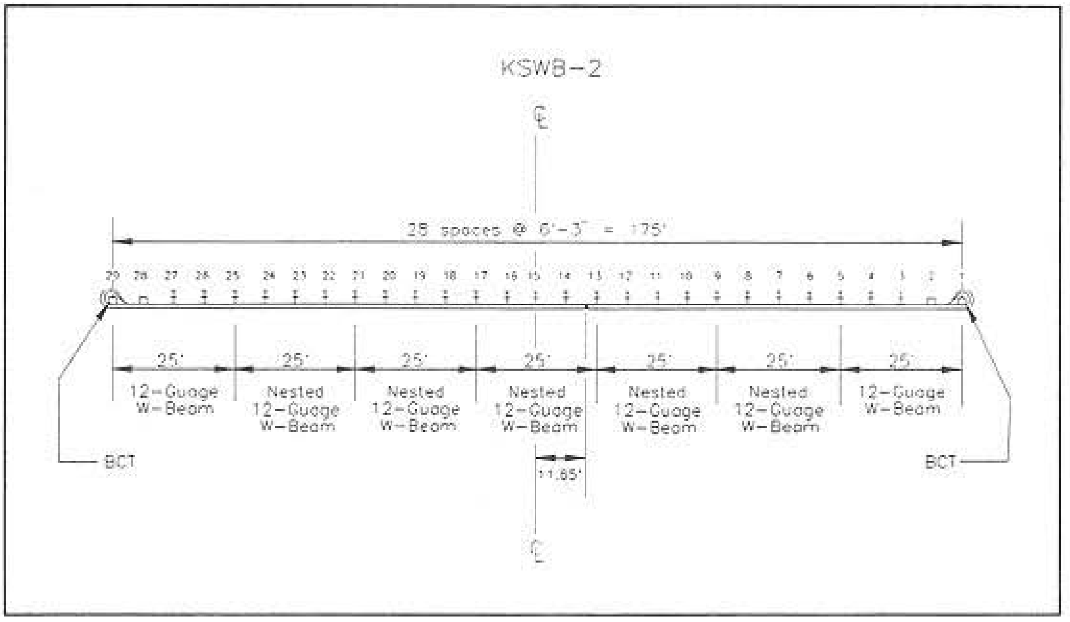

Figure 19. Plan view of KSWB-2 guardrail installation.

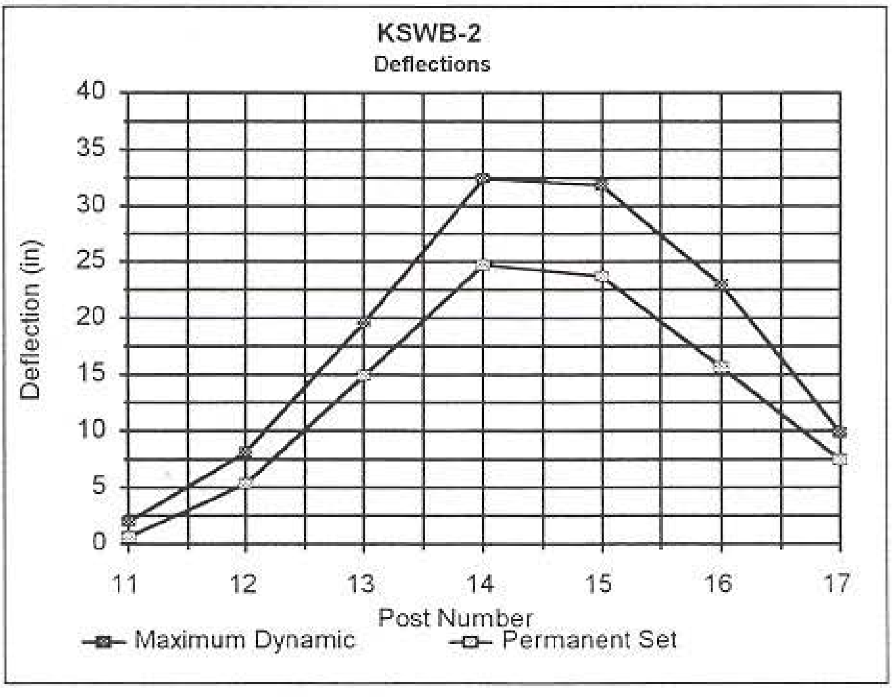

Figure 20. Full-scale crash test post deflections of KSWB-2.

KSWB-3

The third system in the series as shown in Figure 21 used a single W-beam and half-post spacings (3 ft - $1^1/_2$ in.). As before, only the middle five sections employed the strengthening technique of half-post spacings. The total number of posts used in the installation was 49. Post 3 through 47 were 6 ft long W6x9 steel posts with W6x9 steel spacer blocks. Posts 1, 2, 48, and 49 were 3 ft- $6^1/_2$ in. long $5^1/_2$ x $7^1/_2$ inch timber breakaway posts. Steel backup plates were placed between the guardrail and the posts at all non-splice locations. All other pertinent details are the same as previously discussed.

Test KSWB-3 was conducted using a 4,486 lb vehicle impacting the guardrail at 59.7 mph and at an angle of 24.8 degrees. Impact occurred at a point approximately 12 ft upstream of post 25. The impact severity for this test was 94.0 kip-ft. The vehicle exited the guardrail with a speed and angle of 46.1 mph and 9.6 degrees, respectively. The maximum dynamic and permanent set deflections of the posts are illustrated in Figure 22. A maximum dynamic post deflection of 23.5 in. occurred at post 24. The maximum permanent set post deflection of 20.3 in. occurred at the same post. None of the posts were disengaged from the system although posts 24 through 26 contained permanent deformations and marks near the bottom of the posts resulting from contact with the vehicle. Guardrail damage consisted of only moderate deformation and flattening of the lower portion of the impacted 25 ft W-beam section.

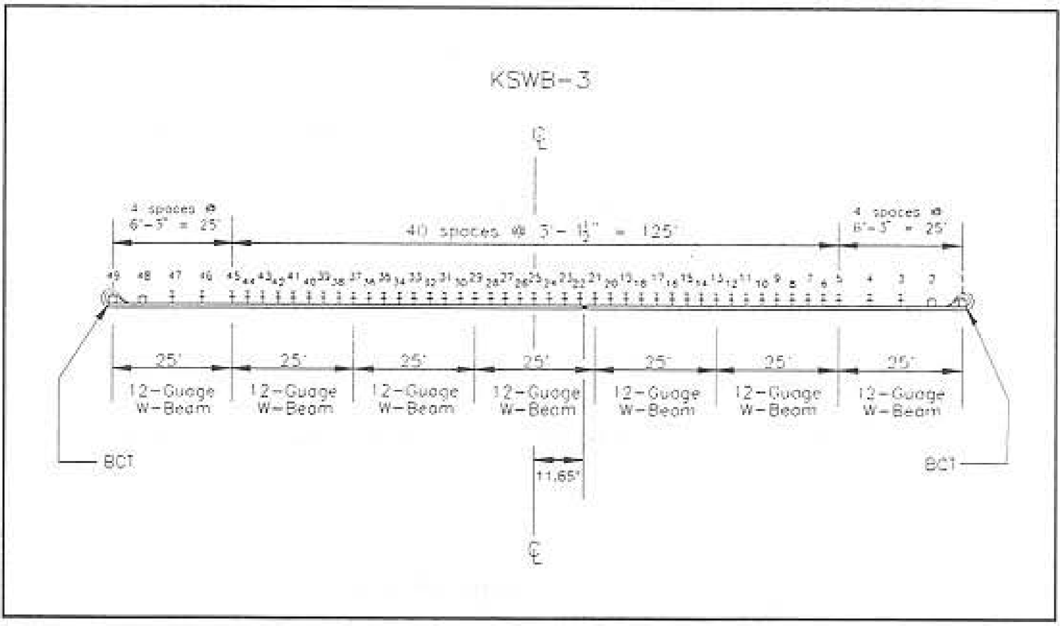

Figure 21. Plan view of KSWB-3 guardrail installation.

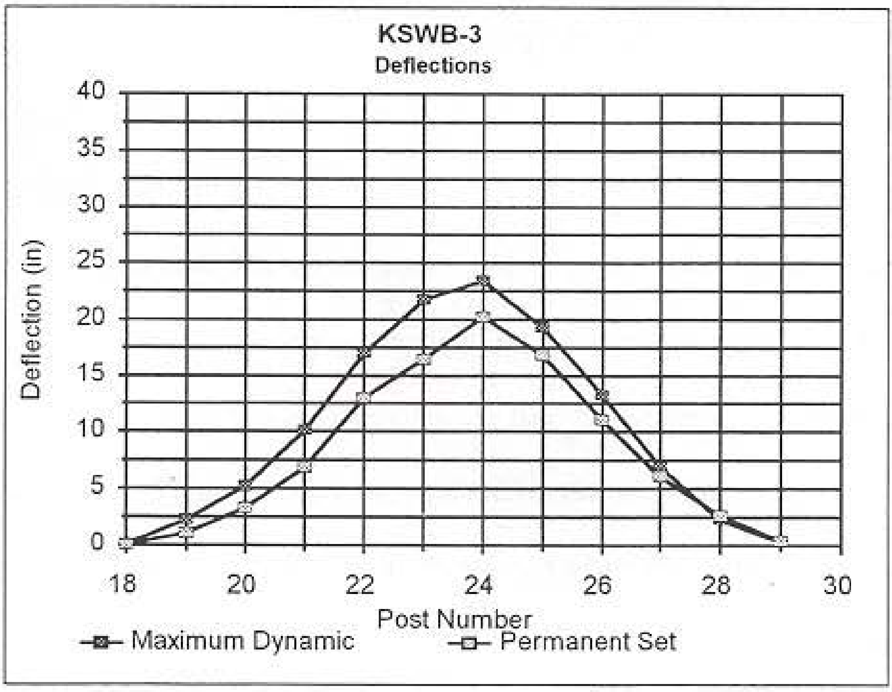

Figure 22. Full-scale crash test deflections of KSWB-3.

KSWB-4

The last system in the series as, shown in Figure 23, employed both strengthening techniques - half-post spacing and nested W-beam. These modifications were also only applied to the middle 5 sections. Forty-nine posts were also used in this installation. The post and rail details are the same as previously discussed in KSWB-3.

Test KSWB-4 used a 4,501 lb vehicle with an impact speed and angle of 60.4 mph and 28.4 degrees, respectively. The vehicle impacted the guardrail approximately 12 ft upstream of post 25. The impact severity for this impact was 124.2 kip-ft. The vehicle left the system with a speed of 46.8 mph and an exit angle of 14.1 degrees. The maximum dynamic and permanent set post deflections are presented in Figure 24. A maximum dynamic deflection of 19.6 in. occurred between post Nos. 23 and 24. The maximum dynamic deflection for a post was 17.6 in. at post 23. The maximum permanent set was measured as 15.9 in. at post 24. Post 24 pulled away from the guardrail, and posts 23 through 25 sustained permanent deformations and marks near the bottom of the posts resulting from contact with the vehicle.

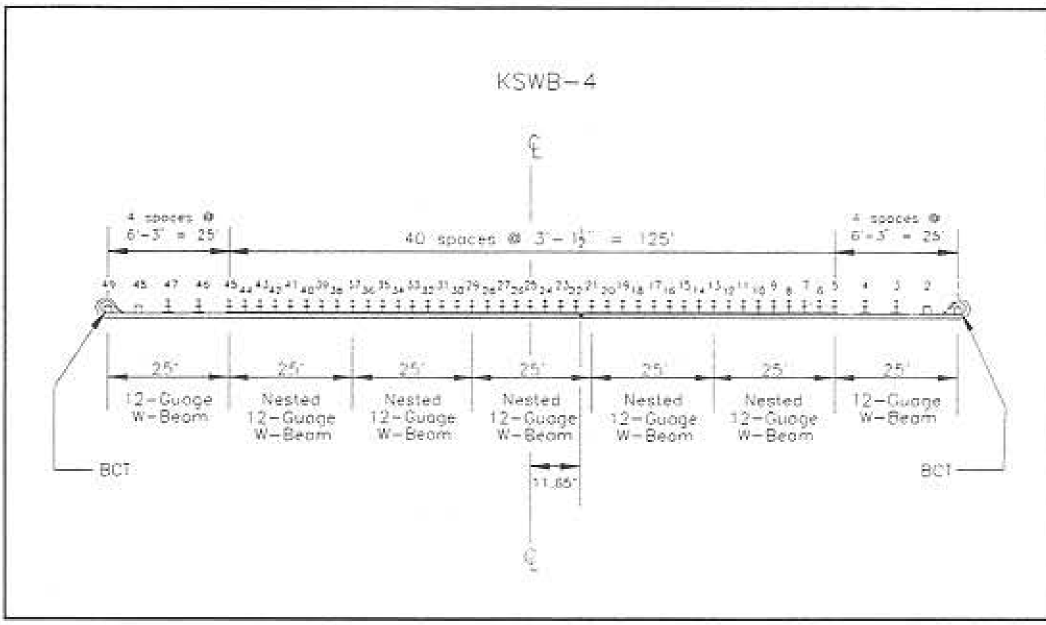

Figure 23. Plan view of KSWB-4 guardrail installation.

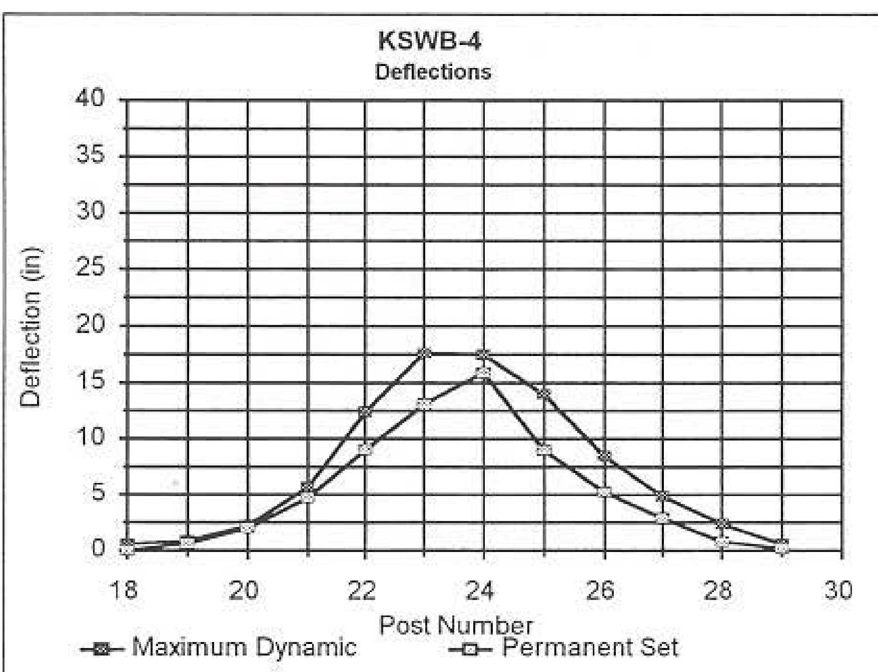

Figure 24. Full-scale crash test deflections of KSWB-4.

A summary of the post deflection results for all four KSWB tests is presented in Table 10. Included in the table are the impact severities, which provide a measure of the lateral impact energy with which the vehicle strikes the guardrail.

Test Designation	KSWB-1	KSWB-2	KSWB-3	KSWB-4
Impact Severity (kip-ft)	101.1	101.0	94.0	124.0
Maximum Dynamic Deflection (in.)	28.0	32.5	23.5	19.6
% Difference from KSWB-1	0.0%	16.1%	-16.1%	-30%
Maximum Permanent Set Deflection (in.)	23.0	24.8	20.3	15.9
% Difference from KSWB-1	0.0%	7.8%	-11.7%	-30.9%

Table 10. Summary of KSWB full-scale crash test post deflections.

When comparing the maximum deflections of the strengthened guardrail systems to the baseline KSWB-1, it is noticed that KSWB-3 and KSWB-4 provide increased resistance to lateral deflections, and as expected, KSWB-4 provided the greatest resistance to lateral deflections. However, the nested W-beam guardrail test KSWB-2 produced maximum dynamic deflections that were 16% greater, although its impact severity was nearly the same as KSWB-1. Despite attempts to control the soil conditions, it is believed that on the day KSWB-2 was tested, the soil moisture content was higher than that of KSWB-1 test conditions. This resulted in larger deflections for the stiffened rail. Along with the soil moisture contents, impact severities for all four tests also varied, ranging from 94.0 kip-ft to 124.2 kip-ft. As a result of these differences, the full-scale tests did not reveal the strengthening effects for each of the modifications in an obvious manner. This dramatically shows how different stiffnesses of the same soil and varying impact severities can produce results that make the various guardrail strengthening techniques difficult to assess from full-scale crash testing alone. Therefore only when the soil stiffness and impact severity variations are eliminated can an objective comparison of the various strengthening techniques be conducted. This is most easily and economically accomplished by using a properly validated computer simulation program.

7.3.2 Computer Validation Results

The post parameters obtained from the steel post bogie tests were incorporated into the BARRIER VII simulations using the same configurations as the KSWB tests. The deflections obtained from the simulations were compared with the measured deflections of the full-scale tests to validate the parameters.

It is necessary to validate the parameters from the post testing program so they may be used in other simulations with confidence. Using results from full-scale tests, such as the KSWB series, simulated deflections from BARRIER VII are compared. If the post input parameters in the simulations must be adjusted to predict the measured deflections, then the remaining parameters must be calibrated in the same manner. Then the calibrated parameters may be used in other simulations.

During the KSWB full-scale crash tests, it was estimated that the moisture content of the soil was higher than the optimum level. Rough estimates of the soil moisture content for these full-scale tests were as high as 27%. According to prior research by Ataulluh (19) soil moisture contents as high as this produce a less stiff guardrail system and result in increased deflections. Therefore, for the validation of the parameters, the strongest and weakest sets of parameters for a higher moisture content were used in simulations of the full-scale tests to predict a performance range for each configuration. The sets are the parameters corresponding with steel posts embedded in clay soil with both optimum and high moisture contents.

KSWB-1

Simulations of the KSWB-1 full-scale tests were conducted using parameters for steel posts embedded in a clay with a high moisture content and an optimum moisture content. The simulation deflection results were compared with the measured deflections from the full-scale test. The maximum dynamic deflections of the full-scale crash test (KSWB-1) and the computer simulations are presented in Figure 25. The permanent set deflections are presented in Figure 26. The simulations were conducted using the same impact conditions as the full-scale test. Example BARRIER VII simulation input data files for all four KSWB validation simulations can be found in Appendix C.

The shape of the measured deflected rail was closer to the predicted shape of the simulated rail with an optimum moisture content. The largest difference occurs on the downstream side of the maximum deflection at post 16. However, the simulated deflections generally agreed with the measured deflections.

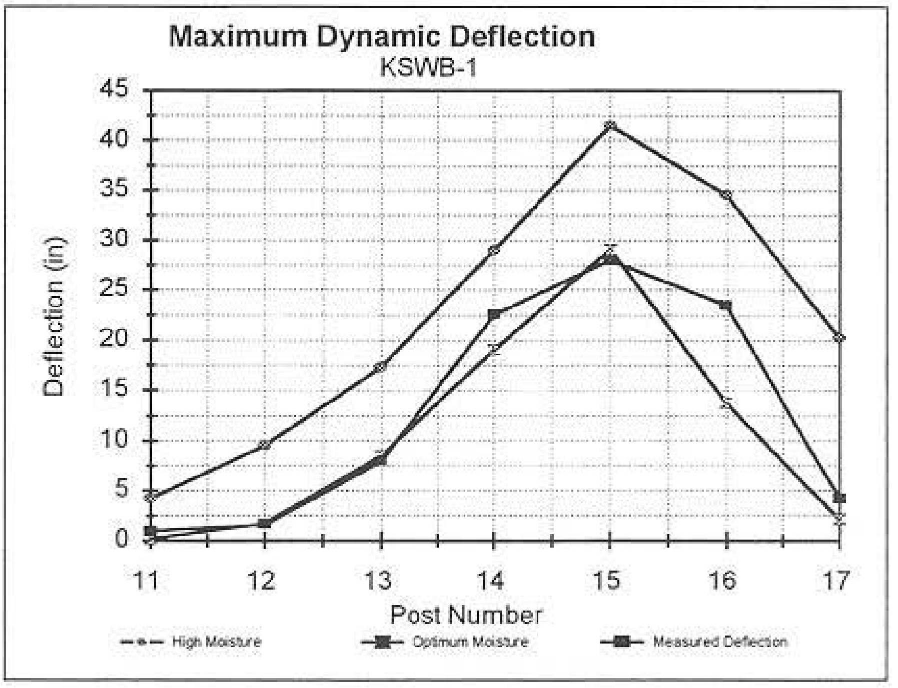

Figure 25. KSWB-1 maximum dynamic deflection comparison.

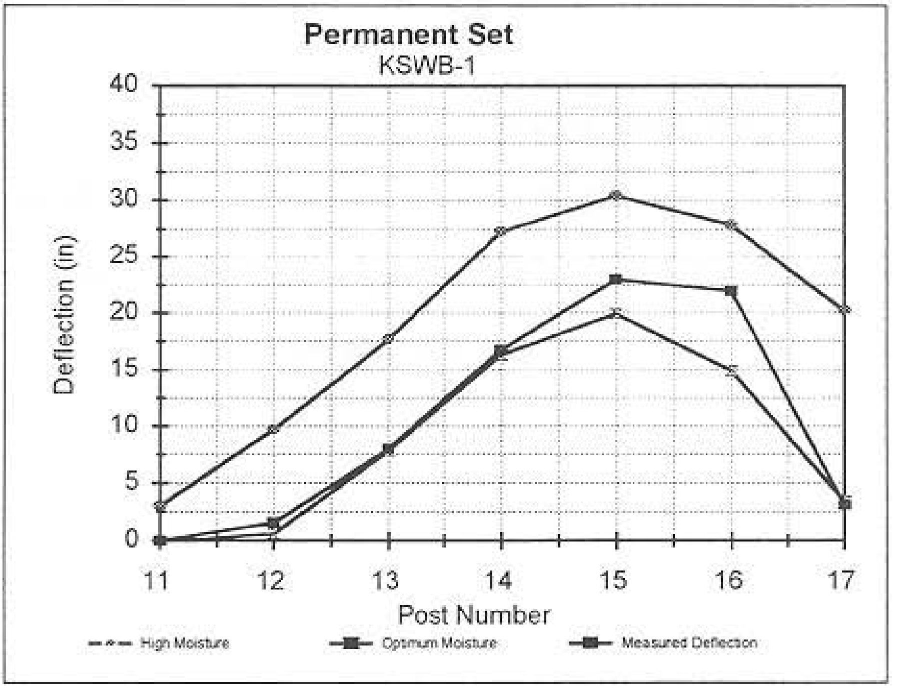

Figure 26. KSWB-1 permanent set deflection comparison.

The maximum permanent set deflections shown in Figure 26 occur at the same post for all three shapes. As with the dynamic deflections, the measured deflections were approximated more closely by the simulation using parameters for a steel post embedded in a clay with an optimum moisture content. The largest difference, once again, occurred on the downstream side. Also, the measured deflected shape was within the range predicted by the simulations. The results of the above validation simulations suggest that the moisture content of the soil for which KSWB-1 was tested was around the optimum moisture content (17%).

KSWB-2

Simulations of the KSWB-2 full-scale tests were also conducted with the aforementioned parameter sets. A comparison of the maximum dynamic deflections and the permanent set deflections from the simulations and the full-scale crash test are presented in Figures 27 and 28, respectively. The same full-scale test impact conditions that were present for the full-scale test were used in the simulations.

The measured maximum dynamic deflected shape for KSWB-2, shown in Figure 27, was within the range predicted by the simulations. The measured maximum dynamic deflection of 32.5 in. was within the range predicted by the simulations of 25 in. to 39 in.

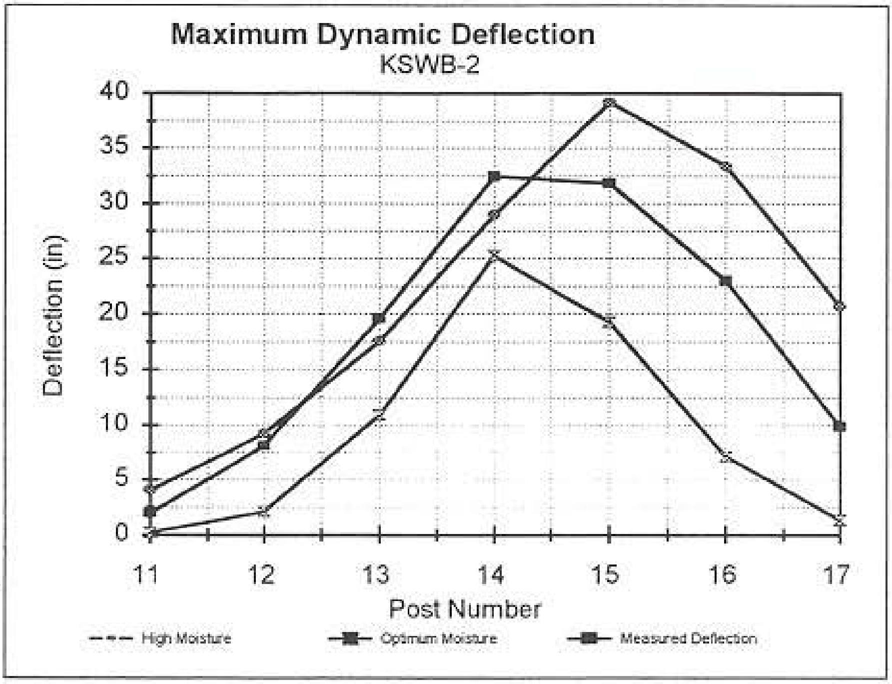

Figure 27. KSWB-2 maximum dynamic deflection comparison.

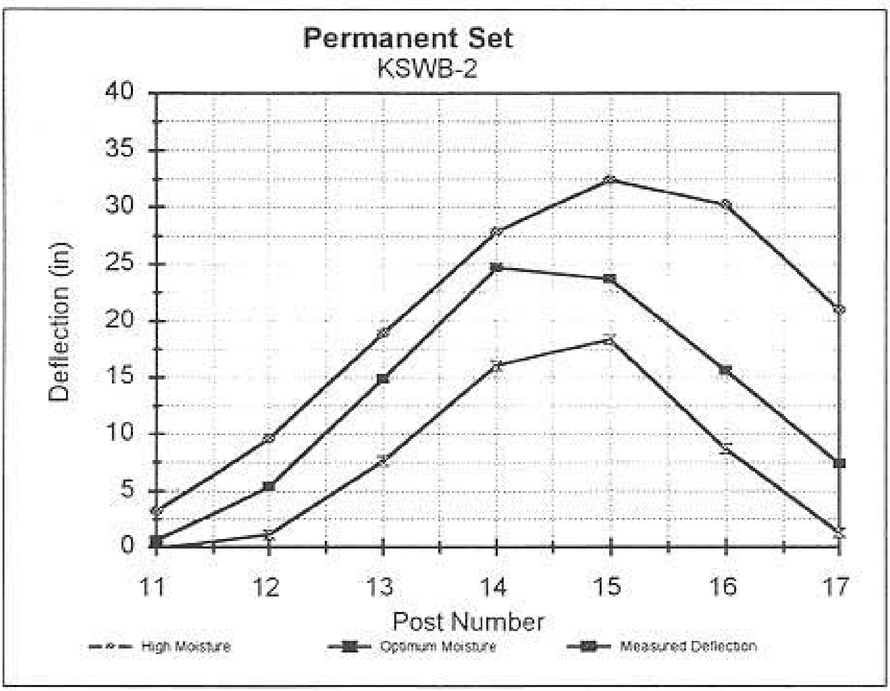

Figure 28. KSWB-2 permanent set deflection comparison.

The permanent set deflections of KSWB-2 are shown in Figure 28. The measured permanent set deflected shape fell within the range predicted by the simulations. From the validation results presented, it is difficult to estimate the moisture content of the soil on the day that KSWB-2 was tested; however, it is reasonable to conclude that the moisture content was within the range investigated.

KSWB-3

The KSWB-3 full-scale test was also simulated with the properties mentioned above. The maximum dynamic and permanent set deflections obtained from the results of the full-scale crash tests (KSWB-3) and the computer simulations using the same impact conditions from the actual full-scale test are presented in Figures 29 and 30, respectively.

The measured maximum dynamic deflected shape for KSWB-3 almost fell completely within the range predicted by BARRIER VII. Deflections on the upstream side of maximum were slightly out of range. However, once again the maximum value was within the range of maximums predicted.

The maximum permanent set deflections from the computer simulations and the full-scale test are presented in Figure 30. The deflections from the full-scale tests were slightly above the values predicted by the simulation conducted with high moisture content clay parameters. These results coupled with the maximum dynamic deflection comparisons suggest that the KSWB-3 test was tested in a clay with a high moisture content.

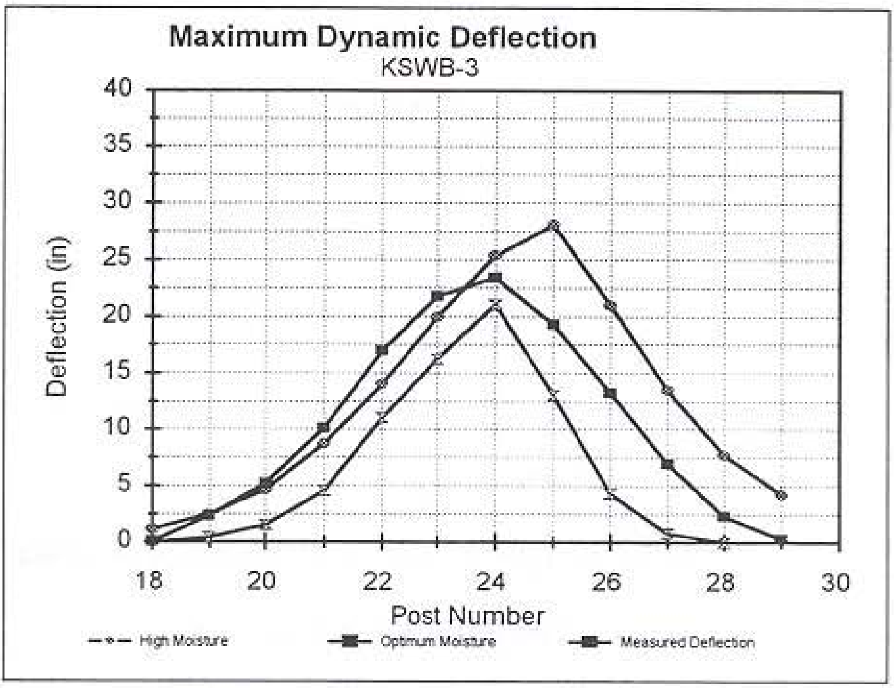

Figure 29. KSWB-3 maximum dynamic deflection comparison.

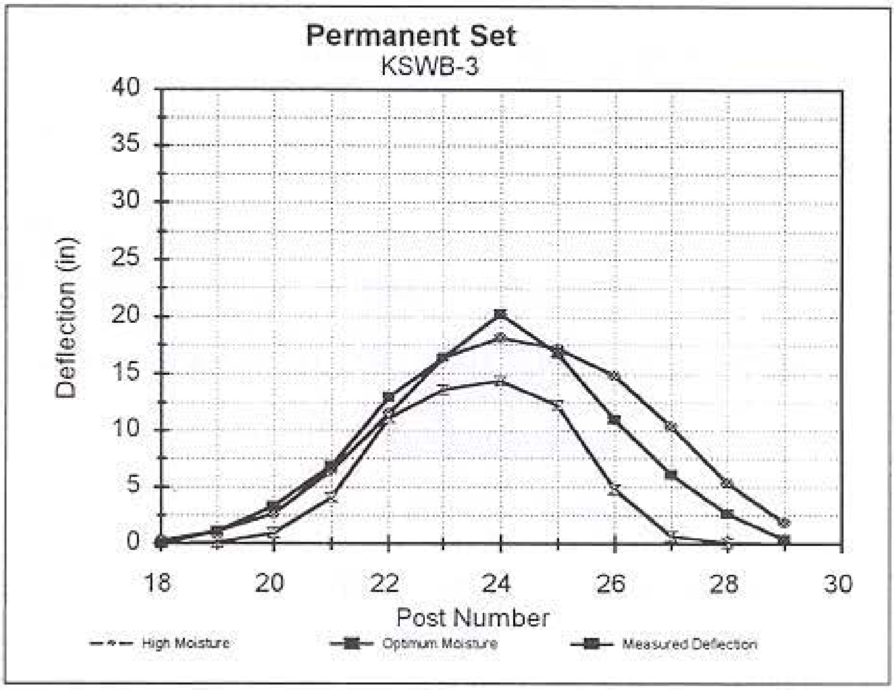

Figure 30. KSWB-3 permanent set deflection comparison.

KSWB-4

The final KSWB configuration was also used in simulations to predict a range of deflections for the full-scale test. The maximum dynamic deflections and the permanent set deflections are presented in Figures 31 and 32, respectively. The computer simulation of the KSWB-4 installation used the same impact conditions as the corresponding full-scale test.

Figure 31 presents the maximum dynamic deflections from the computer simulation and the full-scale test. The deflected shapes of the simulated guardrails were more severe than the full-scale crash test results. The largest difference occurred at the maximum value.

The permanent set deflections for KSWB-4 are presented in Figure 32. As with the dynamic deflection comparison, the measured results were lower than the range predicted by BARRIER VII. However, the largest difference between the range and the actual measured deflection was less than 5 in. From the simulation results, it is reasonable to conclude that the moisture content of the soil on the day of test KSWB-4 was at or near optimum.

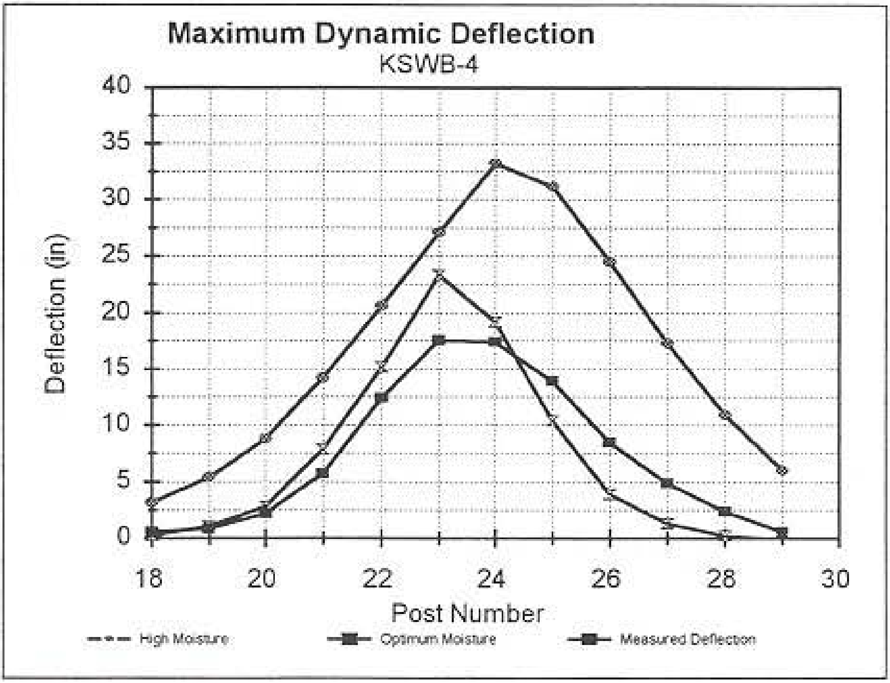

Figure 31. KSWB-4 maximum dynamic deflection comparison.

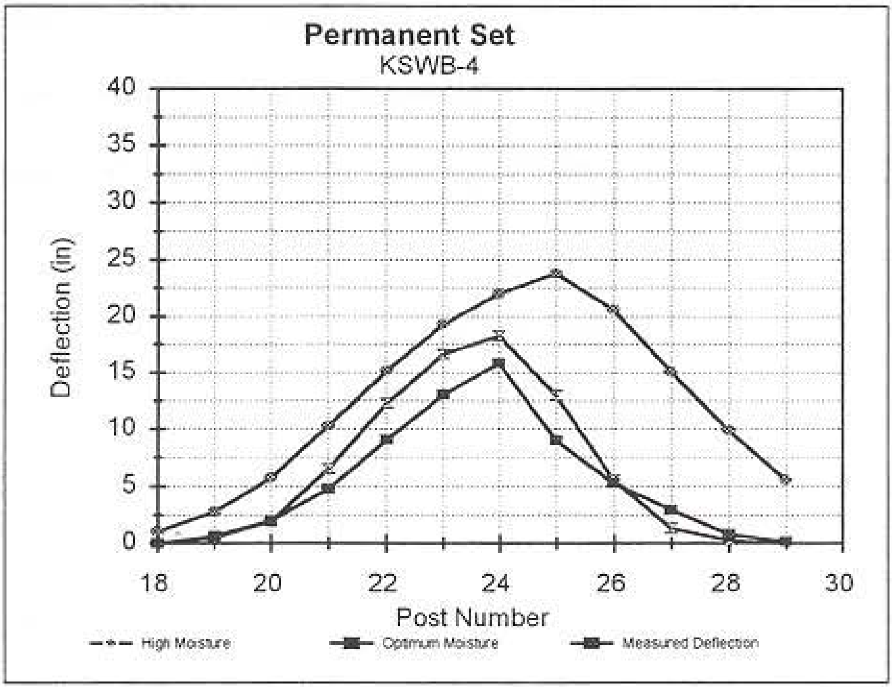

Figure 32. KSWB-4 permanent set deflection comparison.

Table 11 presents a maximum dynamic deflection summary of the BARRIER VII simulations and the full-scale test results of the four KSWB installations.

Test Designation	Measured Maximum Dynamic Deflection (in)	Simulated Maximum Dynamic Deflection Ranges (in.)
KSWB-1	28.0	29.1 - 41.6
KSWB-2	32.5	25.3 - 39.2
KSWB-3	23.5	21.1 - 28.1
KSWB-4	17.6	23.3 - 33.3

Table 11 BARRIER VII Validation Results

Considering the above results of the validation study, the use of the BARRIER VII input parameters obtained from the bogie tests were considered acceptable to determine the performance comparisons of the guardrail strengthening techniques. With the knowledge that the post testing parameters could satisfactorily replicate actual full-scale crash test results, simulations could then be conducted using the other parameters determined from the bogie post testing phase to predict the performance of the guardrail systems with different post and soil conditions.

8. Applied Results

Following the validation of the post parameters with the four KSWB tests, computer simulations of the guardrail crash tests were conducted with the same post and soil conditions as that used during the bogie post tests. By using identical post properties in all four KSWB guardrail simulations, soil stiffness variations were eliminated and objective comparisons of the various strengthening techniques were conducted. Also, comparisons between systems using different post and soil properties were conducted by using identical impact conditions, thus eliminating the impact condition variations that accompanied the full-scale KSWB crash tests. Knowing this, all of the KSWB simulations in this chapter were conducted using the intended KSWB target impact conditions, a 4500 lb sedan impacting at 60 mph and 25 degrees.

Using the timber post data from the bogie post testing, computer simulations were used to predict the dynamic response of similar systems with timber posts, thereby avoiding the cost of four additional full-scale crash tests. In addition to the systems with timber posts embedded to a standard depth in clay, the performance of similar systems with longer posts, different moisture conditions, and sandy soil were also evaluated using the post parameters developed from the post testing program.

The maximum dynamic and permanent set deflections for the guardrail impact simulations using the test matrix conditions found in Table 9 are summarized in Table B-1.

8.1 Effects of Nested W-beams and Half-Post Spacings on Guardrail Performance

A comparison of the maximum dynamic deflections of all of the simulations performed in this study is presented in Table 12. This table is intended to aid in the evaluation of the effects of the various guardrail strengthening techniques. The values in parentheses represent the percent decrease in the maximum dynamic deflection for each system compared to the standard KSWB-1 installation.

Post and Soil Conditions				Maximum Dynamic Deflection (in) (% Decreases in comparison to the Standard Installation)			
Soil Type	**Moisture Content**	**Embedment Length**	**Post Type**	**Standard Installation**	**W-beam Nesting Only**	**Half-Post Spacing Only**	**Both Nesting & Half-Post Spacing**
Clay	Low	Extended	Steel	26.8	25.6 (4%)	22.2 (17%)	18.3 (32%)
			Timber	25.8	24.9 (3%)	20.2 (22%)	17.4 (33%)
		Standard	Steel	29.3	26.4 (10%)	21.9 (25%)	18.8 (36%)
			Timber	25.4	24.5 (4%)	19.2 (24%)	17.6 (31%)
	Optimum	Standard	Steel	26.8	24.7 (8%)	21.4 (20%)	18.2 (32%)
			Timber	24.7	23.6 (4%)	18.9 (23%)	16.3 (34%)
	High	Standard	Steel	40.3	37.7 (6%)	28.7 (29%)	27.4 (32%)
			Timber	38.9	36.2 (7%)	28.9 (26%)	27.2 (30%)
Sand	Unsaturated	Standard	Steel	37.3	34.9 (6%)	27.3 (27%)	25.6 (31%)
			Timber	35	31.8 (9%)	25.6 (27%)	23.6 (33%)

Table 12. KSWB strengthening techniques comparisons.

As expected, the guardrail systems with both nesting and half-post spacing consistently have the lowest maximum dynamic deflections for all soil and post types, reducing the deflections by 30% to 36% compared with the standard installation. The system alternative consisting of half-post spacings with a single W-beam decreased the deflections of the standard installation by 17% to 29%. The simulations in drier clay soils, indicated that the effect of nested W-Beams was greater for systems with half-post spacings in comparison to the effect nesting had on systems with regular full-post spacings. The results from the simulation conducted with steel posts embedded to an extended depth in a clay soil with a low moisture content illustrate this. The deflection of a system employing nested W-Beams alone reduced the deflections by 4% compared with the standard installation. However, the simulation conducted with both modifications, half-post spacing and nested W-Beams, predicted a maximum dynamic deflection of 18.3 in., which was 18% lower than the deflection of 22.2 in. obtained with half-post spacings alone. This difference was not as large for simulations conducted in weaker soils (high moisture content clay and sand).

8.2 Effects of Post Type on Guardrail Performance

The post type does not greatly affect the deflection characteristics of any of the W-beam systems tested. The average difference in maximum dynamic deflection for wood and steel post systems for all simulations was only 7%. The largest difference of maximum dynamic deflection was 3.9 in. for the standard installation (KSWB-1) using standard length posts embedded in a low moisture content clay. The maximum dynamic deflection of this system with timber posts was only 13% smaller. These results agree with the findings of the TTI study (14) that maintained that steel posts behaved similarly to timber posts under laterally applied load.

8.3 Effects of Moisture Content on Guardrail Performance

The BARRIER VII post parameters obtained from Table 9, particularly the yield moments, varied considerably with the moisture content of the clay. The differences between posts embedded in a clay with a low, optimum, and high moisture content is illustrated in Table 13. The low moisture content yield moments were only 6% to 17% lower than the optimum moisture content clay yield moments, whereas the high moisture content yield moments were 52% to 65% lower than optimum. The effect of moisture content on the performance of a post is considerable, confirming what Ataulluh et al. suspected in 1988 (19).

Post Type	Clay Moisture Content	Yield Moment (kip-in.)	% Difference
Timber	Low	237.72	-17%
	Optimum	286.23	
	High	100.91	-65%
Steel	Low	193.20	-6%
	Optimum	205.80	
	High	97.86	-52%

Table 13. Clay moisture content and yield moment comparisons for standard embedment depth.

The deflections of the systems simulated in clay soil with high moisture contents were considerably higher than the deflections from simulations conducted with a drier soil. The predicted deflections from simulations in a clay at a high moisture content were on average 45% higher than those resulting from simulations with a low moisture content. The largest difference occurred in the simulations for timber posts in the standard KSWB-1 configuration with deflections that were 53% higher. The optimum moisture content simulations produced deflections that were only slightly lower than that of the systems placed in soil with a low moisture content, as the deflections decreased by an average of only 4%. These comparisons show that guardrails are particularly vulnerable to weak soil conditions, such as when the moisture content is high. Soils with low to optimum moisture contents are similar in strength and guardrails installed in these soils respond similarly to impacts. Therefore, a guardrail placed in a soil with a high moisture content may not perform up to expectations because of the low resistance the soil provides. These results dramatically illustrate the effects of the moisture content of the clay on the performance of a guardrail in controlling lateral deflections.

8.4 Effects of Post Embedment Depth on Guardrail Performance

A synthesis of Table 9 is presented in Table 14 illustrating the difference between the yield moments of posts embedded to a standard depth and those with an extended embedment of 6 in. The comparison is only performed for a post embedded in a low moisture content clay because there is only test data available for this moisture content. For both post types, the yield moment of the extended post was on average 12% higher than a post embedded to a standard depth.

Post Type	Embedment Depth	Yield Moment (kip-in.)	Difference (%)
Timber	Standard	237.72	17.22 (7%)
	Extended	254.94	
Steel	Standard	193.20	32.76 (17%)
	Extended	225.96	

Table 14. Embedment depth and yield moment comparisons.

By comparing the maximum dynamic deflections of the systems listed in Table 12, no substantial decrease in deflection results from embedding the posts an additional 6 in. The average difference of the maximum dynamic deflections between the two posts was 3%. These results indicate that increasing the embedment depth of a post by 6 in. provides little or no additional resistance when a standard embedment depth of 44 in. is used in low moisture content clay.

8.5 Effects of Soil Type on Guardrail Performance

The maximum dynamic deflections for posts in sand were consistently higher than the posts in clay except when a high moisture content was present. The deflections for systems in clay at low and optimum moisture contents were on average 24% and 28% lower than the deflections in sand, respectively. The largest difference in deflection between systems in sand and clay occurred with the standard configuration (KSWB-1) using steel posts in an optimum moisture content clay. The high moisture content deflections, however, were consistently higher than those of the sand installations by an average of 10%.

9. Conclusions and Recommendations

9.1 Conclusions

The objective of this research was to develop a set of post parameters to be used in simulations of guardrail installations. These simulations would be used to evaluate the effects of strengthening techniques, post type, soil type, embedment depth, and soil moisture content on the performance of guardrails. The objective was achieved through the use of dynamic post tests and the BARRIER VII simulation program. This work is also reported in the thesis by Bierman (28)

The post test study and analysis of the KSWB simulations conducted in this research lead to several general conclusions. Timber and steel posts behaved similarly in all installations and soil conditions. The timber post guardrails performed slightly better in all conditions. The post input parameters in clay illustrate the drastic effect moisture content has on the lateral impact behavior of a post under dynamic load. This effect becomes critical when lateral deflections are to be controlled adjacent to roadside hazards. The deflections for guardrails placed in clay soils at a high moisture content were on average 50% higher than those placed in an optimum moisture content soil. The effect of post embedment on guardrail performance was found to be minimal for $6^{1}/_{2}$ ft posts embedded an additional 6 in. in a low moisture content clay. A guardrail system placed in an unsaturated sand was not as effective at controlling deflections as the same system placed in a clay with a low or optimum moisture content.

Using the results of the full-scale crash tests and computer simulations, the effect of nested W-beams alone at reducing guardrail deflections was found to be marginal and therefore it is not recommended as an alternative to reduce deflections. However, half-post spacing produced a substantial reduction in the maximum deflections of the guardrail. Therefore, the strengthening technique of a half-post spacing is recommended. Compaction of the soil is of primary importance because any benefit derived by either strengthening technique can be reduced or eliminated if the soil cannot provide the required resistance to lateral load.

9.2 Recommendations

Due to the limited time and resources available to the researchers, the number of tests performed on the posts with a wide range of moisture contents was limited. Future research should examine this phenomenon in more detail, and attempt to establish a more dependable relationship between the soil moisture content and the post-soil strength. Also, only the strong axes of the posts were tested, and further research should be conducted to verify the weak axis parameters used in the simulations for this research.

Different sizes of posts of the same material were not included as a study parameter in this research. The results from this research only considered the timber 6 in. x 8 in. and steel W6x9 posts. As a result, the effects of post material, size, and shape on the strength of a post could not be determined.

It should be noted that the bogie impact speed and weight were held constant throughout the testing program. The bogie speed and weight were chosen to reproduce the forces transmitted to a post when a 4500 lb sedan impacts a guardrail at 60 mph and 25 degrees. The results obtained in this research were intended to be used for guardrail simulations conducted with similar impact conditions. No conclusions about the effect of impact severity on the performance of the post can be made using the results of this testing program alone, therefore the conclusions of this research should be used with discretion for installations with different impact conditions than those investigated here.

10. References

1. Powell, G.H., *Computer Evaluation of Automobile Barrier Systems*, FHWA, Report FHWA-RD-73-73, August 1970.
2. Powell, G.H., *BARRIER VII: A Computer Program for Evaluation of Automobile Barrier Systems*, Report FHWA-RD-73-51, FHWA, U.S. Department of Transportation, April 1973.
3. Ross, H.E., Jr., *Analysis and Design of Safety Appurtenances by Computer Simulation*, The Role of the Civil Engineer in Highway Safety, American Society of Civil Engineers, 1983.
4. Post, E.R., *Full-Scale Vehicle Crash Tests on Guardrail-Bridgerail Transition Designs with Special Post Spacing*. Report TRR-03-008-87, Final Report, May 1987.
5. Bligh, R.P., Sicking, D.L., and H.E. Ross, *Development of a Strong Beam Guardrail/Bridge Rail Transition*. Presented at 67th Annual Meeting of the Transportation Research Board, Washington, D.C., January 1988.
6. Tuan, C.Y., Post, E.R., Ataullah, S. and J.O. Brewer, *Development of Kansas Guardrail to Bridgerail Transition Designs Using BARRIER VII*, Transportation Research Record 1233, TRB, National Research Council, Washington, D.C., 1989.
7. Cichowski, G., Skeels, P. C., and W. R. Hawkins, *Appraisal of Guardrail Installations by Car Impact and Laboratory Tests*. HRB, Vol. 40, 1961, pp. 137-178.
8. Graham, D., Burnett, W. C., Gibson, J. L. and R. H. Freer, *New Highway Barriers: The Practical Application of Theoretical Design*. Highway Research Record 174, HRB, Washington, D.C., 1967.
9. Michie, J.D., *Response of Guardrail Posts During Impact*. Research Report No. 03-9051, Southwest Research Institute, San Antonio, Texas, October 1970.
10. Michie, J.D., Gatchell, C.J. and T. J. Duke, *Dynamic Evaluation of Timber Posts for Highway Guardrails*. Highway Research Record 343, HRB, Washington, D.C., 1971, pp. 19-33.
11. Gatchell, C.J., and J. D. Michie, *Pendulum Impact Tests of Wooden and Steel Highway Guardrail Posts*. USDA Forest Service Research Paper NE-311, 1974.
12. Calcote, L.R., and C.E. Kimball, *Properties of Guardrail Posts for Various Soil Types*, Transportation Research Record 679, TRB, National Research Council, Washington, D.C., 1978, pp. 22-25.
13. Calcote, L.R., *Development of a Cost-Effectiveness Model for Guardrail Selection*. Report No. FHWA-RD-78-74, U.S. Department of Transportation, January 1980.

14. Jeyapalan, J.K., Dewey, J.F., Hirsch, T.J., Ross, H.E., and H. Crooner, *Soil-Foundation Interaction Behavior of Highway Guardrail Posts.* Transportation Research Record 970, 1983, pp. 37-47.

15. Eggers, W., Hirsch, T.J., and H.E. Ross, Jr., *Strength of Guardrail Post in Rock.* Report No. FHWA/TX-85/42+343-1(Suppl.), September 1984.

16. Bedewi, N.E., *Dynamic Response of Guardrail Posts in Soil.* Report No. FHWA/RD-86/147, University of Maryland, September 1985.

17. Eggers, W. and T.J. Hirsch, *The Effects of Embedment Depth, Soil Properties, and Post Type on the Performance of Highway Guardrail Post.* Report No. FHWA/TX-86/64+405-1, August 1986.

18. Bronstad, M.E., Calcote, L.R., Ray, M.H., and J.B. Mayer. *Guardrail-Bridge Rail Transition Designs.* Report FHWA-RD-86-178, FHWA, U.S. Department of Transportation, April 1988.

19. Ataullah, S., *An Analytical Evaluation of Future Nebraska Bridgerail-Guardrail Transition Designs using Computer Simulation Model BARRIER VII*, UNL Thesis, August 1988.

20. Stout, J.H., and T.L. Yang, *Force-Deflection Characteristics of Guardrail Posts,* Report No. FHWA-RD-88-193, September 1988.

21. Hargrave, M.W., and A.G. Hansen. *Federal Outdoor Impact Laboratory - A New Facility for Evaluating Roadside Safety Hardware,* Transportation Research Record 1198, TRB, National Research Council, Washington, D.C., 1988, pp. 90-96.

22. *Enhanced Graphics Acquisistion and Analysis (EGAA), Operation Guide and Reference Manual*, Version 3.34.1, R.C. Electronics, Goleta, California, December 1990.

23. *EDR and EDRIS User's Manual*, Instrument Sensor Technologies, Inc, Okemos, Michigan, August 1993.

24. *DynaMax User's Manual, Revision 1.3*, Instrumented Sensor Technologies, Inc, Okemos, Michigan, April 1993.

25. *The DADiSP Worksheet, Data Analysis and Display Software, User and Reference Manuals*, Version 3.0, DSP Development Corporation, Cambridge, Massachusetts, December 1991.

26. Holloway, J.C., M.G. Bierman, B.G. Pfeifer, B.T. Rosson, and D.L. Sicking, *Performance Evaluation of KDOT W-beam Systems.* Research Report No. TRP-03-39-96, Midwest Roadside Safety Facility, Draft Report, Lincoln, Nebraska, March 1996.

27. Michie, J.D. ,*Recommended Procedures for the Safety Performance Evaluation of Highway Appurtenances*, National Cooperative Highway Research Program Report No. 230, Transportation Research Board, Washington, D.C., March 1981.

28. Bierman, M.G., *Behavior of Guardrail Posts to Lateral Impact Loads*, Masters Thesis, Civil Engineering Department, University of Nebraska-Lincoln, December 1995.

11. Appendices

Appendix A: Force-Deflection Results of Bogie Post Tests

Table A-1 lists the classification numbering scheme of the post testing program. Refer to this table to find the post and soil conditions that were present for each set of test data.

Class (PT)	Post Type	Soil Type	Moisture Content	Embedment Depth
1	Timber	Clay	Low	Standard
2	Timber	Clay	Low	Extended
3	Timber	Clay	Optimum	Standard
4	Timber	Clay	High	Standard
5	Timber	Sand	Unsaturated	Standard
6	Steel	Clay	Low	Standard
7	Steel	Clay	Low	Extended
8	Steel	Clay	Optimum	Standard
9	Steel	Clay	High	Standard
10	Steel	Sand	Unsaturated	Standard

Table. A-1. Post / soil testing classification scheme.

Figures A-1 through A-10 present the force-deflection data used in the BARRIER VII post parameter analysis. The dark line on each is the simplified force-deflection model used by BARRIER VII. Annotated on each graph are the actual BARRIER VII post parameters extracted from the models that were presented in Table 8. A description of the procedure used in determining the parameters is presented in Chapter 7.

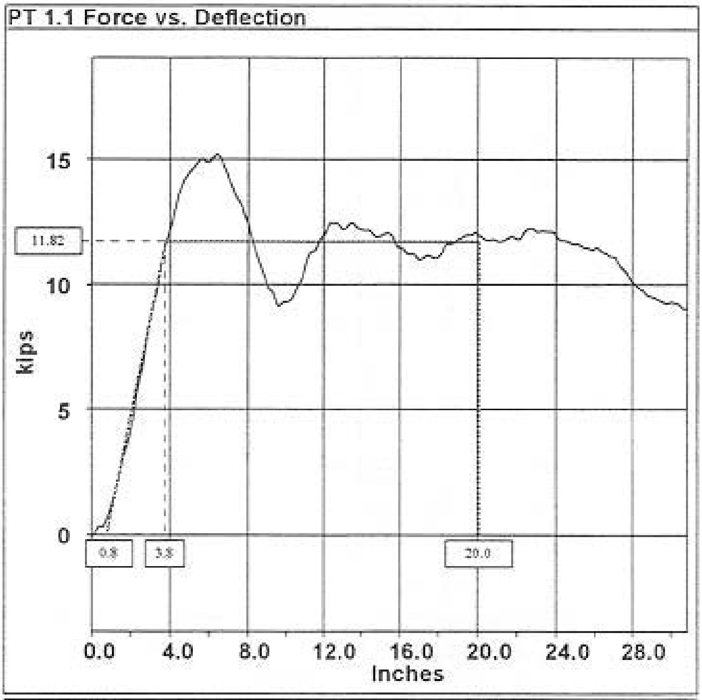

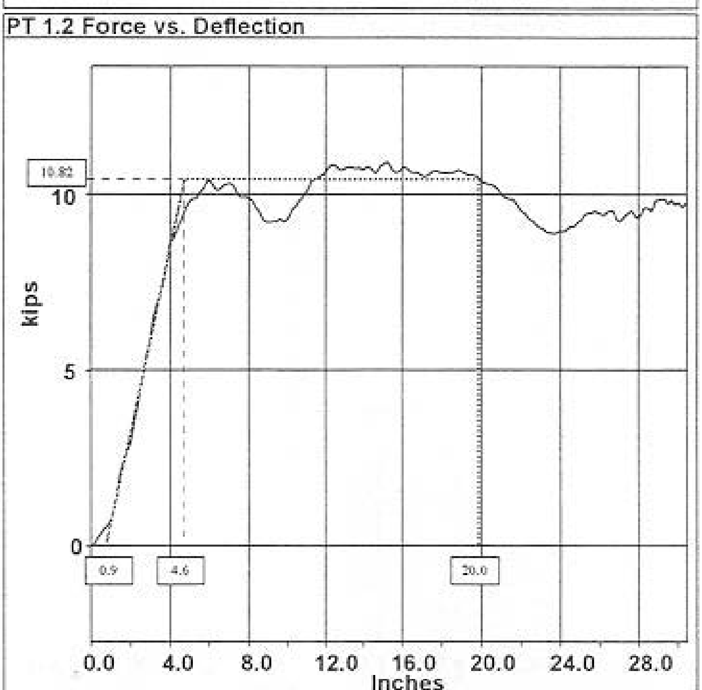

Figure. A-1. PT 1 force-deflection data analysis results.

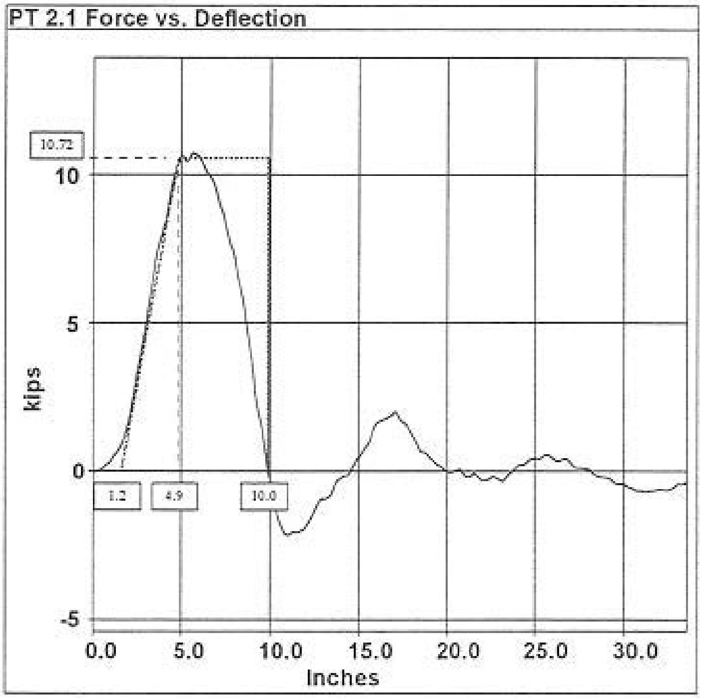

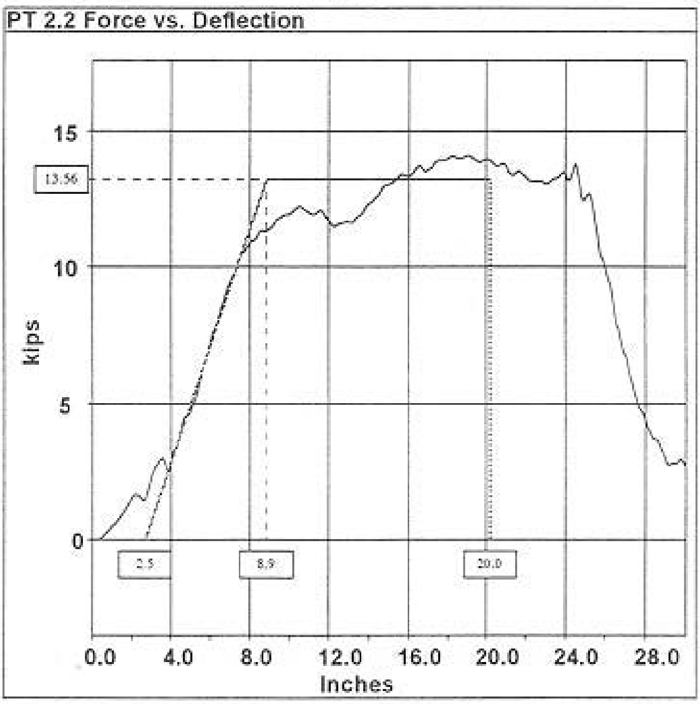

Figure. A-2. PT 2 force-deflection data analysis results.

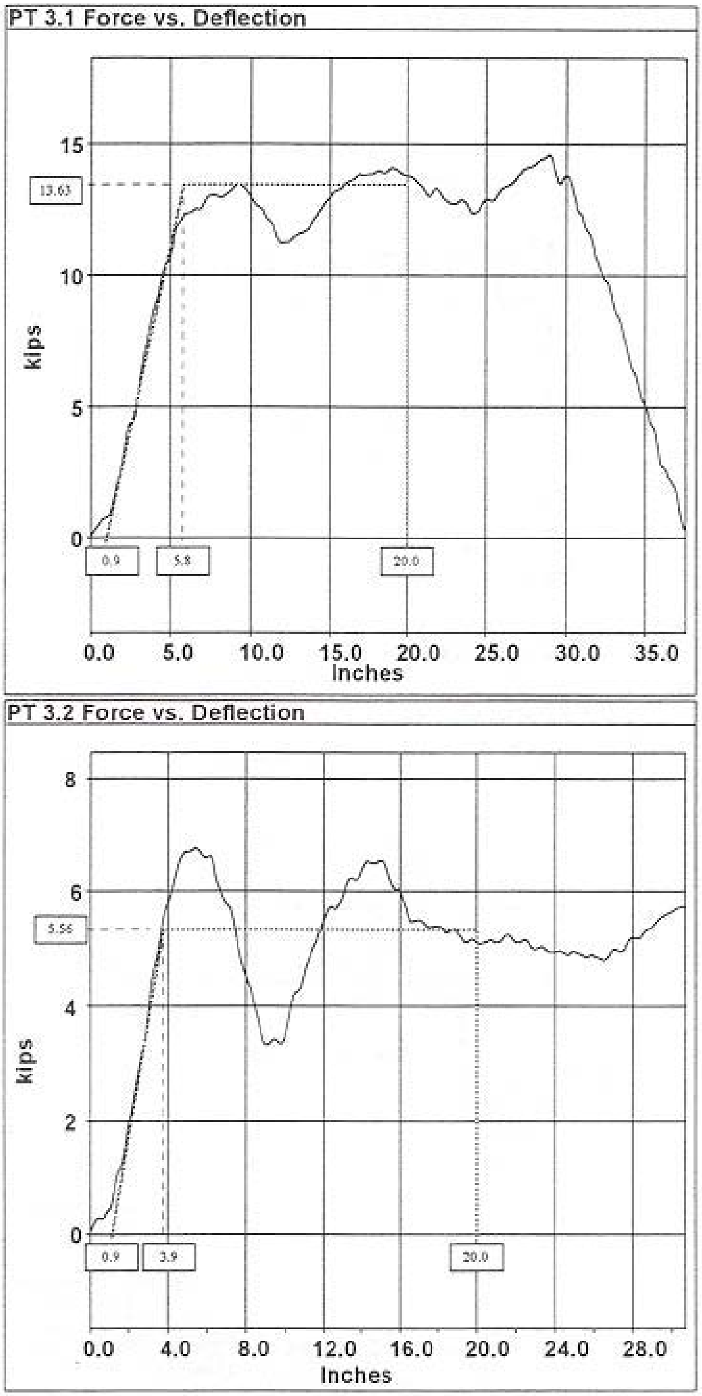

Figure. A-3. PT 3 force-deflection data analysis results.

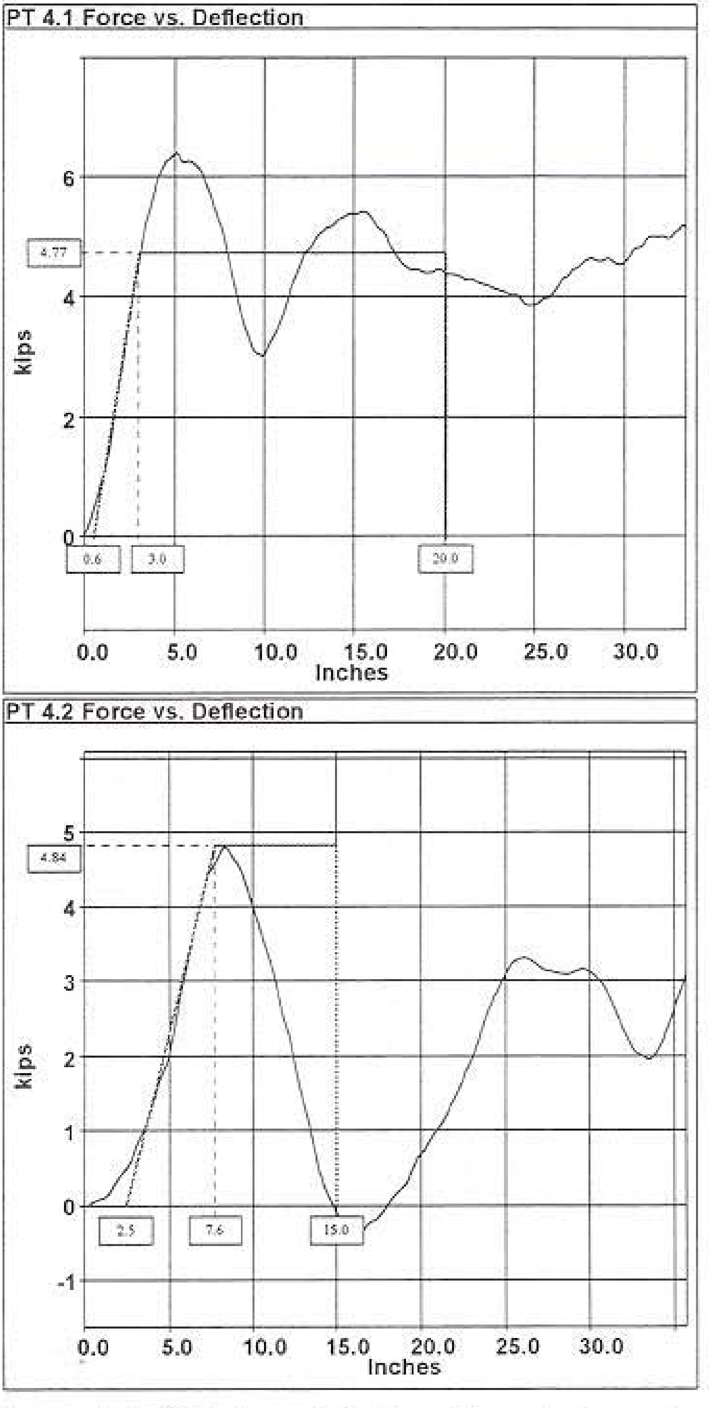

Figure. A-4. PT 4 force-deflection data analysis results.

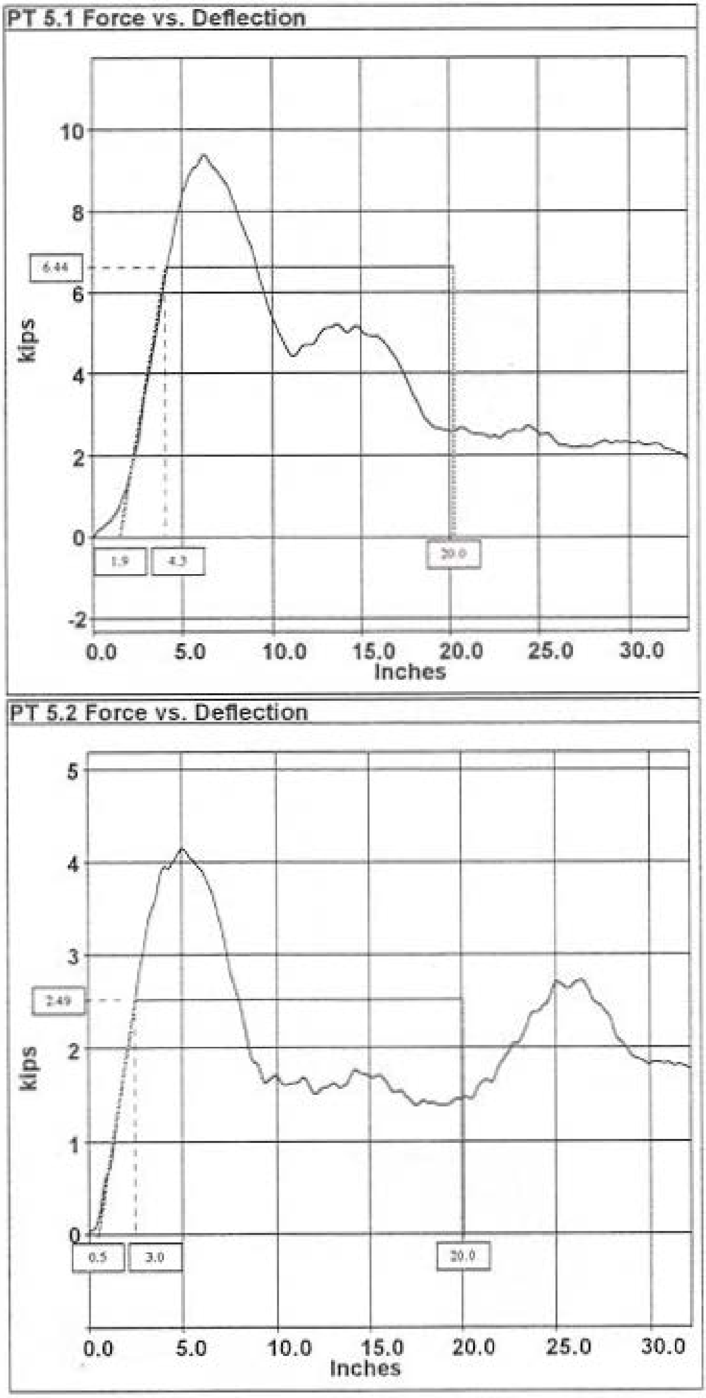

Figure. A-5. PT 5 force-deflection data analysis results.

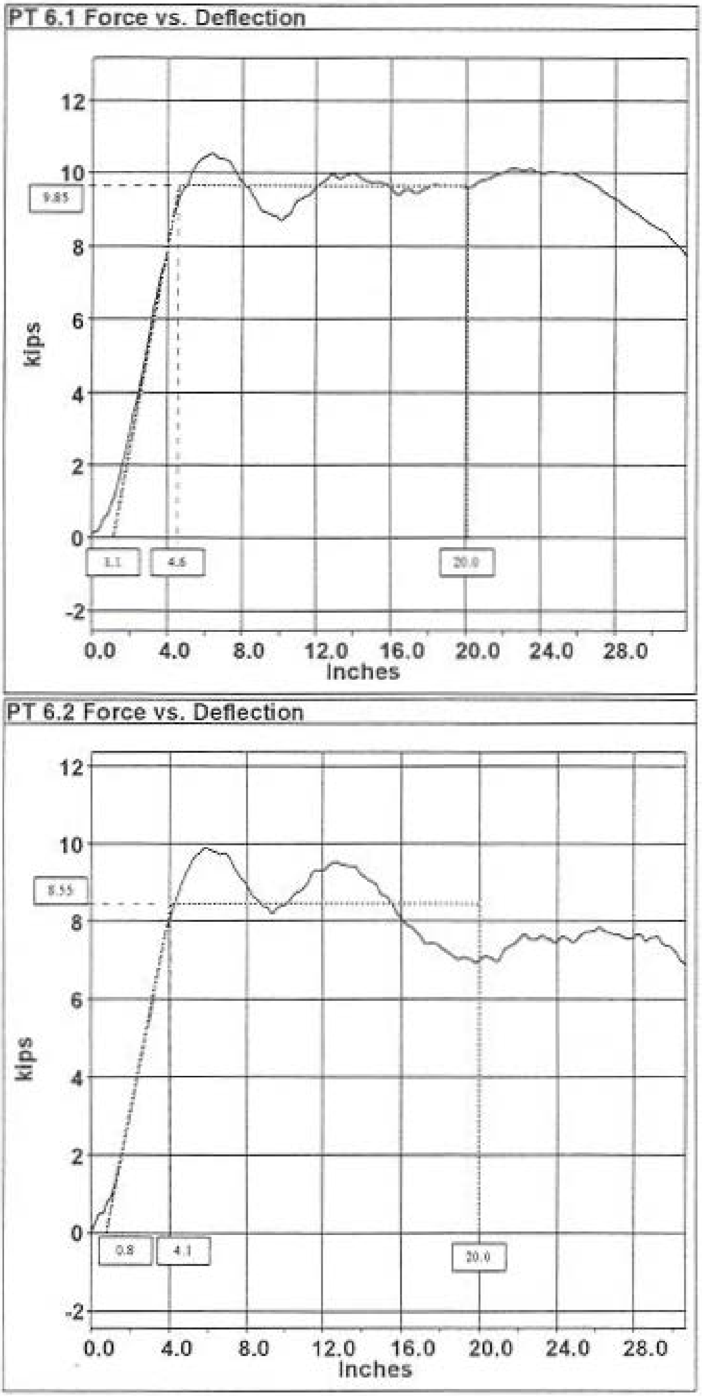

Figure. A-6. PT 6 force-deflection data analysis results.

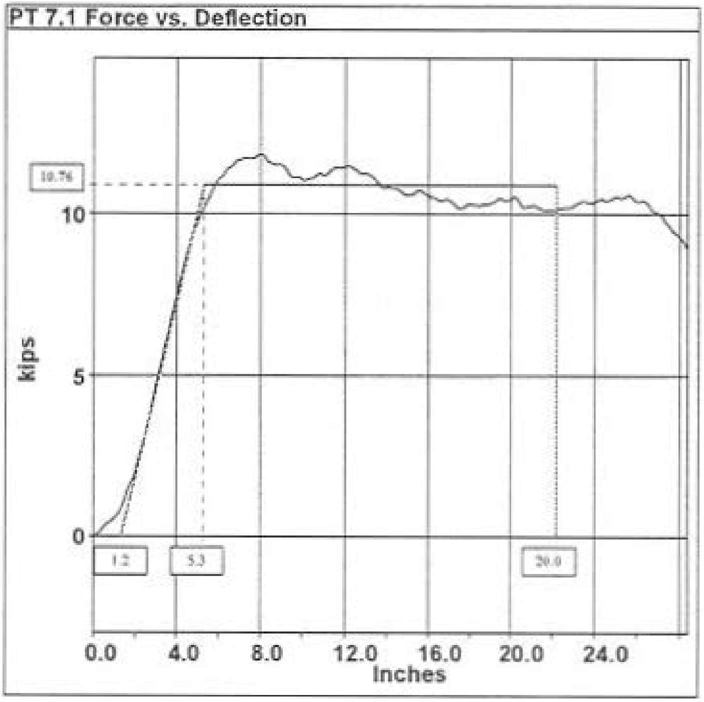

Figure. A-7. PT 7 force-deflection data analysis results.

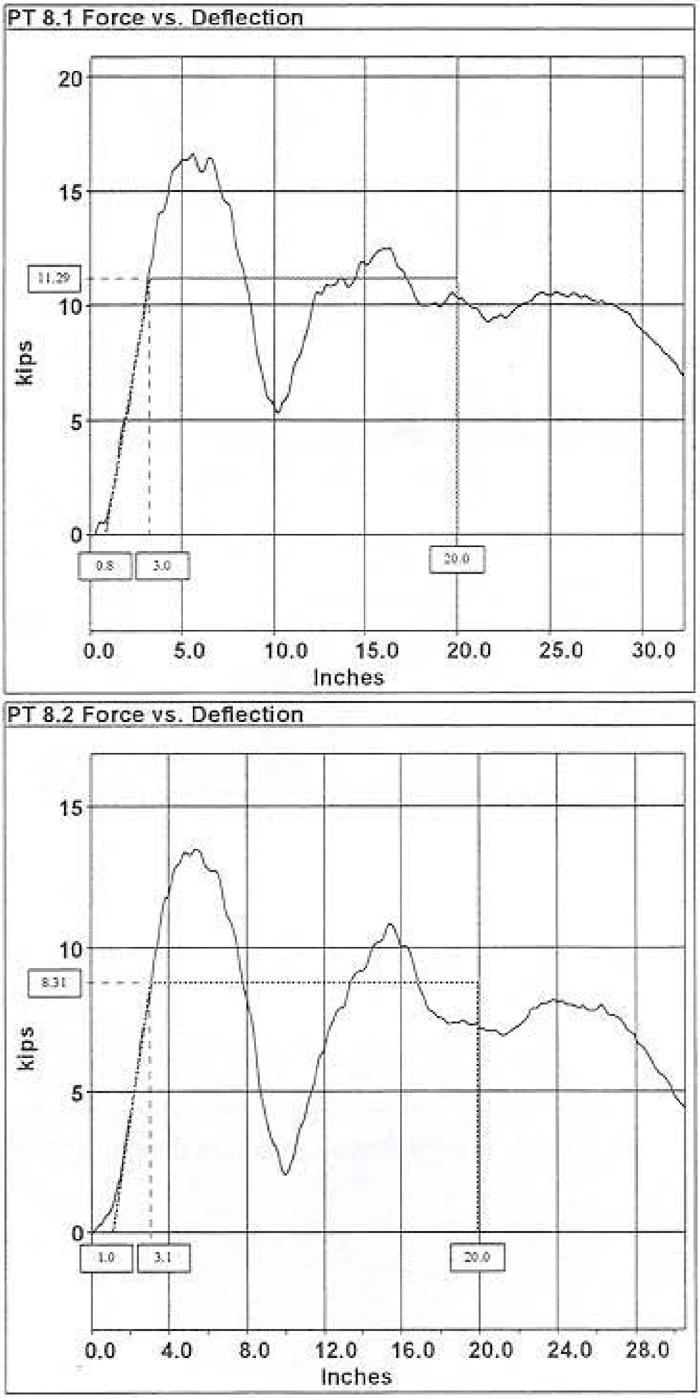

Figure. A-8. PT 8 force-deflection data analysis results.

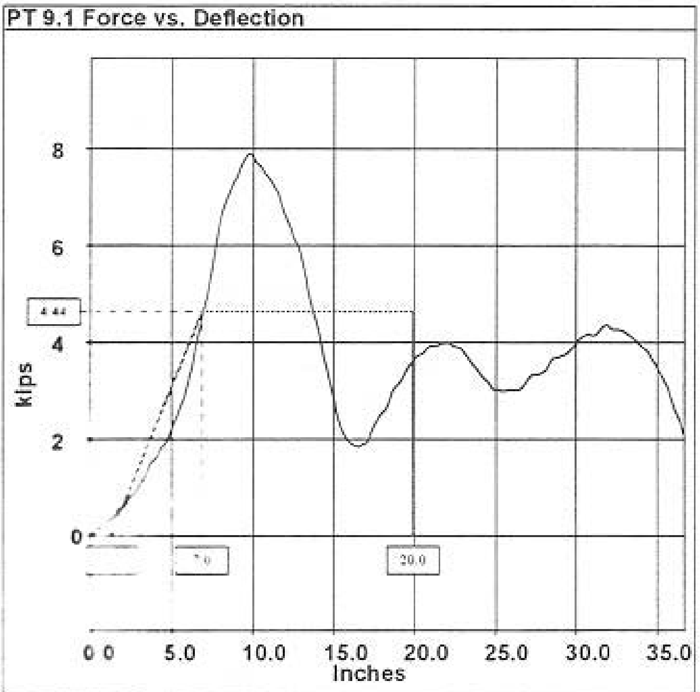

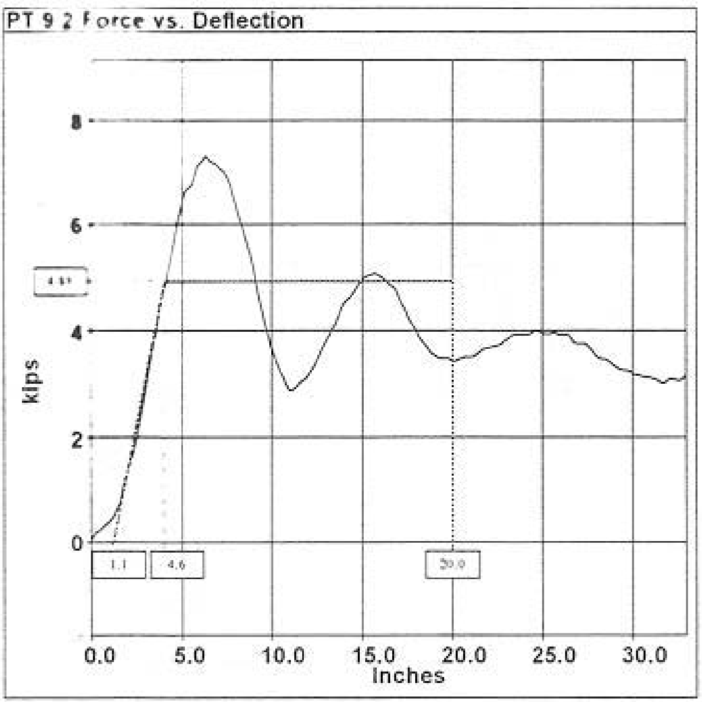

Figure. A-9. PT 9 force-deflection data analysis results.

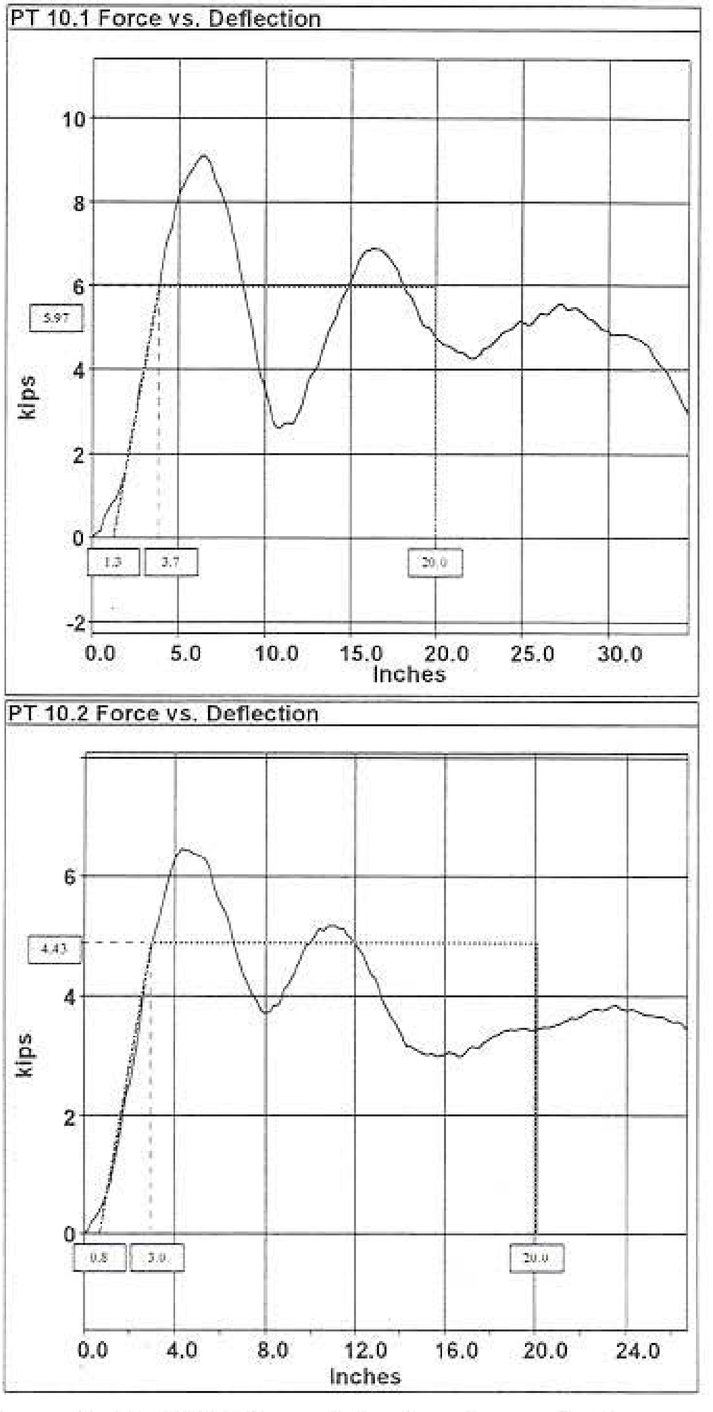

Figure. A-10. PT 10 force-deflection data analysis results.

Appendix B: Deflected Shapes of the Simulated KSWB Systems

Listed in Table B-1 is the maximum dynamic and permanent set deflections of the BARRIER VII simulations conducted in this research. The deflected shapes of the simulated KSWB guardrails can be found in Figures B-1 through B-10. Depicted on each plot are the maximum dynamic and permanent set deflections resulting from BARRIER VII simulations conducted using the appropriate parameters from Table 9 for each post and soil condition. Refer to Table B-1 for a list of the various post and soil conditions present for each simulation.

Post and Soil Conditions				Maximum Dynamic Deflection [Permanent Set Deflection] (in.)			
Soil Type	**Moisture Content**	**Embedment Length**	**Post Type**	**Standard Installation**	**W-beam Nestin Only**	**Half-Post Spacing Only**	**Both Nesting & Half-Post Spacing**
Clay	Low	Extended	Steel	26.8 [17.0]	25.6 [18.5]	22.2 [14.4]	18.3 [13.6]
			Timber	25.8 [16.9]	24.9 [15.1]	20.2 [13.0]	17.4 [12.0]
		Standard	Steel	29.3 [19.1]	26.4 [19.5]	21.9 [14.0]	18.8 [15.3]
			Timber	25.4 [16.8]	24.5 [15.8]	19.2 [14.9]	17.6 [13.0]
	Optimum	Standard	Steel	26.8 [17.2]	24.7 [18.0]	21.4 [13.5]	18.2 [14.9]
			Timber	24.7 [13.9]	23.6 [12.6]	18.9 [13.3]	16.3 [10.5]
	High	Standard	Steel	40.3 [28.1]	37.7 [28.0]	28.7 [19.3]	27.4 [18.4]
			Timber	38.9 [28.6]	36.2 [27.4]	28.9 [19.9]	27.2 [18.9]
Sand	Unsaturated	Standard	Steel	37.3 [25.5]	34.9 [28.2]	27.3 [17.9]	25.6 [18.3]
			Timber	35.0 [23.0]	31.8 [24.8]	25.6 [15.9]	23.6 [18.1]

Table. B-1. Predicted deflections of KSWB configurations with varying conditions.

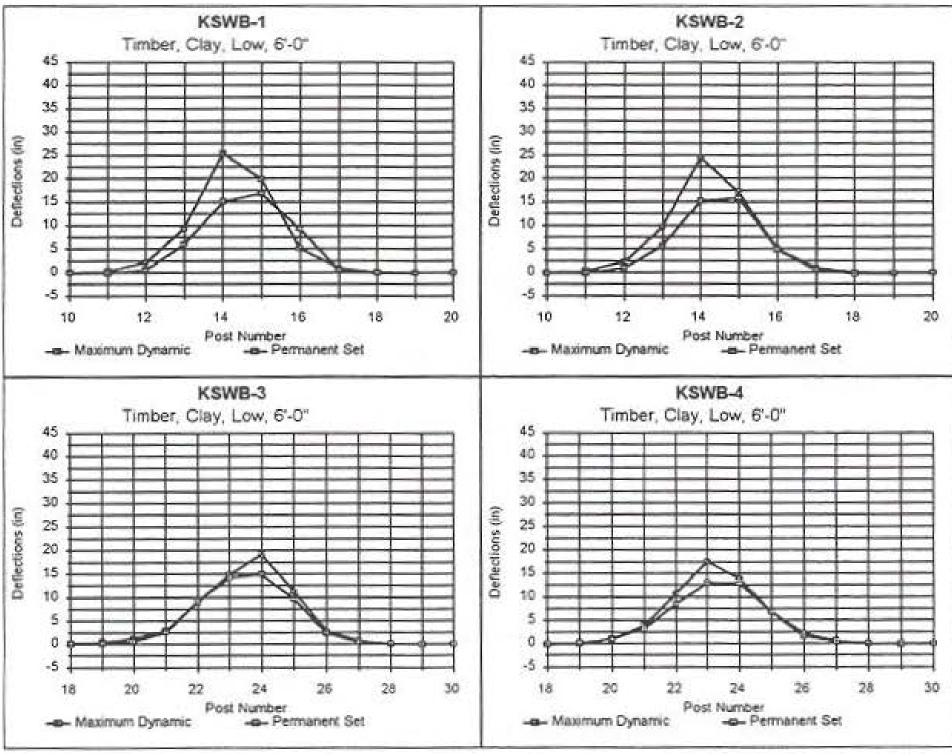

Figure. B-1. Predicted KSWB deflections using PT 1 post parameters.

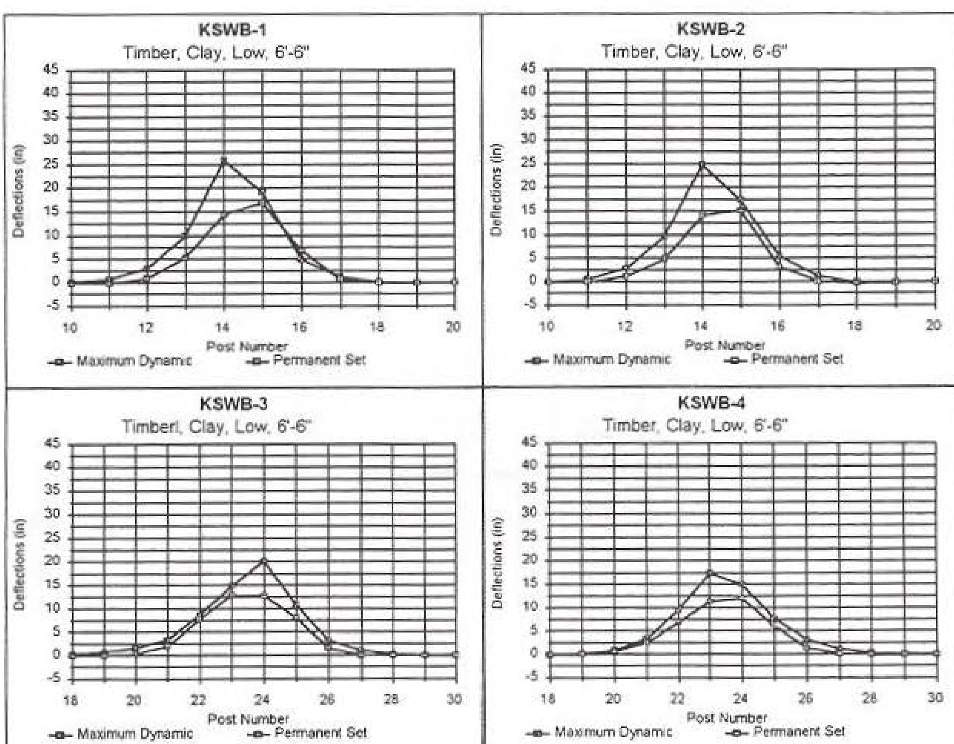

Figure. B-2. Predicted KSWB deflections using PT 2 post parameters.

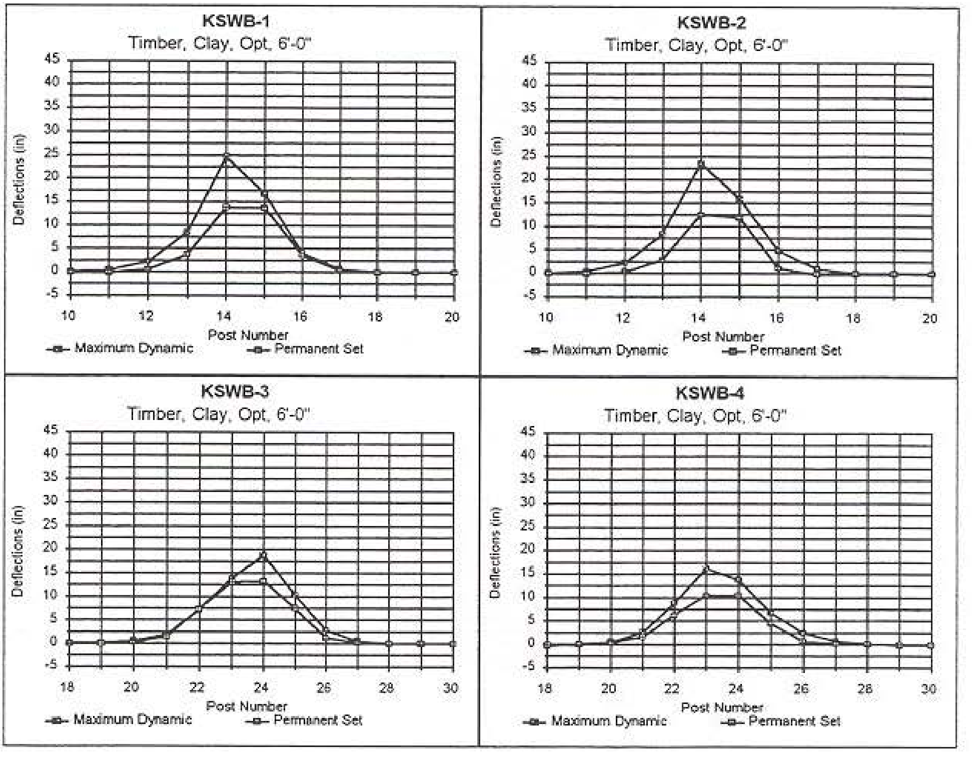

Figure. B-3. Predicted KSWB deflections using PT 3 post parameters.

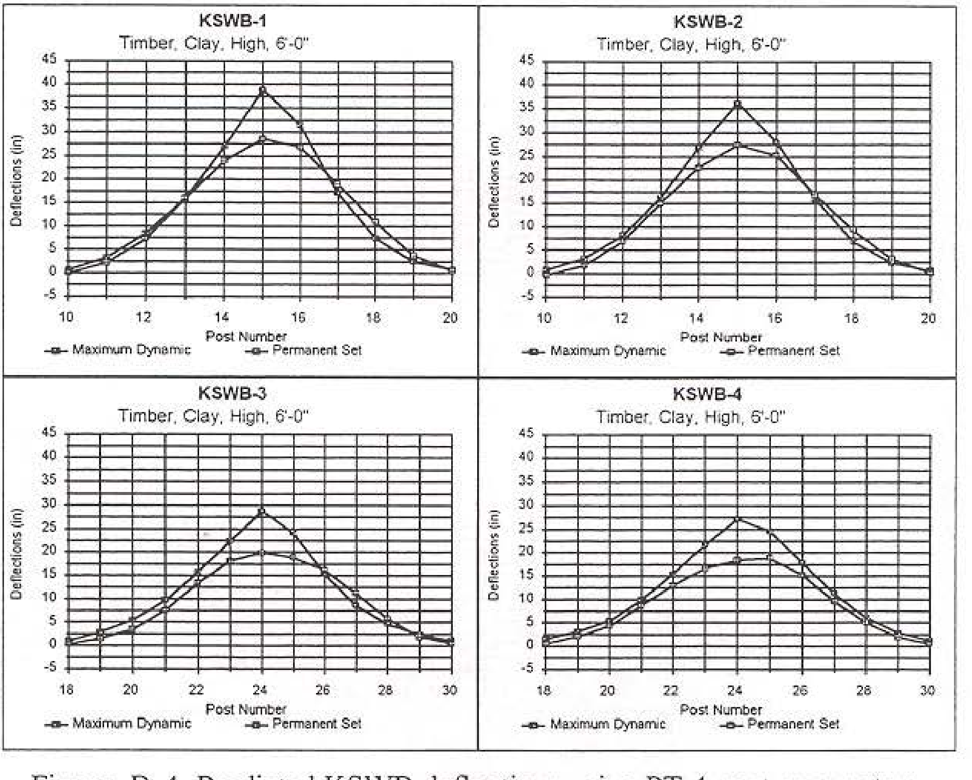

Figure. B-4. Predicted KSWB deflections using PT 4 post parameters.

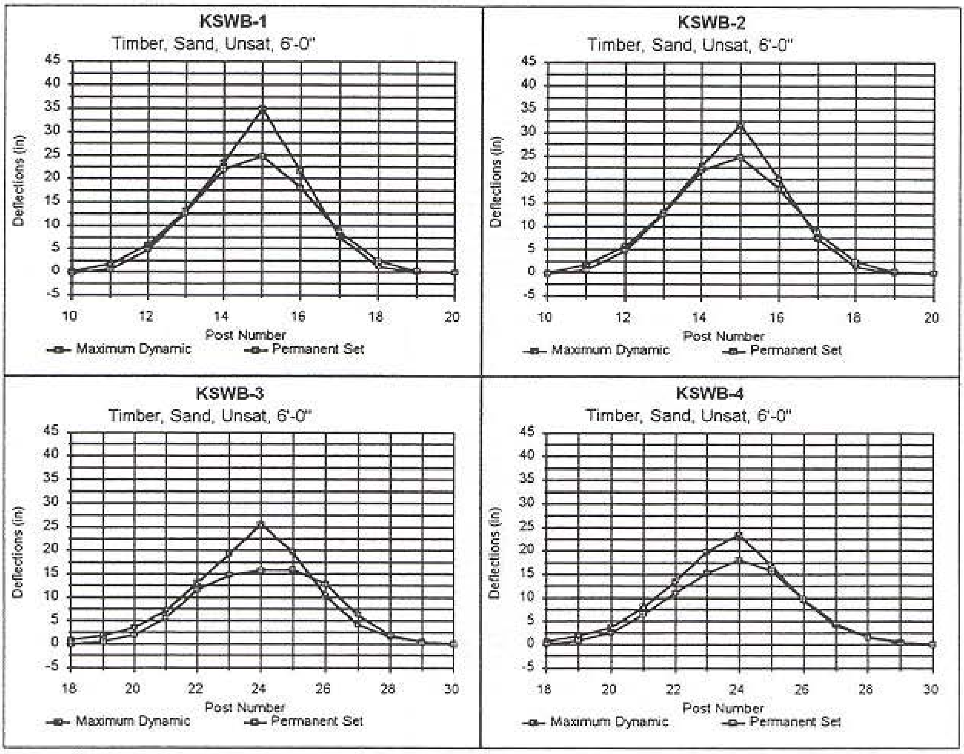

Figure. B-5. Predicted KSWB deflections using PT 5 post parameters.

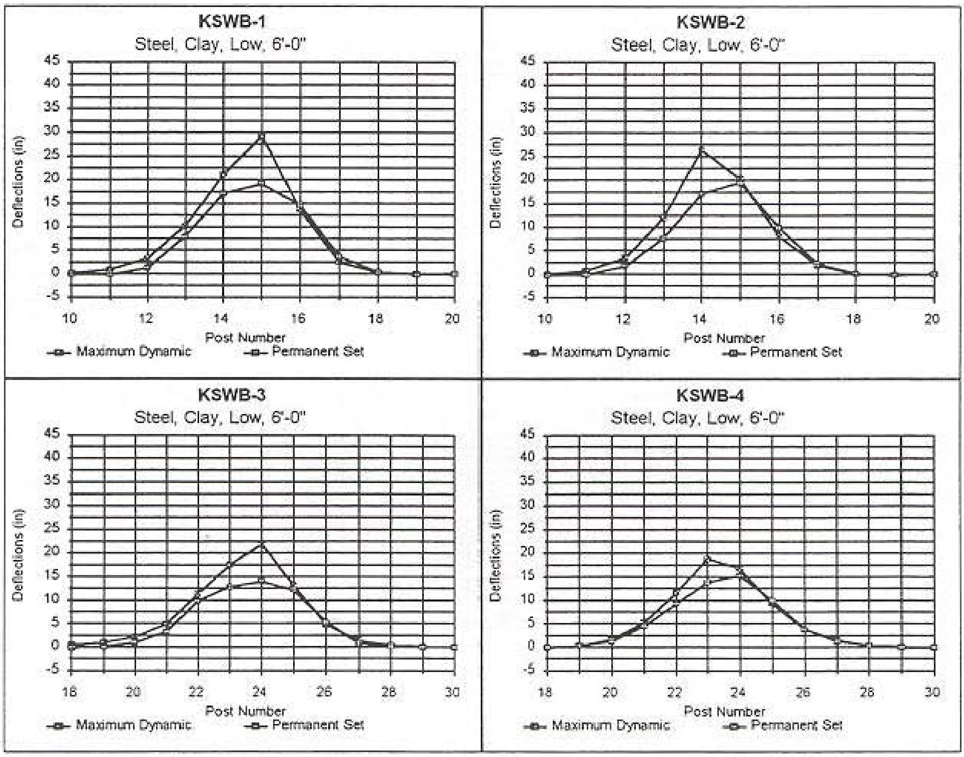

Figure. B-6. Predicted KSWB deflections using PT 6 post parameters.

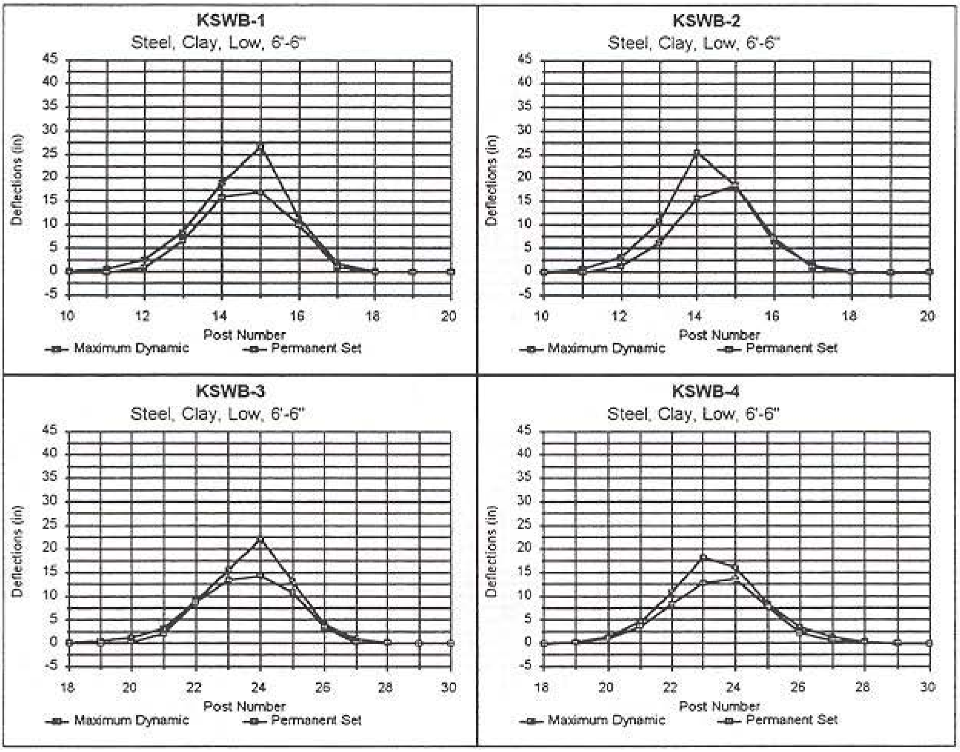

Figure. B-7. Predicted KSWB deflections using PT 7 post parameters.

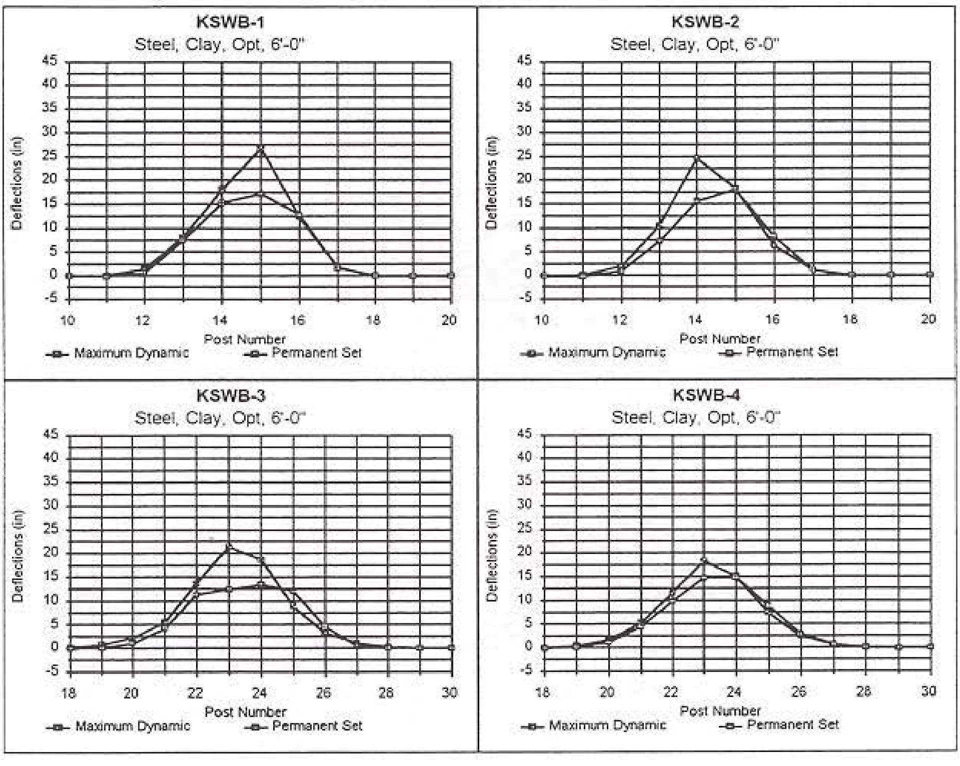

Figure. B-8. Predicted KSWB deflections using PT 8 post parameters.

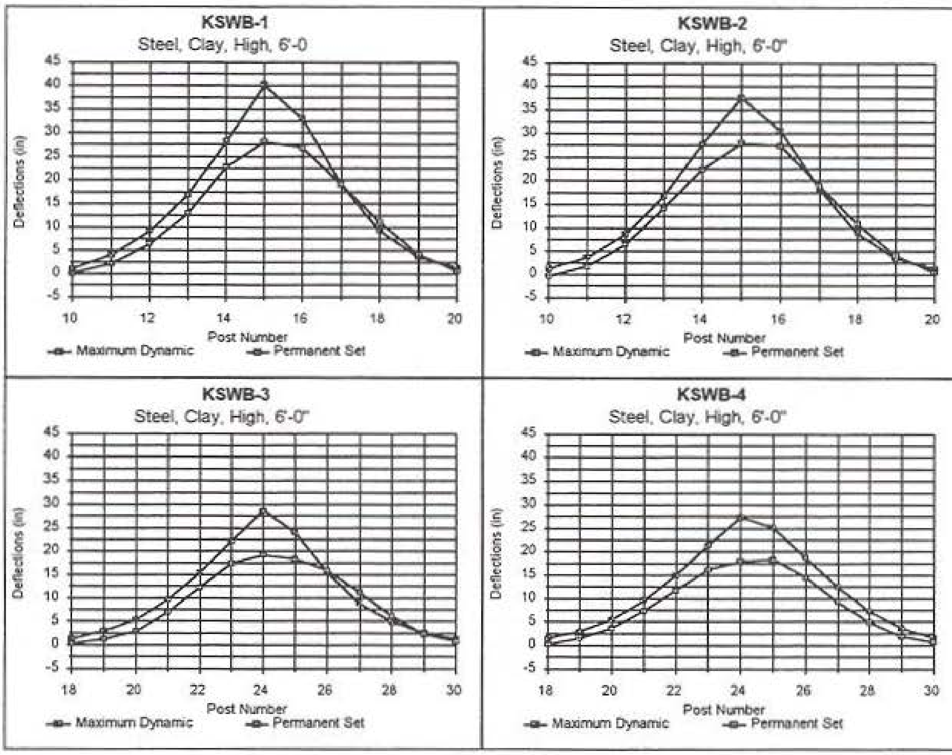

Figure. B-9. Predicted KSWB deflections using PT 9 post parameters.

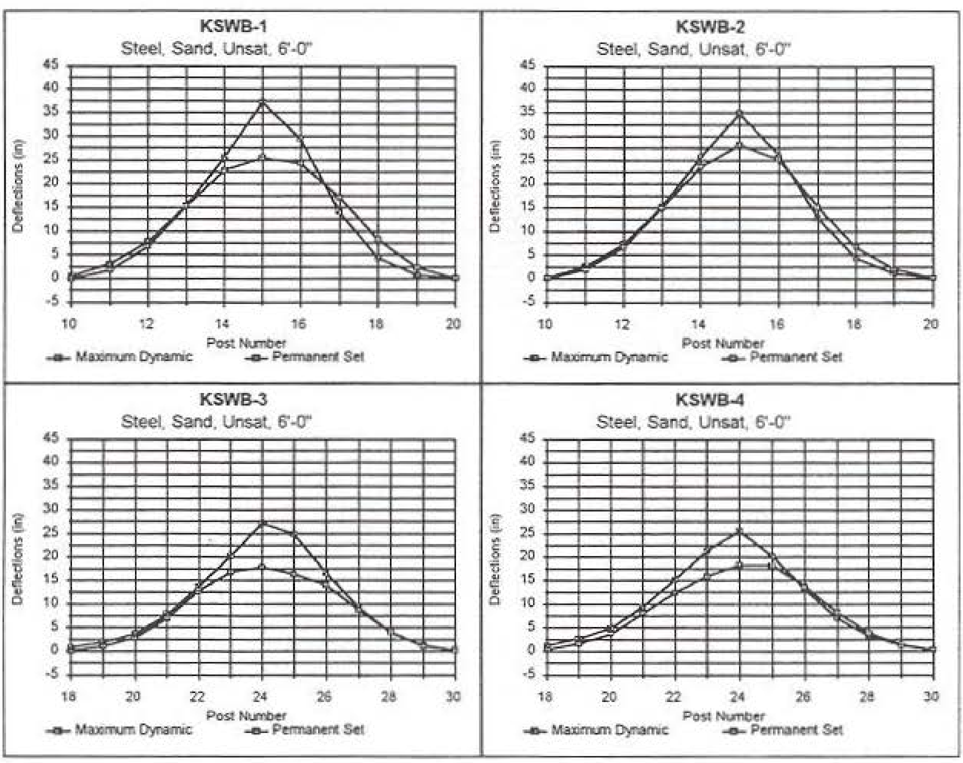

Figure. B-10. Predicted KSWB deflections using PT 10 post parameters.

Appendix C: Sample BARRIER VII Simulation Input Files

BARRIER VII input files used in the validation simulations described in Chapter 7 are given in their entirety on the following pages.

I. KSWB-1 BARRIER VII Simulation Input File

```
Kansas Post Testing, KSWB1, 4399#/61.9mph/25.1deg/Node13
   29     8     7     1    57     4     2     0
  0.001     0.001     2.000       300       1.0           1
    1    10    10    10    10     5     5
    1 0.0         0.0
    5 300.        0.0
    9 600.        0.0
   13 900.        0.0
   17 1200.0      0.0
   21 1500.0      0.0
   25 1800.0      0.0
   29 2100.0      0.0
    1     5     3     1
    5     9     3     1
    9    13     3     1
   13    17     3     1
   17    21     3     1
   21    25     3     1
   25    29     3     1
    1    29 0.35
   29    28    27    26    25    24    23    22    21    20
   19    18    17    16    15    14    13    12    11    10
    9     8     7     6     5     4     3     2     1
  100     1
    1 2.30      1.99       75.0       30000.     3.92       99.5       68.5       0.1
  300     2
    1 21.       0.         1.150      4.540      54.        107.10     205.80     0.1
5.100      12.25      20.00      20.00
    2 21.       0.         102.50     1.5600     64.50      630.00     191.10     0.1
35.00      9.100      20.0       15.5
    1     1     2    28     1   101 0.         0.         0.
   29     1          30     1   302 0.         0.         0.         0.         0.
   31     3          55     1   301 0.         0.         0.         0.         0.
   56    28          57     1   302 0.         0.         0.         0.         0.
 4399.     47000.        20     1     4     0     1
    1 0.040     0.250      7.50       12.
    1 89.35     14.38          1 12.          1    0    0    0
    2 89.35     26.38          1 12.          1    0    0    0
    3 89.35     38.38          1 12.          1    0    0    0
    4 77.35     38.38          1 12.          1    0    0    0
    5 65.35     38.38          1 12.          1    0    0    0
    6 53.35     38.38          1 12.          1    0    0    0
    7 41.35     38.38          1 12.          1    0    0    0
    8 29.35     38.38          1 12.          1    0    0    0
    9 -42.65    38.38          1 12.          1    0    0    0
   10 -54.65    38.38          1 12.          1    0    0    0
   11 -66.65    38.38          1 12.          1    0    0    0
   12 -78.65    38.38          1 12.          1    0    0    0
   13 -90.65    38.38          1 12.          1    0    0    0
   14 -102.65   38.38          1 12.          1    0    0    0
   15 -114.65   38.38          1 12.          1    0    0    0
   16 -126.65   38.38          1 12.          1    0    0    0
   17 -126.65   -38.38         1 12.          0    0    0    0
   18 89.35     -38.38         1 12.          0    0    0    0
   19 48.35     31.0           1 1.           1    0    0    0
   20 -65.65    31.0           1 1.           1    0    0    0
    1 48.35     31.0       0.         633.
    2 48.35     -31.0      0.         633.
    3 -65.65    31.0       0.         467.
    4 -65.65    -31.0      0.         467.
    1 0.0       0.0
    3 910.2     0.         25.1       61.9       0.0        0.0        0.0
```

II. KSWB-2 BARRIER VII Simulation Input File

```
Kansas Post Testing, KSWB2, 4486#/60.5mph/25.4deg/Node13
   29     8     7     1    77     5     2     0
  0.001     0.001      2.000        100       1.0            1
    1    10    10    10    10     5     5
    1 0.0        0.0
    5 300.       0.0
    9 600.       0.0
   13 900.       0.0
   17 1200.0     0.0
   21 1500.0     0.0
   25 1800.0     0.0
   29 2100.0     0.0
    1     5     3     1
    5     9     3     1
    9    13     3     1
   13    17     3     1
   17    21     3     1
   21    25     3     1
   25    29     3     1
    1    29 0.35
   29    28    27    26    25    24    23    22    21    20
   19    18    17    16    15    14    13    12    11    10
    9     8     7     6     5     4     3     2     1
  100     1
    1 2.30      1.99       75.0       30000.     3.92       99.5       68.5       0.1
  300     2
    1 21.       0.         1.15       4.540      54.        107.1      205.80     0.1
5.10       12.25      20.0       20.0
    2 21.       0.         102.50     1.5600     64.50      630.00     191.10     0.1
35.00      9.100      20.0       15.5
    1     1     2    28     1   101 0.         0.         0.
   29     5     6    48     1   101 0.         0.         0.
   49     1          50     1   302 0.         0.         0.         0.         0.
   51     3          75     1   301 0.         0.         0.         0.         0.
   76    28          77     1   302 0.         0.         0.         0.         0.
 4486.     47000.         20     1     4     0     1
    1 0.040     0.250      7.50       12.
    1 89.35     14.38            1 12.           1     0     0     0
    2 89.35     26.38            1 12.           1     0     0     0
    3 89.35     38.38            1 12.           1     0     0     0
    4 77.35     38.38            1 12.           1     0     0     0
    5 65.35     38.38            1 12.           1     0     0     0
    6 53.35     38.38            1 12.           1     0     0     0
    7 41.35     38.38            1 12.           1     0     0     0
    8 29.35     38.38            1 12.           1     0     0     0
    9 -42.65    38.38            1 12.           1     0     0     0
   10 -54.65    38.38            1 12.           1     0     0     0
   11 -66.65    38.38            1 12.           1     0     0     0
   12 -78.65    38.38            1 12.           1     0     0     0
   13 -90.65    38.38            1 12.           1     0     0     0
   14 -102.65   38.38            1 12.           1     0     0     0
   15 -114.65   38.38            1 12.           1     0     0     0
   16 -126.65   38.38            1 12.           1     0     0     0
   17 -126.65   -38.38           1 12.           0     0     0     0
   18 89.35     -38.38           1 12.           0     0     0     0
   19 48.35     31.0             1 1.            1     0     0     0
   20 -65.65    31.0             1 1.            1     0     0     0
    1 48.35     31.0       0.         572.
    2 48.35     -31.0      0.         572.
    3 -65.65    31.0       0.         496.
    4 -65.65    -31.0      0.         496.
    1 0.0       0.0
    3 910.2     0.         25.4       60.5       0.0        0.0        0.0
```

III. KSWB-3 BARRIER VII Simulation Input File

```
Kansas Post Testing, KSWB3, 4486#/59.7mph/24.8deg/Node22
   49     8     7     1    97     6     2     0
 0.001     0.001      2.000        100       1.0            1
    1    10    10    10    10     5     5
    1 0.0         0.0
    5 300.        0.0
   13 600.        0.0
   21 900.        0.0
   29 1200.0      0.0
   37 1500.0      0.0
   45 1800.0      0.0
   49 2100.0      0.0
    1     5     3     1
    5    13     7     1
   13    21     7     1
   21    29     7     1
   29    37     7     1
   37    45     7     1
   45    49     3     1
    1    49 0.35
   49    48    47    46    45    44    43    42    41    40
   39    38    37    36    35    34    33    32    31    30
   29    28    27    26    25    24    23    22    21    20
   19    18    17    16    15    14    13    12    11    10
    9     8     7     6     5     4     3     2     1
  100     2
    1 2.30       1.99       75.0       30000.     3.92       99.5       68.5       0.1
    2 2.30       1.99       37.5       30000.     3.92       99.5       68.5       0.1
  300     2
    1 21.        0.         1.15       4.540      54.        107.1      205.80     0.1
5.10      12.25      20.0       20.0
    2 21.        0.         102.50     1.5600     64.50      630.00     191.10     0.1
35.00      9.100     20.0       15.5
    1     1     2     4     1   101 0.         0.         0.
    5     5     6    44     1   102 0.         0.         0.
   45    45    46    48     1   101 0.         0.         0.
   49     1          50     1   302 0.         0.         0.         0.         0.
   51     3          95     1   301 0.         0.         0.         0.         0.
   96    48          97     1   302 0.         0.         0.         0.         0.
 4486.    47000.          20     1     4     0     1
    1 0.040      0.250      7.50       12.
    1 89.35      14.38           1 12.           1    0    0    0
    2 89.35      26.38           1 12.           1    0    0    0
    3 89.35      38.38           1 12.           1    0    0    0
    4 77.35      38.38           1 12.           1    0    0    0
    5 65.35      38.38           1 12.           1    0    0    0
    6 53.35      38.38           1 12.           1    0    0    0
    7 41.35      38.38           1 12.           1    0    0    0
    8 29.35      38.38           1 12.           1    0    0    0
    9 -42.65     38.38           1 12.           1    0    0    0
   10 -54.65     38.38           1 12.           1    0    0    0
   11 -66.65     38.38           1 12.           1    0    0    0
   12 -78.65     38.38           1 12.           1    0    0    0
   13 -90.65     38.38           1 12.           1    0    0    0
   14 -102.65    38.38           1 12.           1    0    0    0
   15 -114.65    38.38           1 12.           1    0    0    0
   16 -126.65    38.38           1 12.           1    0    0    0
   17 -126.65    -38.38          1 12.           0    0    0    0
   18 89.35      -38.38          1 12.           0    0    0    0
   19 48.35      31.0            1 1.            1    0    0    0
   20 -65.65     31.0            1 1.            1    0    0    0
    1 48.35      31.0       0.         625.
    2 48.35      -31.0      0.         625.
    3 -65.65     31.0       0.         496.
    4 -65.65     -31.0      0.         496.
    1 0.0        0.0
    3 910.2      0.         24.8       59.7       0.0        0.0        0.0
```

IV. KSWB-4 BARRIER VII Simulation Input File

```
Kansas Post Testing, KSWB4, 4501#/60.4mph/28.4deg/Node22
   49     8     7     1   137     7     2     0
 0.001     0.001      2.000        100        1.0            1
    1    10    10    10    10     5     5
    1 0.0         0.0
    5 300.        0.0
   13 600.        0.0
   21 900.        0.0
   29 1200.0      0.0
   37 1500.0      0.0
   45 1800.0      0.0
   49 2100.0      0.0
    1     5     3     1
    5    13     7     1
   13    21     7     1
   21    29     7     1
   29    37     7     1
   37    45     7     1
   45    49     3     1
    1    49  0.35
   49    48    47    46 [illegible]   44    43    42    41    40
   39    38    37    36 [illegible]   34    33    32    31    30
   29    28    27    26 [illegible]   24    23    22    21    20
   19    18    17    16 [illegible]   14    13    12    11    10
    9     8     7     6 [illegible]    4     3     2     1
  100     2
    1 2.30       1.99       [illegible]     30000.     3.92       99.5       68.5       0.1
    2 2.30       1.99       [illegible]     30000.     3.92       99.5       68.5       0.1
  300     2
    1 21.        0.         [illegible]     4.540      54.        107.1      205.80     0.1
5.10       12.25   [illegible]     [illegible]0.0
    2 21.        0.         [illegible]50   1.5600     64.50      630.00     191.10     0.1
35.00      9.100   [illegible]     15.5
    1     1     2     4   [illegible] 0.         0.         0.
    5     5     6    44   [illegible] 0.         0.         0.
   45    45    46    45   [illegible] 0.         0.         0.
   49     5     6    88   [illegible] 0.         0.         0.
   89     1          90   [illegible] 0.         0.         0.         0.         0.
   91     3         135   [illegible] 0.         0.         0.         0.         0.
  136    48         137   [illegible] 302 0.     0.         0.         0.         0.
 4501.     47000.     [illegible]     1     4     0     1
    1 0.040      0.250      [illegible].50  12.
    1 89.35      14.38          1 12.            1     0     0     0
    2 89.35      26.38          1 12.            1     0     0     0
    3 89.35      38.38          1 12.            1     0     0     0
    4 77.35      38.38          1 12.            1     0     0     0
    5 65.35      38.38          1 12.            1     0     0     0
    6 53.35      38.38          1 12.            1     0     0     0
    7 41.35      38.38          1 12.            1     0     0     0
    8 29.35      38.38          1 12.            1     0     0     0
    9 -42.65     38.38          1 12.            1     0     0     0
   10 -54.65     38.38          1 12.            1     0     0     0
   11 -66.65     38.38          1 12.            1     0     0     0
   12 -78.65     38.38          1 12.            1     0     0     0
   13 -90.65     38.38          1 12.            1     0     0     0
   14 -102.65    38.38          1 12.            1     0     0     0
   15 -114.65    38.38          1 12.            1     0     0     0
   16 -126.65    38.38          1 12.            1     0     0     0
   17 -126.65    -38.38         1 12.            0     0     0     0
   18 89.35      -38.38         1 12.            0     0     0     0
   19 48.35      31.0           1 1.             1     0     0     0
   20 -65.65     31.0           1 1.             1     0     0     0
    1 48.35      31.0       0.         630.
    2 48.35      -31.0      0.         630.
    3 -65.65     31.0       0.         496.
    4 -65.65     -31.0      0.         496.
    1 0.0        0.0
    3 910.2      0.         28.4       60.4       0.0        0.0        0.0
```

Appendix D: Optimum Moisture Content Determination

Prior to post testing, a soil analysis was conducted with the clay soil to determine the optimum moisture content. This is the moisture content at which the maximum dry density of the soil can be achieved. This was accomplished by performing a standard Proctor test. A plot of the Proctor curve obtained from the test is illustrated below in Figure D-1. A second order regression curve was fit to the data points in order interpolate values between known points.

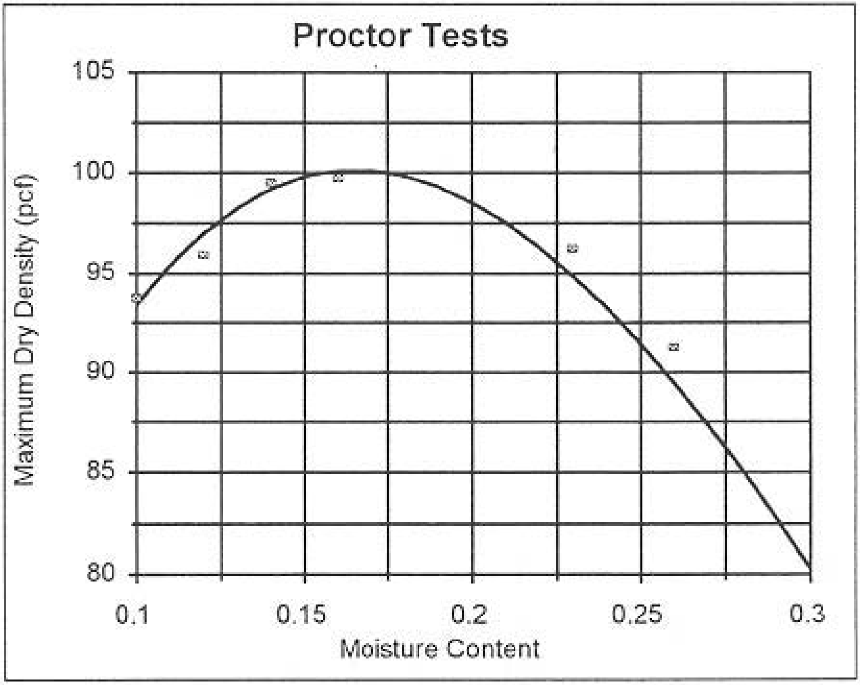

Figure. D-1. Clay soil proctor curve.

Using the proctor curve, the optimum moisture content was determined by interpolating the moisture content at which the curve is maximum and was found to be approximately 17%, yielding a maximum dry density of 100 pcf.

Appendix E: Moisture Content Relationships

Given in Figures E-1 through E-6 are the moisture content relationships for the BARRIER VII parameters - the yield moment (M_A), the stiffness (K_B), and the force (F_B) parameters. Plots are included for both steel and timber posts embedded to a standard depth.

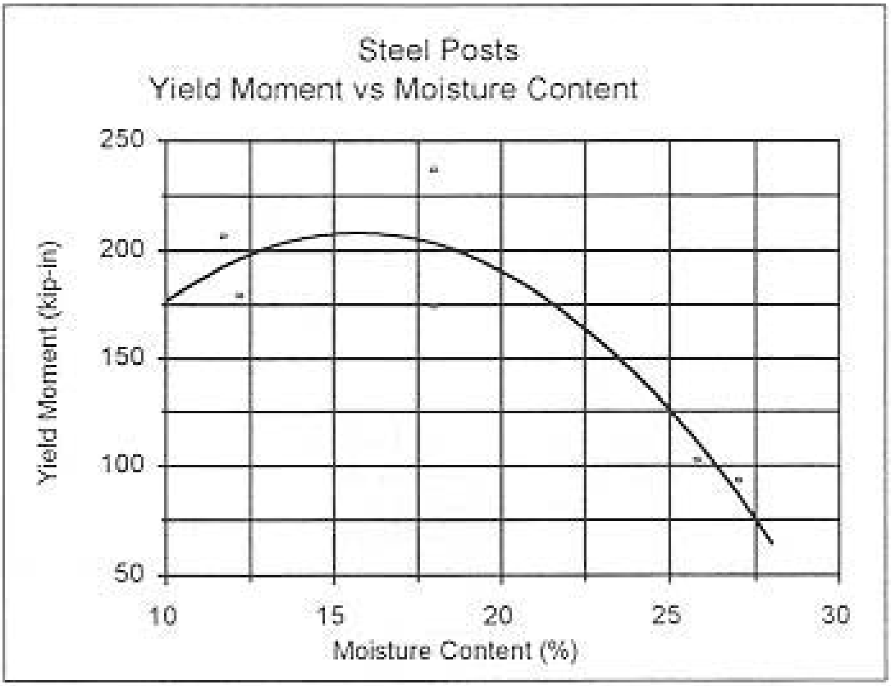

Figure. E-1. Moisture content vs. yield moment for a steel post.

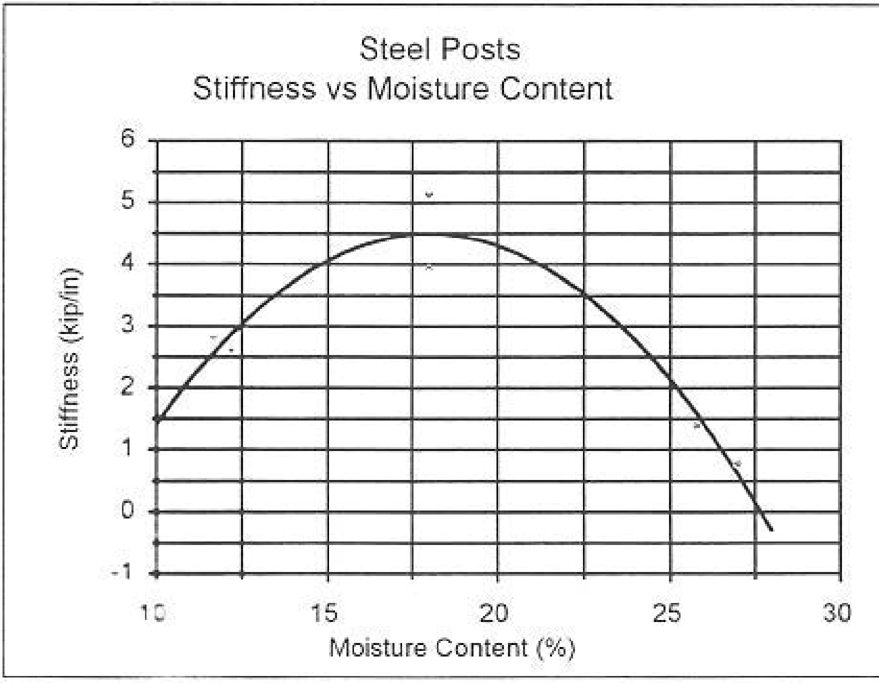

Figure E-2. Moisture content vs. stiffness for a steel post.

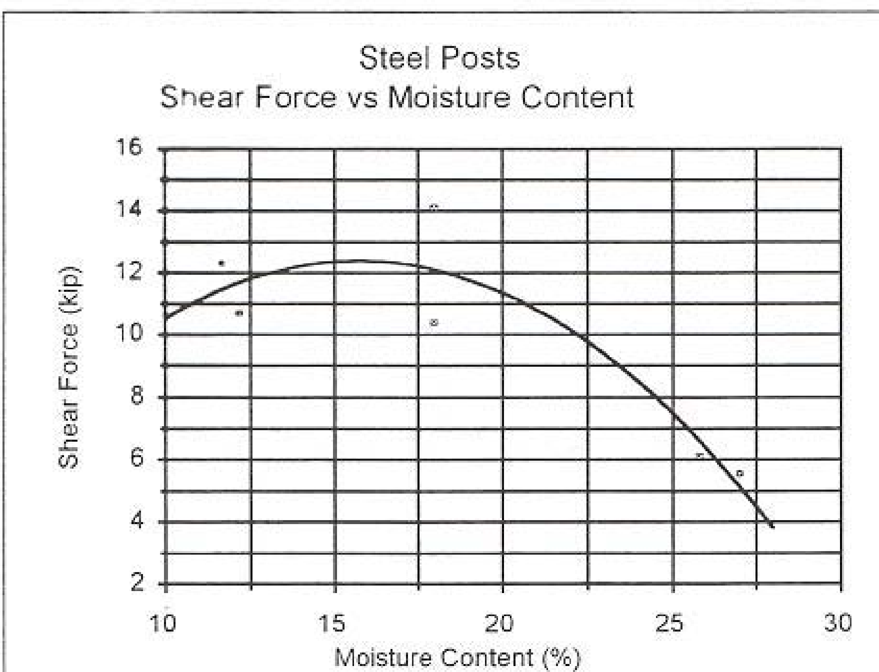

Figure. E-3. Moisture content vs. shear force for a steel post.

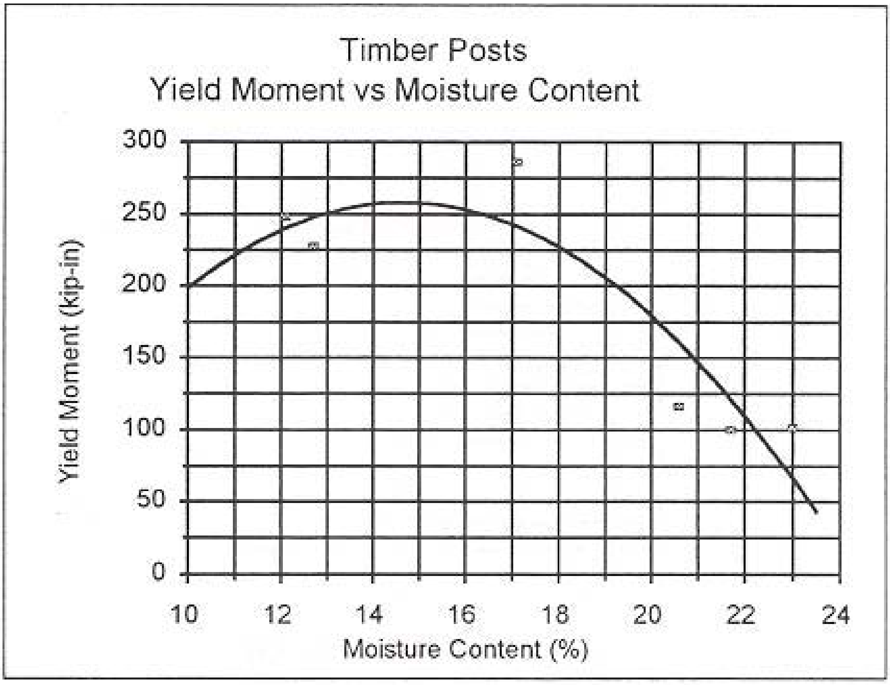

Figure. E-4. Moisture content vs. yield moment for a timber post.

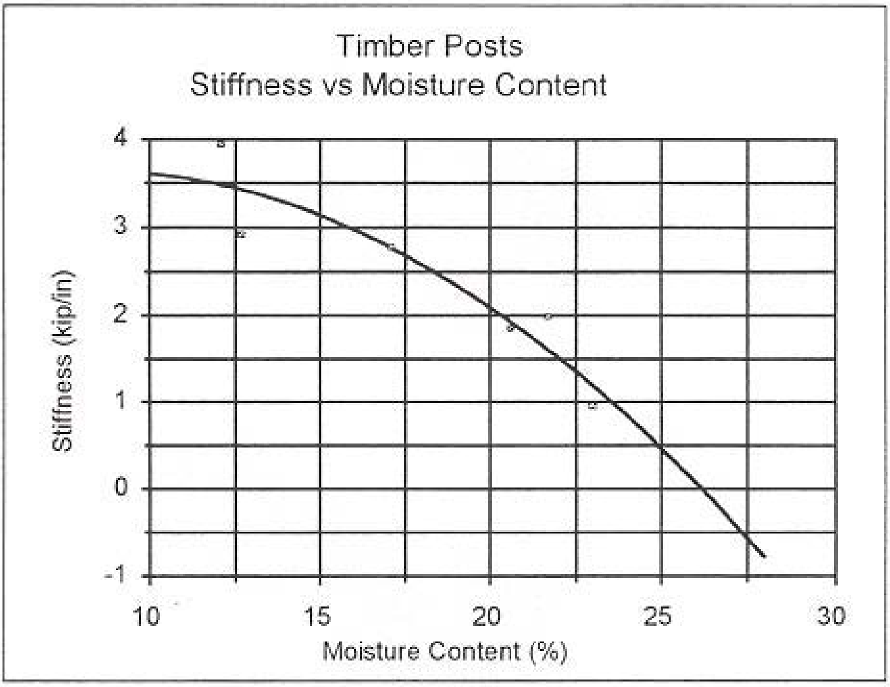

Figure. E-5. Moisture content vs. stiffness for a timber post.

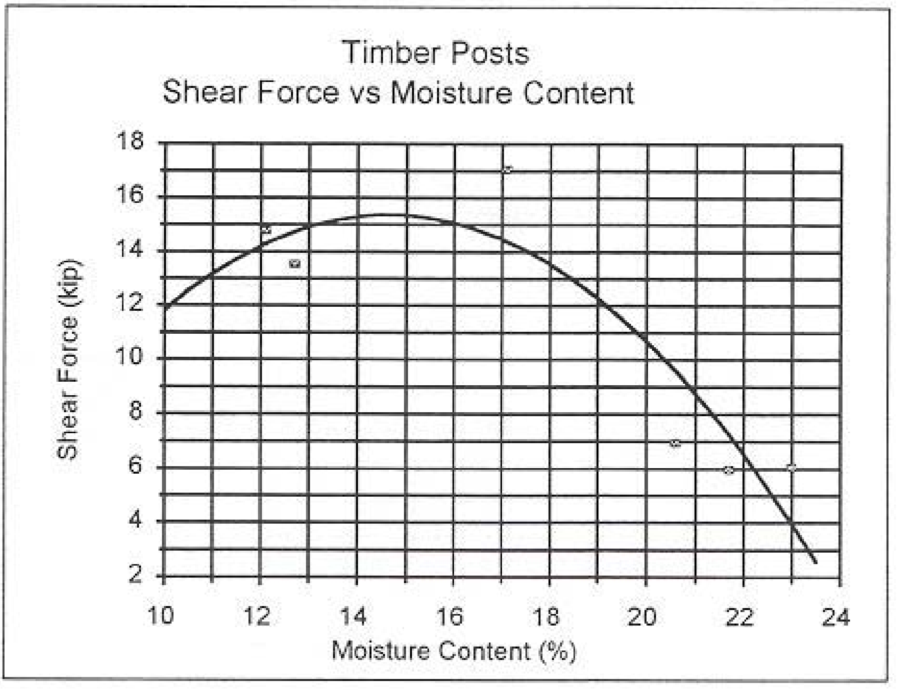

Figure. E-6. Moisture content vs. shear force for a timber post.